SYSTEMATICS, EVOLUTION, AND TAXONOMY OF THE GENUS *APHELINUS* (HYMENOPTERA: APHELINIDAE)

A Thesis

by

XANTHE ALEXIS SHIRLEY

Submitted to the Office of Graduate and Professional Studies of
Texas A&M University
in partial fulfillment of the requirements for the degree of

MASTER OF SCIENCE

Chair of Committee,	James B. Woolley
Committee Members,	John Oswald
	Kevin Conway
	Keith A. Hopper
Head of Department,	David Ragsdale

August 2016

Major Subject: Entomology

ABSTRACT

Aphelinus (Hymenoptera: Aphelinidae) is a genus of parasitoid wasps that has a long history of use in biological control programs against aphids. Past research shows that the classification of *Aphelinus* is greatly complicated by lack of comprehensive literature and the existence of cryptic species. In this body of work, traditional methods using morphological data sets and molecular methods using next generation sequencing were utilized to better discern the evolutionary relationships among species in *Aphelinus*. The evolutionary relationships among 14 species in *Aphelinus* and two outgroups were inferred using phylogenetic analyses (maximum parsimony and maximum likelihood) with amino acid data representing 110 protein-coding genes. The following results were common in both analyses: *A. perpallidus* (subgenus *Mesidia*) is basal to all other *Aphelinus* species; *A. abdominalis* and *A. asychis* are sister to all remaining *Aphelinus*; *varipes* and *mali* groups are monophyletic (but latter with weak support in maximum likelihood analysis). The placement of *A. daucicola* is unstable and differed in the two analyses. These phylogenetic analyses lay a preliminary phylogenetic framework for the classification of *Aphelinus.*

To explore the evolution of morphological characters in *Aphelinus*, character state mapping using the molecular phylogeny described above was used. A set of morphological characters consisting of both traditional morphological characters (wing setae, coloration, antennal measurements) as well as new characters (modified structures on the male scape, male genitalia) was compiled. Nine characters were found to have

strong phylogenetic signal (retention index >0.667). Wing characters were observed to be taxonomically important in diagnosing species groups, corresponding with what has been found in previous work. The structure of the carina around gland pores on the male scape, internal surfaces of the posterior-most sternum in males, and digiti length were also shown to diagnose natural groups of *Aphelinus*.

Through the development of a morphological character set, a revision of the *Aphelinus asychis* species group was conducted. Two new species (one from China and one from Kazakhstan) are described and two existing valid species within the *asychis* group (*A. asychis* and *A. semiflavus*) were redescribed.

DEDICATION

To my parents.

ACKNOWLEDGEMENTS

This work would not have been possible without assistance from others. I would like to thank everyone who was involved in helping me complete my thesis.

Thank you to my committee chair, Dr. Jim Woolley, for the constant guidance, encouragement, and laughs throughout this adventure. Thank you for believing in me. You have shaped me into a better person and scientist. I am incredibly thankful to have been able to work with you, and will always happily remember this chapter of my life.

Thank you to my committee members Dr. John Oswald and Dr. Kevin Conway for the support throughout the course of this research. Thank you to my fourth committee member, Dr. Keith Hopper, for all the assistance and considerable contributions. I am thankful I was able to collaborate with you throughout this project.

I am indebted to Dr. Bob Wharton and his lab, where my love for parasitoid wasps and systematics all started. Thank you for offering me a lab technician job when I was an undergraduate. The positive experiences from that time in my life opened the doors for graduate school for me. Thank you for your friendship and support throughout the years.

Thank you to the folks at USDA-ARS-BIIRL: Dr. Kristen Kuhn, for assisting in the whole genome sequencing work, and Kathryn Lanier and Joshua Rhodes for maintaining *Aphelinus* cultures.

Thank you to all the people who provided parasitized aphids for this research: Bill Ree, Dr. Roy Parker, Dr. Mike Brewer, Dr. Allen Knutson, Dr. Charles Allen, Dr. Greg Sword, Rande Patterson, and numerous others.

Thank you to the wonderful systematists at the Canadian National Collection and at the Smithsonian National Museum of Natural History (NMNH), specifically Dr. Mike Gates, Dr. Gary Gibson and Dr. John Huber. I look up to you all and am happy I was able to visit and meet you all in person. Thank you to the wonderful interns at the NMNH who took me under their wings during my visit there.

Thank you to the labs of Dr. Whitney Cranshaw and Dr. Paul Ode at Colorado State University and the CSU Horticulture Farm for the hospitality and assistance during my time there. Thank you to the numerous organic farms (Happy Hearts Farm, Revive Gardens, Gardens on Spring Creek, Schnorr Farm, Berry Patch Farm, and Sunny Daze Garden) that welcomed me on their land and allowed me to collect parasitized aphids during my time in Colorado.

Thank you to Dr. Richard Stouthamer and Dr. John Heraty for providing me beloved outgroups and Ryan Perry for being my chalcicoid buddy.

Thank you so much to Dr. Andreas Holzenburg and Dr. Mike Pendleton at the TAMU Microscopy Center for the help and guidance during my SEM saga.

Thank you to Kevin Deitz for giving me advice on sequence alignments and Meaghan Pimsler for helping me write the R script for my phylogenetics chapter.

A special thank you to all the wonderful people from the Woolley lab. Thanks to Dr. Ana Dal Molin for helping me make a smooth transition into graduate school when I

first started and for the support and insight all along the way. Thank you to Erin Maxson for all the encouragement. Thanks to each lab technician and undergraduate student worker (Jewel Coffey, Bethany Lefner, Corryn Cadena, Courtney Hendler, Itzel Hodges, Alyssa Mann, and Ada Morales) for all the hard work and help across the years.

Thanks also go to my friends and colleagues in the Department of Entomology at Texas A&M University. To Tyler Raszick, Bryant McDowell, Carl Hjelmen, Emily Boothe, Ivy Wei Chen, Chloë Hawkings, Kelly Beskin, and numerous others: Thank you for the wonderful memories. You are all incredible scientists and I am so honored I was able to share this experience with you all.

Thank you to all my professors (Dr. Micky Eubanks, Dr. Michel Slotman, Dr. Andreas Holzenburg, Dr. Terry Thomas, Dr. Robert Coulson, Dr. John Oswald, Dr. Jim Woolley, and Dr. Mariana Mateos), department faculty (Dr. Pete Teel, Dr. Spencer Johnston, Dr. Greg Sword, Dr. Julio Bernal and Dr. David Ragsdale) and staff (Rebecca Hapes, Ann Pool, Ed Riley, Robert Jensen, Felicita Anzualda, and Angie Rollins) for making my time at Texas A&M University a great experience.

I also want to extend my gratitude to the National Science Foundation, the Department of Entomology, and the Graduate and Professional Student Club for providing financial support.

Finally, I would like to thank my amazing family, especially my mother and father, for their continuous encouragement and support. Words cannot express how much you all mean to me and how thankful I am for your unconditional love.

TABLE OF CONTENTS

Page

LIST OF FIGURES

Page

LIST OF TABLES

Page

CHAPTER I

INTRODUCTION AND LITERATURE REVIEW

Background

Aphelinus Dalman 1820 is a genus of chalcidoid wasps in the family Aphelinidae, subfamily Aphelininae (Hayat 1972). *Aphelinus* is the type genus for this subfamily (Thomson 1876). Aphelininae is characterized by the possession of a linea calva on the forewing and at most six antennal segments (Hayat 1998). The subfamily Aphelininae has been treated as having four tribes: Aphelinini, Eutrichosomellini, Aphytini, and Eretmocerini (Hayat 1998), a hypothesis later tested by Kim and Heraty (2012), (see below).

Aphelinus belongs in the tribe Aphelinini, which is characterized by (1) being parasitoids of aphids, (2) having a prominent hypopygium that extends at least to the apex of the metasoma [in other tribes it extends at most to four-fifths the length of the metasoma], and (3) having a flexible articulation [not a rigid coupling] between tergum VI and the fused tergum VII + VIII (syntergum) of the metasoma, so that during oviposition the syntergum and ovipositor sheaths move upwards and stand erect and the ovipositor stylets are entirely everted. Aphelinini also contains *Protaphelinus* Mackauer 1972, and *Hirtaphelinus* Hayat 1983.

Aphelinus currently contains 92 valid species and 34 synonyms (Noyes 2016) and has been found to be monophyletic in both morphological and molecular phylogenetic studies (Campbell et al. 2000; Munro et al. 2011; Kim and Heraty 2012).

History of Phylogenetic Studies with Aphelinus

Kim and Heraty (2012) conducted a phylogenetic analysis of Aphelininae based on 50 morphological characters. Their results show strong support for the monophyly of Aphelininae (supported by four unambiguous characters).

Aphelinini was supported by two unambiguous characters. *Aphelinus* itself is supported by one unambiguous synapomorphy (Table 1). *Hirtaphelinus*, from Nepal (Hayat 1983), is supported by one unambiguous synapomorphy (Table 1). *Protaphelinus*, a genus of parasitoids of gall-making aphids in the genus *Pemphigus*, is known from the Oriental and Palearctic regions and is supported by two unambiguous synapomorphies (Table 1).

Table 1: Characters that support the monophyly of each genus of Aphelinini (Kim and Heraty 2012).

Genus	Unambiguous Characters
Aphelinus	• Posterior pair of scutellar setae farther apart than anterior pair of scutellar setae
Hirtaphelinus	• Axillar width 0.3 – 0.4× as long as interaxillar distance
Protaphelinus	• Epicoxal pad absent • Posterior margin of metanotum with a median projection, forming a triangular shape

Biology of Aphelinus

The life cycle of all species of *Aphelinus* involves the female adult ovipositing an egg into an aphid. In host instar preference studies, it has been reported that females of *Aphelinus* adults will oviposit in all four nymphal instars, but highest parasitization was found in young and intermediate instars and lowest parasitization in alatoid 4th instars (Cate et al. 1977; Gerling et al. 1990; Suck et al. 2012; Askar and El-Hussieni 2015; Shrestha et al. 2015).

Once the egg of *Aphelinus* hatches within the aphid, the *Aphelinus* larva feeds and grows internally, eventually killing the aphid host. During this process the integument of the aphid turns black and the aphid becomes a "mummy" (Christiansen-Weniger 1994). *Aphelinus* development is completed inside the aphid, and the adult parasitoid emerges through the mummy by chewing a hole, generally through the aphid's dorsum.

This life cycle makes *Aphelinus* useful for biological control of pest aphids and the genus has a long association with biological control research (Raney 1971; Cate et al. 1973; Starks et al. 1976; Clausen 1978; Arce Gomez and Rumiatto 1989; Sell and Kuo-Sell 1989; Elliott et al. 1995).

Aphelinus *in Biological Control*

One of the earliest examples of the use of *Aphelinus* in biological control involves *Aphelinus mali*, which is native to the northeastern United States. *Aphelinus mali* has been used in several parts of the world to control *Eriosoma lanigerum*, the wooly apple aphid. Since 1920, *A. mali* has been introduced into more than 50 countries

with apple growing areas and has been established in more than 40 countries, with varying degrees of aphid control success (Clausen 1956; Clausen 1978).

Aphelinus abdominalis has recently been commercialized. It can be purchased from biological control companies such as Syngenta and Arbico Organics for use as a control agent against a wide variety of aphid species, most notably *Macrosiphum euphorbiae*, the Euphorbia aphid, and *Aulacorthum solani*, the foxglove aphid.

Aphelinus asychis was the subject of significant interest for control of *Therioaphis trifolii*, the spotted alfalfa aphid, in the United States in the 1950's (Hagen and van den Bosch 1968). Field releases in southern California of imported *A. asychis* from southern Europe and the Middle East occurred during 1955. By the summer of 1956, they had become firmly established and consignments were sent to Western states in the following years as the aphid spread in distribution (Clausen 1978).

Aphelinus asychis was also the focus of work on biological control programs of *Schizaphis graminum*, the greenbug, during the 1970's and 1980's (Cate et al. 1973; Johnson et al. 1979; Summy et al. 1979) and *Diuraphis noxia,* the Russian wheat aphid, (Hopper et al. 1998; Prokrym et al. 1998; Brewer et al. 2001) during the 1990's. More recently, research has focused on foreign exploration for natural enemies of *Aphis glycinis*, the soybean aphid, with *Aphelinus* at the forefront as a potential biological control agent (Heimpel et al. 2004; Wu et al. 2004)

Through these endeavors, it has become increasingly apparent that a comprehensive review of the taxonomy of *Aphelinus* is needed to facilitate the

exploration, importation, and release of appropriate *Aphelinus* species for biological control of aphid pests.

Taxonomic Problems Within Aphelinus

The current classification of *Aphelinus* is provided in Table 2. Three specific issues have surfaced that provide the reasons why a comprehensive revision of *Aphelinus* is needed. The first is the taxonomic instability of subgenera, species groups, and related genera. Generic-level names that have been used include *Mesidia*, *Mesidiopsis*, and *Paulianaphelinus*. *Mesidia* was treated as a subgenus of *Aphelinus* by Boucek and Graham (1978), and this was followed by Hayat (1983). Graham (1976) noted the similarity of *Mesidia* and *Mesidiopsis*, and *Mesidiopsis* was treated as a synonym of *Aphelinus* (*Mesidia*) by Hayat (1990). This group is distinguished by longer segments in the antennal funicle, particularly the basal two segments, which are longer than wide, and a short ovipositor in females (Mackauer 1972). The monophyly of subgenus *Mesidia* and its relationships with other *Aphelinus* remain to be tested using rigorous methods. *Paulianaphelinus*, described from a single, brachypterous, African species, is probably a synonym of *Aphelinus*, as there is no indication that the type species, *P. maricusae* Risbec, represents a distinct lineage.

Many workers have used informal species groups in *Aphelinus*, perhaps best developed in Hayat (1998). These include four species groups in *Mesidia* (the *annulipes*, *argiope*, *automatus* and *subflavescens* groups) and at least five in *Aphelinus* (the *abdominalis*, *asychis*, *mali*, *nepalensis* and *varipes* groups). The intergroup and

intragroup relationships of these, especially those in *Mesidia*, need to be explored further.

Table 2: Taxonomic structure of *Aphelinus* following Hayat 1998 and unpublished data.

Subgenus	Species group	# Species	Distribution
Indaphelinus		1	Oriental
Mesidia	*argiope*	3	Holarctic, Oriental
Mesidia	*automatus*	7	Holarctic, Ethiopian
Mesidia	*subflavescens*	1	Neotropical, Ethiopian
Paulianaphelinus		2	Nearctic, Neotropical, Ethiopian
Aphelinus	*abdominalis*	4	Cosmopolitan
Aphelinus	*asychis*	2	Cosmopolitan
Aphelinus	*mali*	15	Cosmopolitan
Aphelinus	nr. *mali*	6	Cosmopolitan
Aphelinus	*nepalensis*	2	Oriental
Aphelinus	*varipes*	15	Cosmopolitan
Aphelinus	unplaced	34	Cosmopolitan
Total		**92**	

The second issue is the regional, not global, focus of most *Aphelinus* literature. Apart from Hopper et al. (2012), who treated the *mali* complex worldwide, all of the taxonomic literature on *Aphelinus* treats only regional faunas. The Palearctic fauna is the largest and best known (Nikolskaya 1952; Yasnosh 1963; Ferrière 1965; Nikolskaya and Yasnosh 1966; Hayat 1972; Graham 1976; Yasnosh 1978; Liao et al. 1987; Hayat 1990; Hayat 1991b; Hayat 1991a; Hayat and Fatima 1992; Huang 1994; Yasnosh 2002; Li and Zhang 2004; Japoshvili and Abrantes 2006).

Papers are available too on species in Africa (Prinsloo and Neser 1994), Argentina (De Santis 1948), Australia (Girault 1913b; Girault 1913a; Girault 1915; Girault 1929; Girault 1932; Hayat and Fatima 1992), Israel (Zehavi and Rosen 1988), and North America (Haldeman 1851; Ashmead 1888; Dalla Torre 1898; Howard 1908; Girault 1911; Howard 1914; Howard 1917; Timberlake 1924; Gahan 1925; Carver 1980; Evans et al. 1995), but no comprehensive keys to species exist in these regions. Available keys for specific geographical regions are shown in Table 3. Because of the general lack of continental and global-scale treatments, it is difficult for most specialists to confidently identify species from much of the world and consequently, species concepts have largely been based on regional faunas.

Table 3: Keys to *Aphelinus* species by geographical region.

Region	Source
Egypt	Abd-Rabou, 2002 Abd-Rabou, 2005 Nikol'skaya 1952 Ferrière 1965
Europe	Graham, 1976 Yasnosh 1978
India	Hayat, 1972 Hayat, 1998
China	Huang, 1994 Liao et al., 1987
Iberian Peninsula	Japoshvili & Abrantes, 2006
Rep. of Georgia	Japoshvili & Karaca, 2009
Spain	Mercet, 1929
South Africa	Prinsloo & Neser, 1994
Southern Primorye Province	Yasnosh, 1994
Israel	Zehavi & Rosen, 1989

The third issue is the recognition that the classification of *Aphelinus* is complicated by the existence of at least three known complexes of cryptic species. Cryptic species differ little in morphological characters but are phylogenetically distinct lineages that differ in biology and are usually reproductively isolated from one another. The known cryptic species complexes in *Aphelinus* are the *mali* complex (Hopper et al. 2012), the *varipes* complex (Heraty et al. 2007) and the *asychis* complex (Kazmer et al. 1996).

Project to Revise the Aphelinus *Species of the World*

The objectives and work outlined in this thesis are part of a larger project, funded by NSF (DEB 1257601), to revise the *Aphelinus* species of the world. The objectives of the larger project are to assemble material of *Aphelinus* from all known major collections, revise species concepts worldwide, provide a foundation of molecular data for phylogenetic analysis using next-generation-sequencing (NGS) methods, develop an informatics infrastructure for the project using the MX system, and deliver both written and electronic products. The specific role of this thesis is described below (see Thesis Objectives and Summary of Chapter Contents). Dr. Jim Woolley has overall management responsibility for the project and is in charge of the collection-based taxonomy, digital imaging, and bioinformatics components of the project. Dr. Keith Hopper and Dr. Kristen Kuhn, USDA/ARS/Biological Insect Introduction Research Laboratory, Newark, DE, are in charge of generating NGS molecular data, and for assembling partial or complete genomes of *Aphelinus* species for use in phylogenomics

analyses. To date, 14 complete genomes of *Aphelinus* species and one outgroup species (*Aphytis melinus*) have been assembled and annotated through this project.

A comprehensive and robust classification of *Aphelinus,* and specifically of the *Aphelinus asychis* species group, will greatly facilitate the use of species in this group in biological control programs against important agricultural pests. Clarification of *Aphelinus* species names will also aid in studies of parasitoid speciation, host switching, and mate recognition, where *Aphelinus* species provide excellent model systems. The revision and associated digital electronic products proposed below will benefit both specialists in parasitoid taxonomy and biological control researchers. A robust phylogenetic framework is needed to provide a foundation for a corresponding classification and to support future applied entomological work.

Thesis Objectives

1. Use molecular data (generated by collaborators) to conduct maximum parsimony and maximum likelihood phylogenetic analyses to provide a phylogenetic framework for the genus.
2. Develop a set of morphological characters to be used to investigate the phylogenetic structure of the genus *Aphelinus*, including in-depth exploration of pores on the male scape.
3. Map morphological data onto the phylogeny produced from molecular data to investigate evolutionary patterns of morphological character change.
4. Revise the *Aphelinus asychis* species group through the development of a morphological character set.

Summary of Chapter Contents

This body of work incorporates both traditional morphological methods as well as molecular methods with next generation sequencing. An in-depth review of previous molecular work with *Aphelinus* will be discussed in Chapter II, followed by the results of my phylogenetic analysis with amino acid data from next generation sequencing. For the morphology work, I wanted to use traditional morphological characters as well as investigate new possible characters that could be taxonomically important. The use of modified structures on the male scape as taxonomic characters is investigated in Chapter III through a survey of the male scape using scanning electron microscopy. In Chapter IV, morphological characters are coded for all the series that have been sequenced to date, and the morphology is mapped onto the molecular phylogeny from Chapter II. The evolution of these characters and inference about character state homology will be addressed in Chapter IV. Chapter V is a taxonomic study and revision of the *Aphelinus asychis* species group.

Nomenclatural Disclaimer

Publication of this work for the purposes of scientific nomenclature is specifically disclaimed under Article 8.2 of the International Code of Zoological Nomenclature (ICZN 1999).

CHAPTER II

MOLECULAR PHYLOGENY OF THE GENUS *APHELINUS* DALMAN, 1820 (HYMENOPTERA: APHELINIDAE)

Introduction

Past research shows that the taxonomy of *Aphelinus* is greatly complicated by the existence of cryptic species that differ little in the morphological characters traditionally used for *Aphelinus* classification (Kazmer et al. 1996; Heraty et al. 2007; Hopper et al. 2012). Molecular data analyzed in a phylogenetic framework can help in recognition of cryptic species and to better discern the evolutionary relationships among species of *Aphelinus*. With information about these relationships, more accurate taxonomic decisions can be made and a more natural classification can be constructed.

Previous Molecular Work

Aphelinus has been found to be monophyletic in both morphological and molecular phylogenetic studies (Campbell et al. 2000; Kim and Heraty 2012; Munro et al. 2011; Heraty et al. 2007; Heraty et al. 2013).

Campbell et al. (2000) conducted a maximum parsimony analysis for Chalcidoidea using 28S-D2 data. Three *Aphelinus* species were included: *A. asychis*, *A. albipodus*, and *A. varipes*.

Kim and Heraty (2012) conducted a phylogenetic analysis of Aphelininae based on 50 morphological characters scored for 16 genera. Their results provide strong support for the monophyly of the Aphelininae, supported by eight characters, and they

discussed the four lineages within the subfamily: Aphelinini, Aphytini, Eretmocerini, and Euthrichosomellini. Aphelinini, supported by six characters, contains *Aphelinus*, *Protaphelinus* Mackauer 1972, and *Hirtaphelinus* Hayat 1983. Monophyly of *Aphelinus* itself is supported by one unambiguous synapomorphy (posterior pair of scutellar setae farther apart than anterior pair).

Munro et al. (2011) conducted maximum parsimony and maximum likelihood phylogenetic analyses across the Chalcidoidea using 18S and 28S ribosomal gene regions. Within Aphelininae, seven genera (*Aphelinus, Marietta, Aphytis, Eutrichosomella, Samariola, Centrodora,* and a putative new genus) and 22 species were represented. Three species of *Aphelinus* were included in this study, and *Aphelinus* was found to be monophyletic and the sister taxon to the other Aphelininae genera included in the analysis.

Phylogenetic work within *Aphelinus* with emphasis on the *varipes* species group was conducted by Heraty et al. (2007). In this study, relationships among eight populations of six species within the *A. varipes* species group and outgroups consisting of two populations of *A. asychis*, one population of *A. mali*, one population of *A.* near (nr.) *mali*, and one population from the genus *Marietta* were analyzed using four nuclear and two mitochondrial gene regions. Within the *varipes* species group, four clades were obtained: (1) *A. kurdjumovi*, (2) *A. hordei*, (3) *A. atriplicis*, *A. varipes*, *A. albipodus*, and (4) *A. certus*. Heraty et al. (2007) also found that the taxa that were phylogenetically distinct were also reproductively incompatible with the exception of *A. atriplicis* and *A. certus*. The *A. mali* and *A.* nr. *mali* populations formed a clade, and represent the sister

group to the *varipes* group clade. Together these two clades form the sister group to the *A. asychis* clade. The *A. mali* and *A.* nr. *mali* clade had bootstrap value of 79. All other clades were supported by bootstrap values of 100. Extremely short branch lengths were obtained across these clades, especially within the *asychis* clade and the *varipes* group clade. Also, there was virtually no homoplasy in this data set (CI = 0.88, RI = 0.94).

A robust phylogenetic analysis of the Chalcidoidea with both morphological (233 morphological characters) and molecular data (two nuclear gene regions) (Heraty et al. 2013). The relationship of *Aphelinus* with other genera varied according to method used.

A lot is still left to learn about *Aphelinus*, specifically exploring and testing the monophyly of and phylogenetic relationships within and between species groups. Heraty (2007) explored relationships within the *varipes* group, but the number of species within *varipes* group included in that study was limited to six out of a possible 15 (40%). Additional molecular work with broader taxon sampling and including representatives from other species groups and subgenera is needed in order to obtain a clearer phylogenetic framework of *Aphelinus* and to confirm monophyly of the genus. This framework is needed in order to circumscribe complicated species groups and subgenera of *Aphelinus* and to address the taxonomic issues described in Chapter I.

Because DNA sequences are less complex than those of proteins (4 nucleotides vs. 20 amino acids) and possible substitution saturation at the third codon position, amino acid sequences were used for phylogenetic analyses in this study.

Research Objectives

1. Use next-generation sequencing to produce large numbers of phylogenetically informative characters within and between species groups of *Aphelinus.*
2. Conduct a phylogenetic analysis using amino acid sequence data derived from the next generation sequencing.

Materials and Methods

Genome Sequencing, Assembly, and Annotation

All DNA extraction, whole genome sequencing, as well as genome assembly and annotation, was done by my collaborators (Dr. Keith Hopper and Dr. Kristen Kuhn) at USDA, ARS, Beneficial Insects Introduction Research Unit (BIIRU). DNA extraction was conducted following the Qiagen DNEasy protocol. They sequenced (sequencing was done at the Delaware Biotechnology Institute Sequencing & Genotyping Center) and assembled the genomes of 14 species in 6 species complexes in Aphelinus and one outgroup (Table 4). They analyzed the genome assemblies for putative genes and mapped the mRNA sequences to the genomes. For genome *de novo* assemblies, they used primarily Illumina HiSeq paired-end libraries (250-440 bp inserts with 2x100-150nt sequencing of the ends). However, for the *A. atriplicis* genome, they added Illumina mate-pair libraries (~5 kb inserts with 2x100nt sequencing of the ends), and PacBio RS long-read (N_{50}=22kb) libraries, prepared with standard Illumina and PacBio kits and protocols. For Illumina paired-end sequencing, they used 0.3-1 channel flow-cell per species, which gave coverage of 30x to 140x. Using the CLC Bio GenomeWorkbench (clcbio.com), they trimmed the reads for quality and made *de novo* assemblies.

Assembly sizes were 272-358 Mb long with N50 = 2-37 kb, depending on the amount and type of sequence data. The contigs were in general small and numerous, and the assembly sizes were only 73-90% of the genome sizes estimated from flow cytometry, apparently because of frequent sites with repetitive DNA that are difficult to assemble. Nonetheless, these assemblies had 96-98% of the expected eukaryotic genes and 87-93% of the expected arthropod genes in the BUSCO gene sets (Simão et al. 2015). Using AUGUSTUS (Stanke and Morgenstern 2005) for automated gene discovery, 23,867-34,977 putative genes per genome were found, with the number of genes depending strongly on genome size. They sequenced mRNA from whole adult males and females of 12 species using RNA-Seq on the Illumina HiSeq, which produced reads that mapped to 92-100% of the putative genes. To discover the function of these genes, they compared their amino acid sequences to proteins in the RefSeq database (ncbi.nlm.nih.gov) using BLASTP (Altschul et al. 1990). They also searched for information about their functions using Blast2GO (Conesa et al. 2005). BLASTP analysis ($E \leq 0.001$) revealed matches for 71-83% (18,646- 24,823) of the genes found in these species. Blast2GO showed only 28-38% (8,098-10,190) had functional annotations.

All 14 *Aphelinus* species are in culture in the Hopper lab at USDA-ARS-BIIRL. Dr. Richard Stouthamer from University of California, Riverside, provided *Aphytis melinus* from the insectary of Foothill Agricultural Research Center, Browns Valley, California. Voucher specimens are located at Texas A&M University Insect Collection (TAMUIC) and USDA-ARS-BIIRL.

Table 4: List of taxa for which whole genome sequences were used in this study.

Ingroup/Outgroup	Subgenus in *Aphelinus*	Species group in *Aphelinus*	Taxon	Source
Ingroups	*Aphelinus*	*asychis*	*Aphelinus* nr. *asychis*[1]	China, Harbin
	Aphelinus	*mali*	*Aphelinus coreae*[1]	Korea
			Aphelinus glycinis[1]	China, Xiuyan
			Aphelinus rhamni[1]	China, Beijing
	Aphelinus	*daucicola*	*Aphelinus* nr. *daucicola*[1]	USA, Delaware
	Aphelinus	*varipes*	*Aphelinus atriplicis*[1]	Rep. of Georgia
			Aphelinus certus[1]	Japan
			Aphelinus hordei[1]	France
			Aphelinus kurdjumovi[1]	Rep. of Georgia
			Aphelinus varipes[1]	France
			Aphelinus nr. *certus*[1]	USA, Texas
			Aphelinus nr. *certus*[1]	Korea
	Aphelinus	*abdominalis*	*Aphelinus abdominalis*[1]	Originally purchased from Syngenta Bioline
	Mesidia	unplaced	*Aphelinus perpallidus*[1]	Texas, USA
Outgroups	n/a	n/a	*Aphytis melinus*[2]	California, USA
			Nasonia vitripennis[3]	See Werren et al. 2010

1 species that collaborators sequenced and in culture at USDA-ARS-BIIRL
2 species that collaborators sequenced, from other sources, not in culture at USDA-ARS-BIIRL
3 species whose sequence data was obtained through NCBI

Analysis of Protein Sequences

Amino acid data files for all species were received in FASTA format. The number of putative protein-coding genes per species ranged from 22,702 to 35,861. To find homologs of these genes between species, a local BLAST database was constructed. BLAST was downloaded from the NCBI website to a Windows computer. A local BLAST database was set up following the instructions from the Bioinformatics Resources Archives from the Virginia Commonwealth University's Bioinformatics and Bioengineering Summer Institute (http://www.vcu.edu/csbc/bbsi/inst/archives/bioinf/SetupLocalBlast.html). *Aphelinus atripiclis* had the best annotation and was therefore selected as the reference species. Pairwise local BLAST searches were conducted using

A. atriplicis as the reference and an individual query species, which was each of the other 13 *Aphelinus* species. The e-value, a metric that refers to the expected number of random hits when searching the local BLAST database, was set at 0.001.

Local BLAST search results were output in tabular format 6. This format displays the gene number in the query species that matches the gene number in the reference database. Percent identity, alignment length, number of mismatches, number of gap openings, query start position, query end position, target start position, target end position, e-value, and bit score are also given for each gene match.

The local BLAST search found sequences that were putatively homologous, but not necessarily orthologous. The local BLAST search could have yielded paralogous matches. To address this, all sequence matches that had more than one hit in either the reference or query species were removed, therefore removing any apparent paralogs. To do this, each output file from each species was opened in Microsoft Excel. I identified the genes that were duplicates in the reference *A. atriplicis* gene column, and those that were duplicates in the query gene column using the conditional formatting tool. Under the "home" tab, conditional formatting was selected, and then "highlight cell rules", and then "duplicate values". This was first done with the *A. atriplicis* gene column, and then with the query gene column. Using the filter option, cells that were not highlighted in either column were moved to the top. Those that were highlighted, designating duplicates, were removed. Next, using the sort option, the sequences were organized by percent identity from largest to smallest.

Initially, sequences that had less than 97% identity match to *A. atriplicis* were selected. This was done by creating a new column with the header titled "<97%" in the spreadsheet. An "x" was inserted next to the rows that corresponded to this criterion. The filter tool was then used. The filter tool was used on the "<97%" column to just display the rows marked with an "x". These specific genes were then pasted into a new spreadsheet. This protocol was applied to all reference vs. query species pairs. In the new spreadsheet, which contained only the filtered genes for all species, the highlight duplicate feature was used again. In this case, it was used to identify the genes that were found in all 14 species under these criteria. Using these filtration criteria and identifying the genes that were found across all species, only eight genes remained. Because I was interested in obtaining a larger number of genes for phylogenetic analysis, I reset the stringency of identity to less than 100% (rather than 97%) identity for the next trial. Applying the same filtering procedure resulted in a set of 110 genes (Appendix A).

Subsequent local BLAST searches were conducted using the outgroups. *Aphytis melinus* (Hymenoptera: Aphelinidae), which like *Aphelinus* is in the subfamily Aphelininae, was used as a "near" outgroup. The genome for *Nasonia vitripennis* (Hymenoptera: Pteromalidae) is available through NCBI and was downloaded and used as a "far" outgroup.

A script was created in R to pull the 110 gene sequences from the original data files of each species into a new data file that contained data for all 15 species and one gene. Once this step was completed, there were 110 separate FASTA files, one for each gene. Each of these FASTA files was individually aligned using MAFFT

(http://mafft.cbrc.jp/ alignment/server/). Three trials with three different iterative refinement methods for alignment (L-INS-i, E-INS-i, G-INS-i) were used to assess sensitivity of phylogenetic results to alignments. The aligned sequences were downloaded as FASTA files from MAFFT, opened in Mesquite to visually recheck the alignments, then saved as Nexus files. During this step, eleven *Aphytis melinus* sequences and 21 *Nasonia vitripennis* sequences were observed to have major alignment problems and were thus removed. The genes that had outgroup removal were then realigned, and the outgroup sequences were treated as missing. The 110 Nexus files were then consolidated into one interleaved Nexus file for phylogenetic analyses.

Phylogenetic Analyses

Maximum parsimony analyses were performed in PAUP* GUI version 4.0a147 (Swofford 2003) using a branch and bound search. Data from each iterative refinement method (L-INS-i, E-INS-i, G-INS-i) were run separately. For each analysis, node support was calculated using nonparametric bootstrap with 1000 replicates. Bremer support was calculated for clades A-E (Fig. 1).

The maximum parsimony analyses indicated that the E-INS-i alignment produced data with more phylogentic signal (higher retention index (RI)) and less homoplasy (higher consistency index (CI)) than the other alignments (L-INS-i or G-INS-i). The E-INS-i aligned data set was thus utilized or subsequent maximum likelihood analysis. PartitionFinder (Lanfear et al. 2012) was used to estimate an optimal set of models of molecular evolution across the 110 genes.

PartitionFinder sorted the 110 genes into 13 partitions, of which nine used the JTT substitution matrix (Appendix B). I ran maximum likelihood analyses using both the partitioned data and unpartitioned data. The maximum likelihood analyses were performed in RAxML 8.2.8 (Stamatakis 2014) on the CIPRES server (https://www.phylo.org). Node support was calculated using bootstrap with 1000 replicates.

Results

Maximum Parsimony

The same tree topology (Fig. 1) was recovered using data from all three types of iterative refinement methods. The following relationships were found: *A. perpallidus* is basal and the sister taxon to all other *Aphelinus* species; *A. abdominalis* and *A. asychis* are sister groups and together form the sister taxon to all remaining *Aphelinus*; the *mali* group and *A*. nr. *daucicola* were obtained as a monophyletic group, with *A.* nr. *daucicola* sister the sister taxon to the three *mali* group species; the *mali* + *A.* nr. *daucicola* clade forms the sister taxon to the *varipes* group; all seven species from the *varipes* species group were obtained as a monophyletic group.

All nodes except three had bootstrap values of 100 (Table 5). These nodes are designated with asterisks in Figure 1. Bremer support values for clades A-E (Fig. 1) are reported in Table 6.

Table 5: Bootstrap values for Figure 1 nodes that had values less than 100 in each type of alignment method for maximum parsimony analyses.

Alignment method	*mali*+*daucicola* node	*mali* node	*hordei*+*kudjumovi* node
L-INS-i	59.85	90.40	97.55
G-INS-i	69.62	90.55	99.48
E-INS-i	55.78	90.97	98.70

Table 6: Bremer support values for corresponding clades in Figure 1 for each type of alignment method for maximum parsimony analyses.

Alignment method	Clade (Fig. 1)				
	A	**B**	**C**	**D**	**E**
L-INS-i	587	459	16	3	229
G-INS-i	579	455	15	8	227
E-INS-i	585	462	17	2	236

Branch lengths from the maximum parsimony analysis calculated using MINF optimization in PAUP* give the numbers of unambiguous amino acid substitutions supporting each node. The branch lengths found on the maximum parsimony tree using MINF optimization for each iterative refinement method are reported in Table 7. The corresponding branch numbers are illustrated in Figure 2.

Table 7: Maximum parsimony tree (Fig. 2) branch lengths using different alignment methods.

Branch #	E-ins-i	L-ins-i	G-ins-i	Branch #	E-ins-i	L-ins-i	G-ins-i
1	207	214	192	**16**	349	330	353
2	1798	1793	1797	**17**	209	231	327
3	9892	10016	10044	**18**	530	526	526
4	10099	10230	10236	**19**	139	130	125
5	371	364	359	**20**	218	218	635
6	2276	2275	2321	**21**	349	376	391
7	885	859	886	**22**	162	155	145
8	1307	1304	1287	**23**	139	130	141
9	1483	1469	1663	**24**	103	106	101
10	2055	2063	2074	**25**	96	93	97
11	247	253	253	**26**	110	133	155
12	134	131	138	**27**	63	71	70
13	820	835	966	**28**	104	99	220
14	626	616	614	**29**	234	293	402
15	974	954	990	**30**	141	139	215

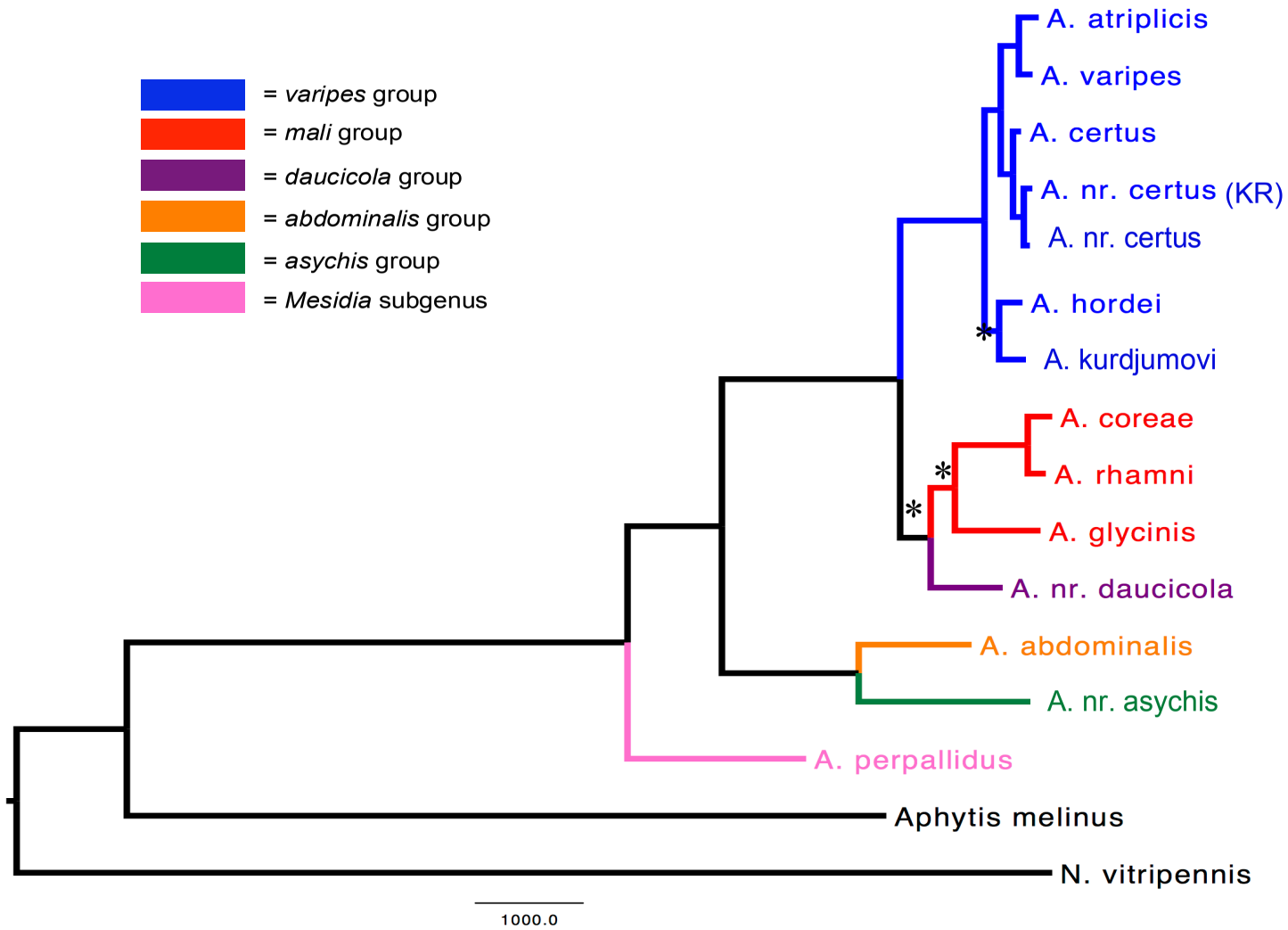

Figure 1: The most parsimonious tree found by maximum parsimony analysis using data from the E-INS-i alignment. Nodes that have bootstrap values less than 100 are asterisked, the values of which can be found in Table 5. Bremer support values for A-E are reported in Table 6.

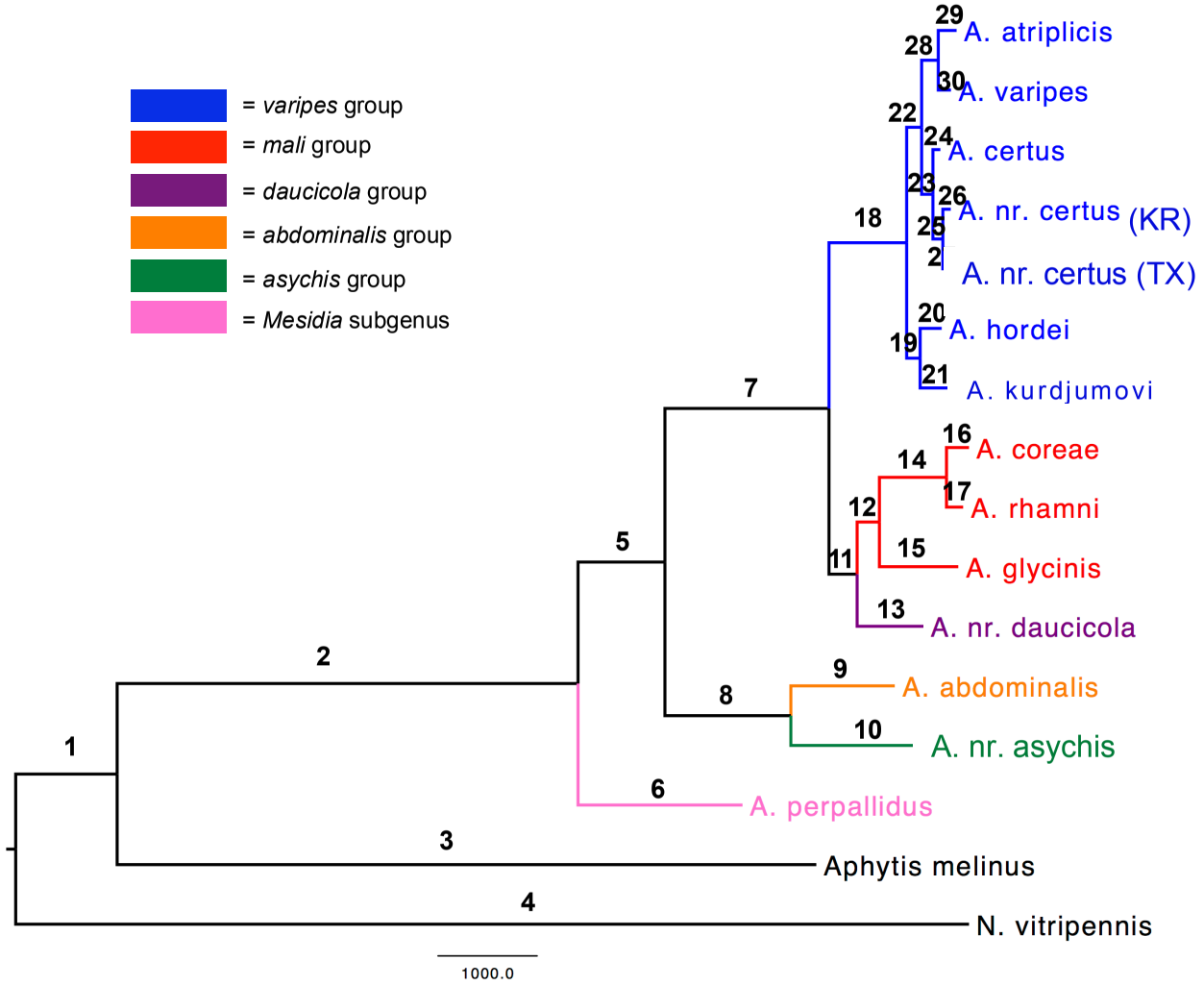

Figure 2: The most parsimonious tree found by the maximum parsimony analysis using data from the E-INS-i alignment method with branch numbers labeled. Branch length values are shown in Table 7.

For testing evolutionary relationships, characters that are homologous are required. With homologous characters, better inferences can be made because these characters are similar in different species because they were inherited from a common ancestor. This is in contrast to homoplastic characters in which similarities are not derived from a common ancestor. The consistency index (CI) is a measure of homoplasy (Florey et al. 1992). A CI of 1 means the dataset has zero homoplasy and the characters are perfectly homologous. The CI of the three alignment datasets ranged from 0.9204 – 0.9232 (Table 8). The CI without autapomorphies ranged from 0.7975 – 0.8015. The retention index (RI), a measure of phylogenetic signal or amount of similarity actually used as synapomorphies (Florey et al. 1992), ranged from 0.7789 – 0.7915.

As all three types of iterative alignment methods yielded the same tree topology, the best-scoring method (highest CI with and without autapomorphies and highest RI) which was E-INS-i, was used for maximum likelihood analyses.

Table 8: Tree statistics for maximum parsimony analyses using different alignment methods. The tree topology recovered was identical for each alignment method.

Alignment method	Length of dataset	Parsimony informative characters	Tree length	Autapomorphies	RI	CI	CI without autapomorphies
E-ins-i	62141	6726	36100	16800	0.7915	0.9232	0.8015
L-ins-i	62029	6685	36388	16879	0.7864	0.9218	0.7975
G-ins-i	61864	6904	37707	16990	0.7789	0.9204	0.8004

Maximum Likelihood

The same topology was recovered in the partitioned and the unpartitioned maximum likelihood analyses. The maximum parsimony (Fig. 2) and maximum likelihood (Fig. 3) trees show the same relationships, except for the position of *A.* nr. *daucicola.* In the maximum parsimony analysis, *A.* nr. *daucicola* came out within the *mali* group. In the maximum likelihood analysis, *A.* nr. *daucicola* formed the sister taxon to the *mali* + *varipes* clade. On trees formed using both analytical techniques, nodes involving the position of *A.* nr. *daucicola* have the lowest bootstrap support on the trees. Maximum likelihood nodes that have bootstrap values less than 100 are asterisked in Figure 3 and their values are reported in Table 9.

Table 9: Bootstrap values for Figure 3 nodes that have values less than 100.

Dataset	***mali* node**	***mali* + *varipes* node**	***hordei* + *kurdjumovi* node**
partitioned	65	61	100
unpartitioned	68	58	95

Discussion

The molecular phylogenetic hypotheses resulting from both the maximum parsimony and maximum likelihood analyses indicate the monophyly of the included species of *Aphelinus*. These results are congruent with the findings of prior research (Campbell et al., 2000; Kim and Heraty 2012; Munro et al., 2011; Heraty et al., 2007; Heraty et al., 2013). However, taxon sampling remains incomplete. Current taxon sampling is ~15% of species from the genus. Material from the remaining two *Aphelinus* subgenera,

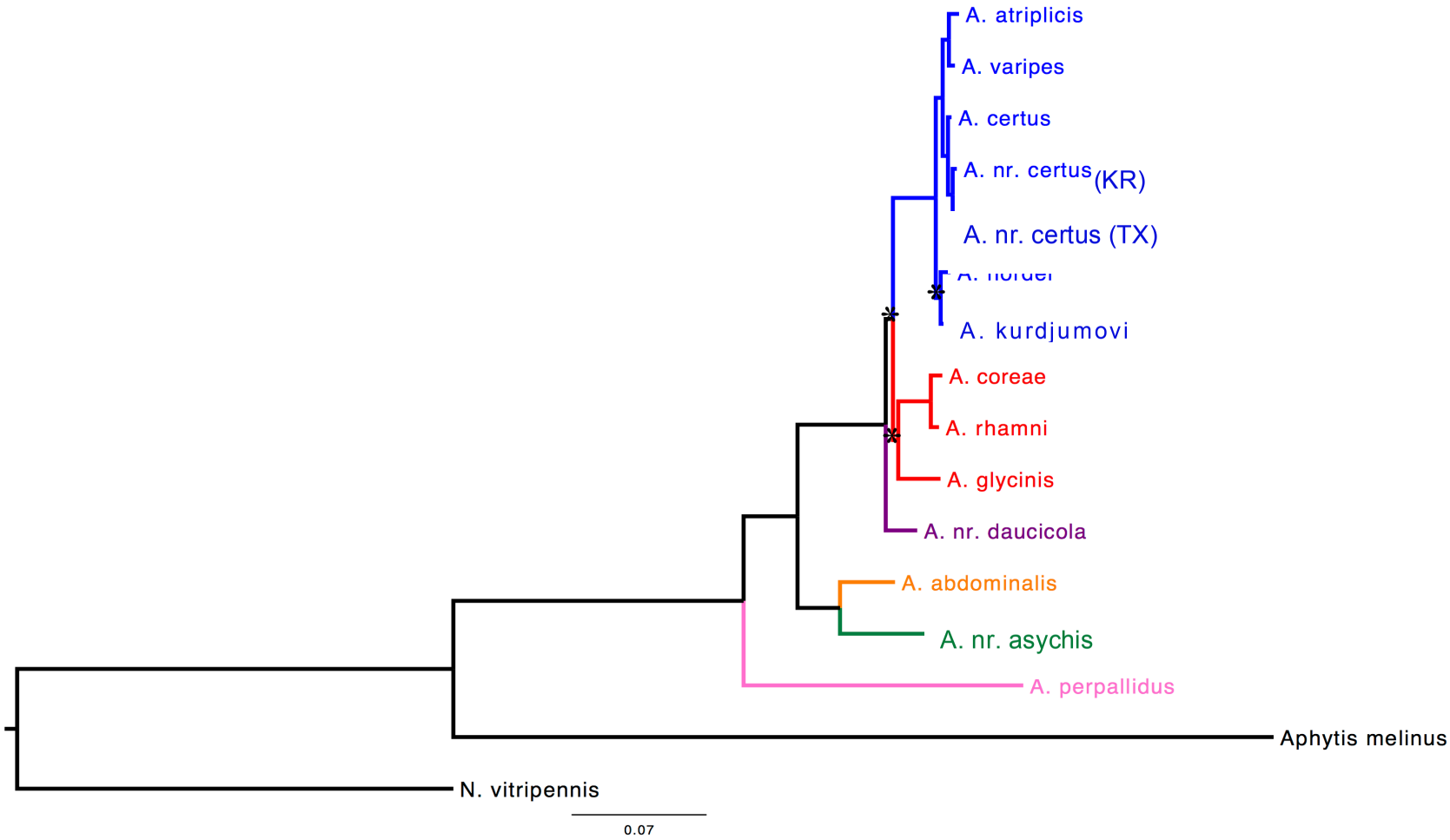

Figure 3: The tree found by maximum likelihood analysis using data from the E-INS-i alignment. The nodes that have bootstrap values less than 100 are denoted with asterisks and the values are reported in Table 9.

Indaphelinus and *Paulianaphelinus,* have yet to be included. Additional work should also include additional non-*Aphelinus* taxa.

Species Groups

The species groups that were originally defined using morphology were also recovered here using molecular data. In both the maximum parsimony and maximum likelihood analyses, all *varipes* group species clustered in one clade. The relationships of the *varipes* group are similar to those reported in Heraty et al. (2007) in that *A. atriplicis* and *A. varipes* are obtained as each other's closest relatives. Also, the *A. certus* clade was found to be sister to the *atriplicis* + *varipes* clade. However, Heraty et al. (2007) obtained *A. kurdjumovi* as the sister taxon to the remainder of the *varipes* group, with *A. hordei* as sister taxon to the remaining *varipes* species, whereas in this study *A. kurdjumovi* and *A. hordei* together form a clade sister group to the rest of the *varipes* group.

In Heraty et al. (2007), *A. mali* and the representative from the *daucicola* group (at that time referred to as nr. *mali* group) form a clade sister group to the *varipes* group. My current study supports *mali* group as sister to the *varipes* group, but the placement of the *daucicola* group representative differs. In my maximum likelihood analysis, all *mali* group species form a clade, and *A*. nr. *daucicola* was recovered as the sister taxon to the *mali* + *varipes* clade. In my maximum parsimony analysis, *A.* nr. *daucicola* is sister to the *mali* group clade. The *A.* nr. *daucicola* + *mali* group clade is sister group to the *varipes* group. However, the placement of nr. *daucicola* had low support values in both

maximum parsimony and maximum likelihood analyses. In Heraty et al. (2007), the *mali* + *daucicola* clade also had low support (bootstrap = 79).

Basal Aphelinus *Taxa Relationships*

Aphelinus asychis has unique courtship behavior, oviposition behavior, and sexual dimorphism of antennal segment proportions, differing from other *Aphelinus* species. In past work (Heraty et al. 2007), and in my preliminary work, *A. asychis* was recovered as sister taxon to other analyzed *Aphelinus*. When data for *A. abdominalis* was included, it was interesting to that *A. abdominalis* formed a clade with *A. asychis*. Morphological similarities between these two species groups are explored in Chapter IV.

The subgenus *Mesidia* has often been treated as a separate genus (Mackauer 1972), so it was not surprising that *A. perpallidus*, a representative of *Mesidia*, was obtained as the sister taxon to all other members of *Aphelinus* included for analysis.

Conclusions

These phylogenetic analyses help lay a preliminary phylogenetic framework for the classification of *Aphelinus*. I found (1) that *A. perpallidus* is sister taxon to all other included *Aphelinus* species (supporting its differentiation at subgenus rank) (2) that *A. abdominalis* and *A. asychis* are members of a clade that is sister group to other included *Aphelinus* sp.; (3) that the *varipes* and *mali* groups are monophyletic (but the latter is weakly supported in maximum likelihood analysis); and (4) that the placement of *A.* nr. *daucicola* is unstable.

To further develop this phylogenetic framework, future work should broaden in taxon sampling, particularly by including more representatives from the *daucicola*,

abdominalis, asychis, and *nepalensis* species groups of subgenus *Aphelinus*; additional taxa from subgenus *Mesidia*; and further outgroups.

CHAPTER III

SURVEY OF GLANDULAR RELEASE AND SPREAD STRUCTURES ON THE MALE SCAPE OF *APHELINUS* DALMAN, 1820 (HYMENOPTERA: APHELINIDAE)

Introduction

Successful mating relies on discriminating conspecific from heterospecific individuals. Intraspecific communication with sex-attractant or identifying pheromones is often a key component in the quest for locating mates. It has been observed in parasitic Hymenoptera that once putative conspecific females and males have located each other, complex antennal waving and subsequent antennal contact is carried out by the male (Dahms 1973; Goodpasture 1975; Gordh and DeBach 1978). In these studies, antennal contact by the male on the female, hereafter referred to as antennation, generally occurs after both parties have assumed a courtship position. Courtship position refers to the posture in which the female has become motionless, the male has mounted the female, both members are facing the same way, and the male's head is parallel above the female's head.

Dahms (1973), observing *Melittobia* (Chalcidoidea: Eulophidae), was among the first to report male antennation during activities undertaken in the courtship position. Goodpasture (1975) observed antennation by males in four species of *Monodontomerus* (Chalcidoidea: Torymidae) during courtship position activities. Gordh and DeBach (1978) observed antennation of the male while in the courtship position in *Aphytis*

lingnanensis (Chalcidoidea: Aphelinidae). Van den Assem et al. (1980) showed that antennal contact between the male and female through the process of antennation is important in courtship in several species of Pteromalidae and Eulophidae (both Chalcidoidea). These courtship behavior studies triggered investigations into the morphology and histology of antennal structure related to antennation behaviors.

History of Antennation Histology Research in Parasitic Hymenoptera

Dahms (1973) observed antennation prior to copulation. Dahms (1984a) presented scanning electron microscopy (SEM) evidence for the existence of a dermal gland opening on the ventral surface of the male scape in the same *Melittobia* species. He proposed that this structure served as a secretion release site, which played a vital role in chemical communication during courtship in *Melittobia* rather than being a sensory structure. These findings triggered immense curiosity across the field of parasitoid Hymenoptera, and subsequent researchers used both SEM and transmission electron microscopy (TEM) to examine modified structures on the ventral portion of the male antennae across the parasitic Hymenoptera. Later work, described below, investigated whether or not these ventral areas, which were previously thought to be sensory in function, were also in fact secretion release sites for glandular complexes. The corpus of these works helps assess how widespread the secretory function of male antennomeres is in relation to antennation during courtship, and how diverse the modified structures can be in parasitic Hymenoptera.

Non-Chalcidoid Hymenoptera

Using SEM, Bin and Vinson (1986) found a prominent projection on the ventral side of the fifth antennomere (third funicular segment) of *Trissolcus basalis* (Platygastroidea: Scelionidae) males. Using TEM, they reported that this ventral projection is used for releasing and spreading a secretion produced by a glandular complex consisting of bicellular secretory units with type III secretory cells (as characterized by Noirot and Quennedey (1974)) located inside the fifth antennomere. They reported that this structure could be similar to the dermal gland from Dahms' (1984a) work.

Isidoro and Bin (1995) found an elevated plate with numerous pores on the ventral side of the fourth antennomere of *Amitus spiniferus* (Platygastroidea: Platygastridae). The site was observed as empty in one specimen and in another specimen it was filled with a secretion "similar to squeezed toothpaste". This plate was interpreted as a site that released and spread a recognition pheromone during courtship antennation. Isidoro et al. (1996) suggested that the phrase "release and spread area" be used to refer to this antennal region, and that the phrase "release and spread structure" (hereafter RSS) be used for the suite of modified structures involved with releasing the products of the glandular complex during courtship antennation. Longitudinal and transverse sections of the plate revealed a glandular complex consisting of bicellular secretory units with type III secretory cells.

Isidoro et al. (1999) looked at a variety of species of Cynipidae and Figitidae (Cynipoidea) and found various morphological modifications (e.g., hollowed out

regions, raised plates, tyloid-like structures) on the ventral side of either the third, or the third and fourth male antennomeres. Using TEM, they found that these modified structures possess pores that connect to an internal glandular complex consisting of bicellular secretory units with type III secretory cells, and they reported these as RSS modifications.

Sacchetti et al. (1999) found a carina with numerous pores on the ventral side of the fourth antennomere (second funicular segment) of male *Trichopria drosophilae* (Proctotrupoidea: Diapriidae). This structure is considered the RSS with a glandular complex consisting of bicellular secretory units composed of type III secretory cells. Romani et al. (2008) based their work on the foundation of Sacchetti et al. (1999). They wanted to confirm that the RSS and glandular system found in the 1999 work was necessary for successful courtship and copulation. To test this, glue was used to cover the fourth antennomere of the male. This prevented transfer of any substance from the antennal gland to the female. No copulation occurred in any of the trials involving glue-covered RSS, whereas 100% successful mating occurred in trials without glue covering the gland. These results suggested that the RSS is the source of important mate recognition pheromones that are transmitted from males to females during courtship. They went on to investigate whether the glandular secretions only worked with antennal contact, or if short-range volatiles were also involved. To test this, the male's left antenna and the female's right antenna was cut off so that no antennal contact would occur between the male and female during courtship. In trials where the contralateral antennae were ablated, no mating occurred. However when the ipsilateral antennae were

ablated, or neither side ablated, 100% successful mating occurred, suggesting that physical antennal contact is necessary during courtship for successful copulation.

Male *Pimpla turionellae* (Ichneumonoidae: Ichneumonidae) possess tyloids with numerous pores on the ventral side of the 8th and 9th antennomeres (Bin et al. 1999). Using TEM, they identified this as the RSS for a glandular complex consisting of bicellular secretory units composed of type III secretory cells. A courtship behavior study further demonstrated that males perform antennation in courtship position, with the tyloids coming into direct contact with the female's antennae. Glue trials, in which the 8th and 9th male antennomeres were covered with glue, demonstrated that physical antennal contact was also necessary for successful mate acceptance and copulation in this species.

Non-Aphelinid Chalcidoid Families

Amornsak et al. (1998) looked at antennal morphology in males and females of *Trichogramma australicum* (Chalcidoidea: Trichogrammatidae). They found strong sexual dimorphism, in which males had an abundant number of pores distributed across the club that were not found on females and were thus hypothesized to have a male-specific function important in courtship. Courtship behavior studies to test for the occurrence of antennation, and TEM work to assess gland type, are needed to further understand the system operating in *T. australicum*.

Guerrieri et al. (2001) investigated the male antennae of *Leptomastix dactylopii*, *Rhopus meridionalis*, and *Asitus phragmitis* (all Chalcicoidea: Encyrtidae). Males of *Leptomastix dactylopii* were shown to have a single row of 8-12 separate raised

structures, each with three uniform apical teeth, on the ventral side of the ultimate 9th antennomere. Males of *Rhopus meridionalis* were shown to have similar structures, but they consisted of a single row of 4-8 separate raised structures, each with three non-uniform apical teeth (middle tooth twice as long as lateral teeth), and were located on the ventral area of the penultimate 8th antennomere. Males of *Asitus phragmitis* were shown to have a depressed region with a single row of 4-7 peg-like structures that were all pointed distally, and were located on the ultimate 9th antennomere. Each of these regions was reported as the RSS for its species with the glandular complexes consisting of unicellular secretory units with type I secretory cells.

Aphelinidae

Using SEM, Pedata and Isidoro (1993) found pores on modified structures on the ventral areas of the fourth and fifth antennomeres (second and third funicular segments) of male *Encarsia asterobemisiae* (Chalcidoidea: Aphelinidae). TEM work confirmed the presence of two glandular complexes, one in the fourth antennomere and one in the fifth, both consisting of unicellular secretory units with type I secretory cells. Male courtship antennation has been observed in this species and the structures on both antennomeres are hypothesized to function as RSS. These authors mention the presence of similar structures in *Encarsia aurantii* and *Encarsia opulenta*, which may prove to be glandular, rather than sensory as previously though.

Gordh and DeBach (1978) reported antennation by *Aphytis melinus* (Chalcidoidea: Aphelinidae) males while in the courtship position. Romani et al. (1999) performed an ultrastructural investigation of the male antennae of *A. melinus* and found

a depressed oval area with numerous setae on the ventral area of the ultimate 6th antennomere. With TEM, they demonstrated that rather than being sensory in function, this was actually the RSS, with glandular complexes consisting of unicellular secretory units with type I secretory cells. They noted that the RSS of *A. melinus* differs from other RSS' reported in Hymenoptera in that the pores are so small that the external openings are not visible with SEM.

In summary, the body of work reviewed above shows that many structures on the ventral area of the male antennae that were once thought to be sensory are actually glandular, and serve as RSS during courtship antennation. The detailed morphological structure of RSS, and their antennomere location differs greatly among taxa. The type of secretory cells in the glandular complexes also vary, with those in the Chalcidoidea being type I, and those outside the Chalcidoidea being type III. Experimental studies of courtship behavior have demonstrated that contact between the products of the RSS and the female antennae are required in mediating courtship and for successful copulation.

To date there have been no detailed published investigations of potential RSS morphologies in *Aphelinus*.

Antennal Sex Gland Work in Aphelinus

Courtship behavior studies recently undertaken at the University of Delaware have shown that male antennation occurs during courtship in all nine species of *Aphelinus* examined (Rhoades 2015). These nine species represent three *Aphelinus* species groups: *varipes*, *mali*, and *daucicola*.

Unpublished research by collaborators (Fernando Bin and associates, Univ. Perugia, Italy) demonstrated that there are modified structures on the ventral area of the scape within the *Aphelinus varipes* species group. TEM work showed the presence of a glandular complex, suggesting that these structures on the scape are the RSS.

Species in the *asychis* group also use wing fanning in addition to antennation during courtship behavior (personal communication from Keith Hopper). During observation of *Aphelinus* specimens using light microscopy, it was noted that the arrangement and shape of the modified male scape structures differs among species groups. While the *varipes* and *mali* groups had prominently raised structures, raised structures appeared absent in the *asychis* group.

A survey of the modified structures on the male scape in *Aphelinus* using SEM was needed to better understand their diversity across the genus, and whether or not they are taxonomically informative.

Research Objectives

1. Survey and compare the modified structures found on the ventral area of the male scape in several different *Aphelinus* species groups.
2. Confirm or refute the absence of these structures on the scapes of males in the *asychis* species group.

Materials and Methods

Specimen Preparation

High quality *Aphelinus* material in alcohol from the TAMU Insect Collection was used. Eight species collected in six countries and in six species groups were studied (Table

10). All specimens were critical point dried (CPD) using a Tousimis Samdri-790, following factory protocols given by Tousimis Research Corporation. After CPD, two males from each collecting event were mounted using black carbon tape onto standard 12.7mm Ted Pella pin stubs. All specimens were gold sputter-coated using a Technics (Anatech Ltd) Hummer I, following factory protocol. Gold was sputtered on specimens for a total of five minutes, in one minute intervals separated by one minute "rests". Due to time and resource constraints, only two male specimens from each collecting event were examined. All antennomeres on both the left and the right antennae were examined in each specimen.

Table 10: *Aphelinus* taxa used in survey of structures on male scape

Subgenus	Species group	Species	Origin
Aphelinus	*abdominalis*	*abdominalis*	Netherlands
Aphelinus	*asychis*	*asychis*	China
Aphelinus	*asychis*	*asychis*	France
Aphelinus	*daucicola*	nr. *daucicola*	USA
Aphelinus	*mali*	*coreae*	Korea
Aphelinus	*varipes*	*albipodus*	Japan
Aphelinus	*varipes*	*varipes*	USA
Mesidia	none	nr. *perpallidus*	USA

Microscopy

SEM images were acquired using a Tescan Vega 3 microscope. All images were acquired using secondary electron emission in high vacuums with beam acceleration voltages ranging from 15 kV to 30 kV. The beam intensity used was either 3 or 5 and the scan speed was either 6 or 7. Image acquisition details and scale bars are given in the legend for each image.

Results

Substantial variation was found in the morphological structures of the male scape in the species examined (Figs. 4 and 5). The most notable observations are as follows.

Pores of presumed secretory function are present on the scapes of members of the *asychis* species group (Figs. 4B, 4C); these were previously thought to be absent. Pores in the *asychis* group males are more or less sessile, not raised above surface of surrounding cuticle, and are arranged in a line on a rounded carina that is not bordered by or set within an adjacent depression.

In non-*asychis* group males, the pore line is surrounded by a depression, and individual pores are located on distinctly raised areas. Among species with pores on distinctly raised areas, the raised form varied from truncated pedicels (Figs. 4D, 5A, 5B, 5C), rounded pedicels (Fig. 4A), or a crenulate ridge (5D).

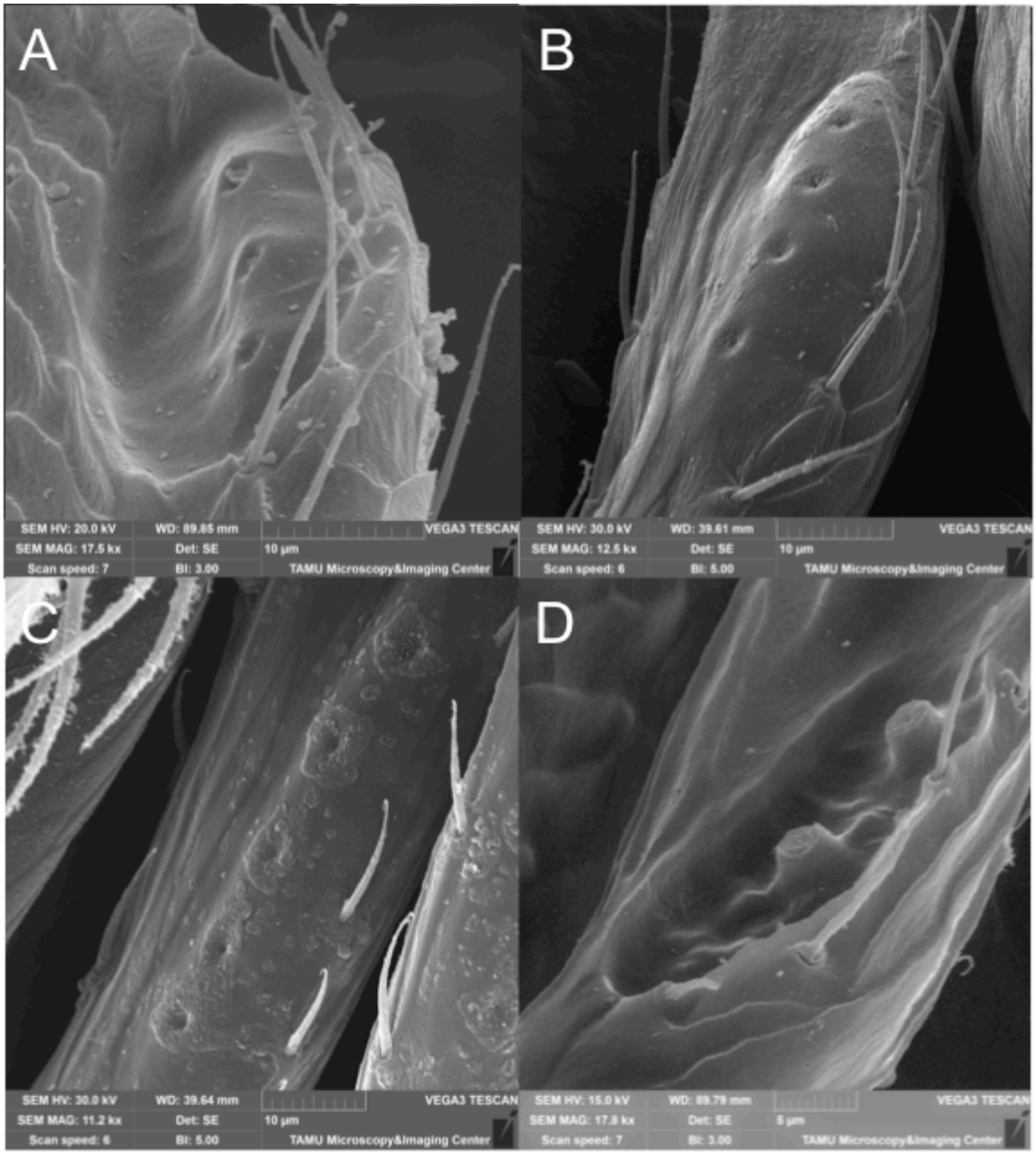

Figure 4: SEM images of the ventral surfaces of male *Aphelinus* scapes **A**: *A. abdominalis*; **B**: *A. asychis* (China); **C**: *A. asychis* (France); **D**: *A. coreae*

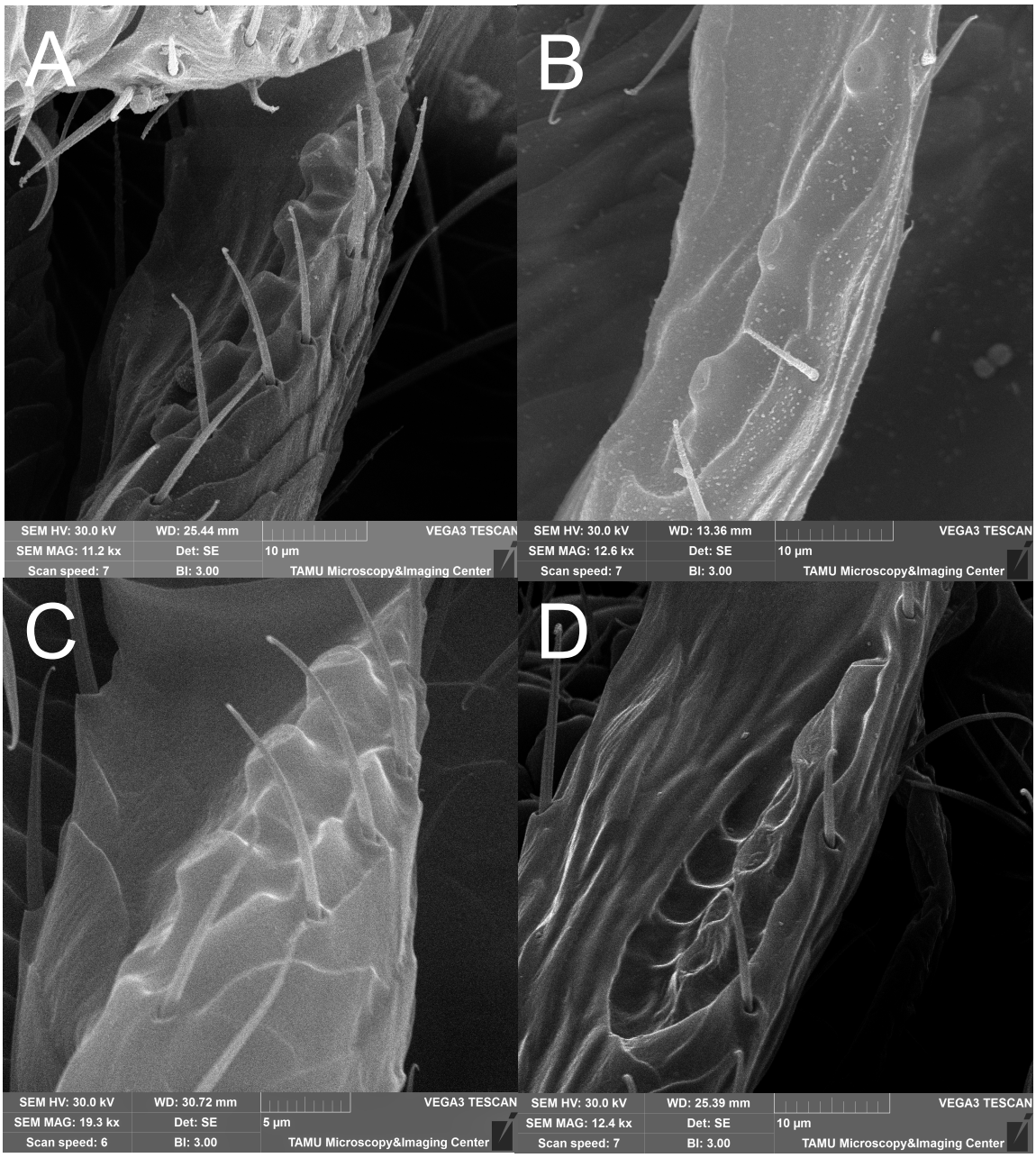

Figure 5: SEM images of the ventral surfaces of male *Aphelinus* scapes: **A**: *A.* nr. *daucicola*; **B**: *A. varipes*; **C**: *A. albipodus*; **D**: *A.* (*Mesidia*) nr. *perpallidus*

From the results of this study, several characters were added to my character matrix in mx for character coding. As discussed in Chapter IV, my intent was not to use morphological characters as primary data to infer common ancestry, but rather to explore the evolution of these characters in a phylogenetic context. The evolution of these characters and inferences about character state homology will be addressed in Chapter IV.

The new characters are as follows:

1: Number of gland pores on male scape. State 0: 0 pores. **State 1**: 1 pore. **State 2**: 2 pores. **State 3**: 3 pores. **State 4**: 4 pores. **State 5**: 5 pores. **State 6**: >5 pores.

2: Conformation of cuticle surrounding gland pore on male scape. State 0: no gland pores present. **State 1**: pore openings not raised above surface of surrounding cuticle (Figs. 4B, C). **State 2**: pore openings located on distinctly raised areas, truncated and flat on top (Figs. 4D, 5A, 5B, 5C). **State 3**: pore openings located on distinctly raised areas, rounded on top (Fig. 4A). **State 4**: pore openings located in recessed area along distinctly raised, crenulate ridge (Fig. 5D).

3: Location of gland pores on male scape. State 0: no gland pores present. **State 1**: most proximal gland in basal third of scape. **State 2**: most proximal gland in apical third of scape. **State 3**: most proximal gland in middle third of scape.

4: Carina delimitation around gland pores on male scape. State 0: no gland pores present. **State 1**: carina completely surrounds pores. **State 2**: carina at proximal end of pores only. **State 3**: no carina around pores. The carina represents the lateral edges of

recessed area surrounding pores. The delimitation of the carina is most easily visible in slide mounts (Fig. 11).

Discussion

Species Groups

Through the literature review, it is clear that the antennomere on which gland pores are found varies considerably within the parasitic Hymenoptera. The SEM results here suggest that the gland pores in *Aphelinus* occurs only on the first antennomere (scape). However, variation of the conformation of the cuticle surrounding the gland pores across taxa surveyed was detected. This preliminary survey of the *Aphelinus* gland pores indicates that, taken together, these modified structures on the male scape could be diagnostic for the species groups of *Aphelinus*. Dahms (1984b) also found that these modified structures on the ventral area of the scape could be a useful taxonomic tool and utilized it in a revision of the genus *Melittobia*.

Aphelinus asychis *Species Group*

Males in the *asychis* group wing-fan as well as antennate. Given the less conspicuous pores on their antennae, it was initially thought that males in the *asychis* group do not have pores. Therefore, the confirmation of the presence of pores on members of *asychis* group is very interesting. Dahms (1984a) compared his work on *Melittobia* with van den Assem et al.'s (1982) work on *Melittobia* and noted with interest that antennation and morphology of the modified structures on the ventral area of the male scapes varied between the *Melittobia* species groups. The species group that did not have extensively modified structures on the males' scapes did not incorporate antennation as strongly into

its courtship behaviors as the species groups that had more prominently modified male scapes. Perhaps we are seeing a similar trend in *Aphelinus*, where the less modified male scapes of the *asychis* group do not play the same role that the more highly modified male scapes do in other species groups of *Aphelinus*. Additional work on courtship behavior needs to be done with the *asychis* species group, together with TEM work to confirm that the observed pores are connected to an internal glandular system.

Conclusion

This study serves as a first step in understanding the interesting and modified structures on *Aphelinus* male scapes. From this, we can begin to understand mate selection strategies in this group, as well as add to the knowledge base of sex glands in parasitic Hymenoptera. In addition to sexual selection and taxonomy, morphologically distinctive components of the male scape suggest that they may also be useful for phylogenetic inferences within *Aphelinus*, and may have broad phylogenetic signal across the genus. This will be discussed further in Chapter IV.

Future TEM work is needed to investigate whether or not the glandular complex in *Aphelinus* is consistent with the type I secretory cells documented in other chalcidoid taxa.

CHAPTER IV

EVOLUTION OF MORPHOLOGICAL CHARACTERS IN *APHELINUS* DALMAN, 1820 (HYMENOPTERA: APHELINIDAE)

Introduction

In an age of growing popularity of molecular work in systematics studies, it is important to note the unique value that morphological data can provide to the field of systematics. One benefit of morphology in systematic studies is that it allows the inclusion of fossils. Molecular data is unattainable for vast majority of fossils, so morphology is essential in inferring phylogenies that include fossil taxa and understanding their relationships with extant taxa and ancestral character states (Smith 1998; Wiens 2000). In addition to investigating evolutionary histories, the field of systematics provides scientific names and identification keys for organisms (Michener 1970). Traditional taxonomy is the part of systematics concerned with these topics, and morphology is the fundamental connection between the two. Not only does morphology help researchers understand what makes species different, but also facilitates in understanding what allows them to survive in their niche (Ferry-Graham et al. 2002). Observing specialization of morphological forms and investigating functional morphology has become important in understanding ecological interactions, which in turn can strengthen systematic studies. Morphological and molecular approaches both provide valuable information to systematics studies and a coordinated effort between the two is necessary to make real progress in assessing Earth's biodiversity (Wiens 2000).

In this study, the intent was not to use morphological characters as primary data to infer common ancestry, but rather to explore the evolution of these characters in *Aphelinus* in a phylogenetic context. This can be achieved with character state mapping, also known as character optimization or character tracing, where character states are optimized onto a phylogeny. I chose to use the molecular phylogeny derived from massive amounts of amino acid data from Chapter II as a robust framework to explore morphological evolution in *Aphelinus*. Thus, homology of shared character states or homoplastic similarities in morphological characters could be inferred.

Due to the use of the phylogeny derived from Chapter II, the series of specimens that were coded for morphology in this chapter were limited to the taxa used in Chapter II. Thus the results and discussion of the evolution of morphological characters in this chapter are based upon that specific set of taxa.

Terminology for Characters

Because of the enormous diversity of Hymenoptera, different terms have been used to describe the same structure, or the same term has been used to describe different structures. This problem is most acute when a single term is used to describe different non-homologous structures. The Hymenoptera Anatomy Ontology project (Yoder et al. 2010) is an ongoing effort to catalog and standardize the terminology used to describe morphological structures across the Hymenoptera. Gibson et al. (1997; 1998) are additional resources for terminology used for Chalcidoidea morphology.

Heraty et al. (2013) was one outcome of a collaboration by much of the world community of chalcidoid taxonomists to develop a set of phylogenetically informative

morphological characters across Chalcidoidea. They followed Gibson et al.'s (1997) terminology with additional terms for head characters from Kim and Heraty (2012). Heraty et al. (2013) vetted their terminology with the HOA for consistency. To continue this practice of providing consistent terminology, Appendix C lists the morphological terms used in this chapter, followed by a definition and a URI (uniform resource identifier) that links to more information on that character in the Hymenoptera Anatomy Ontology project's database.

Choice of Characters

Morphological characters of *Aphelinus* have been thoroughly discussed by Hayat (1972; 1983; 1998), Graham (1976), Hennessey (1981a; 1981b), and Ferrière (1965). Several characters from these works have been suggested for use in distinguishing subgenera of *Aphelinus* (overall body color, size comparisons of F1-3, length of ovipositor compared to mid-tibia) and for distinguishing species groups (number of setae on the submarginal vein, arrangement of setae in the interspace between the basal cell and the linea calva, arrangement of setae in the costal cell).

Wing characters have traditionally been very important in the taxonomy of *Aphelinus*. Graham (1976) noted key differences in wing setation among the British species of *Aphelinus*. Hennessey (1981b) studied the patterns of these setae and discussed their function in at-rest wing coupling. He proposed that the arrangement of setae bordering the linea calva engages the retinaculum on the opposite forewing and is responsible for holding the forewings in a fixed position during non-flight. This forewing restraint could be a means of keeping the wings from being contaminated by

honeydew produced by their host, as of the 18 chalcidoid families studied, forewing restraint mechanisms are most common in Aphelinidae and Encyrtidae, most species of which parasitize honeydew-producing Hemipterans.

Hennessey (1981a) went on to survey the setal patterns to discuss their taxonomic importance. He surveyed the forewings of 13 species in the subgenera *Aphelinus* and *Mesidia* and discussed setal patterns and standardized nomenclature for wing regions. Arrangement of setae in the costal cell, number of setae in the basal cell, number of setae proximad to the linea calva, and presence/absence of setae at the posterior end of the linea calva were reported to be taxonomically important in *Aphelinus*, following and expanding on Graham (1976). Hayat (1972; 1983; 1998) expanded on these works and added two additional important taxonomic wing characters: number of setae on the submarginal vein and how the setae are arranged proximad to the linea calva.

The list of morphological characters used in this chapter was initially based on the works discussed above. I then added several morphological characters (four characters based on the gland pores of the male scape and six characters based on male genitalia) based on my own study of *Aphelinus* specimens. A total of 37 characters were studied, as described in the methods section below. This chapter expands on previous morphological work done with *Aphelinus*, with the following objectives:

Research Objectives

1. Investigate traditional morphological characters and discover new morphological characters to help with diagnoses of taxa within *Aphelinus.*
2. Examine morphological characters in the context of a robust molecular phylogeny to better understand the evolutionary relationships among species groups and the evolutionary history of morphological characters.

Materials and Methods

Specimens

Specimens were stored in 95% ethanol in freezers. Most were then critical point dried using a Samdri 790 CPD unit. Critical-point-dried specimens were then card mounted with Franklin International's water soluble Titebond Liquid Hide Glue. Selected specimens were slide mounted following Noyes (1982) protocol. All card-mounts and slide-mounted specimens were assigned individual barcoded accession numbers (e.g., TAMUIC X0852885, USNM ENT 4532898, etc.).

Due to the use of the molecular phylogeny as the framework for this study, taxon sampling was limited to the taxa used in Chapter II (Table 11). Although *Nasonia vitripennis* was used as an outgroup for the molecular phylogeny, due to its relatively remote relationship to *Aphelinus, N. vitripennis* could not be scored for most of the morphological characters. I therefore omitted *N. vitripennis* from these comparisons.

Table 11: *Aphelinus* taxa examined for study of morphological evolution.

Ingroup/Outgroup	Subgenus in *Aphelinus*	Species group in *Aphelinus*	Taxon	Source
Ingroups	*Aphelinus*	*asychis*	*Aphelinus* nr. *asychis*	China, Harbin
	Aphelinus	*mali*	*Aphelinus coreae*	Korea
			Aphelinus glycinis	China, Xiuyan
			Aphelinus rhamni	China, Beijing
	Aphelinus	*daucicola*	*Aphelinus* nr. *daucicola*	USA, Delaware
	Aphelinus	*varipes*	*Aphelinus atriplicis*	Rep. of Georgia
			Aphelinus certus	Japan
			Aphelinus hordei	France
			Aphelinus kurdjumovi	Rep. of Georgia
			Aphelinus varipes	France
			Aphelinus nr. *certus*	USA, Texas
			Aphelinus nr. *certus*	Korea
	Aphelinus	*abdominalis*	*Aphelinus abdominalis*	Syngenta
	Mesidia	unplaced	*Aphelinus perpallidus*	Texas, USA
Outgroup	n/a	n/a	*Aphytis melinus*	California, USA

Data Management

Label data from borrowed material was first captured in a local Microsoft Excel spreadsheet. Label data from specimens belonging to the TAMU Insect Collection were barcoded and databased in the TAMUIC database. All label data from both borrowed and local material was uploaded to the mx database. OTU's were created for each species. A character matrix was created in mx and all morphological coding was done within mx.

Morphological Character Set

1: Forewing, basal cell, number of setae. State 0: more than 10. **State 1**: 6-10. **State 2**: less than 6. The basal cell in this character refers to the most proximal area of the forewing, not including the setae directly proximad to the linea calva (Fig. 6; bc).

2: Forewing, basal cell/linea calva interspace, number of setae. State 0: more than 60 setae. **State 1**: between 30 and 60 setae. **State 2**: less than 30 setae. This character refers

to the number of setae on the proximal side of the linea calva, excluding the basal cell area (Fig. 6; lc).

3: Forewing, basal cell/linea calva interspace, arrangement of setae. State 0: 1 complete line of setae (extending from marginal vein to posterior edge of wing) and 1 or 2 incomplete lines of setae (terminating before posterior edge of wing). **State 1**: setae arranged in 2 complete lines and 2-3 incomplete lines. **State 2**: one complete line of setae and a few setae in angle between this line and marginal vein. **State 3**: more than two complete lines of setae.

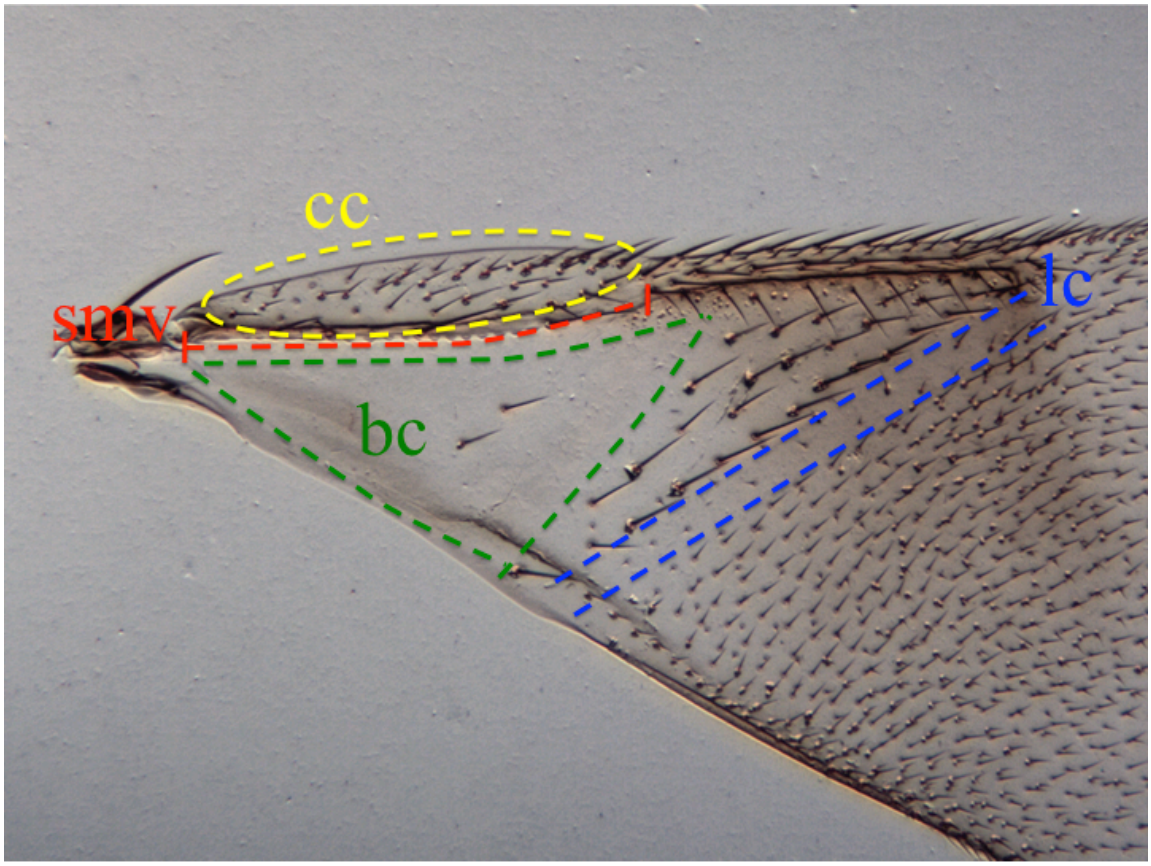

Figure 6: *Aphelinus* forewing, base, dorsal view. Abbreviations: cc = costal cell; smv = submarginal vein; bc = basal cell; lc = linea calva

4: Forewing, submarginal vein, number of setae (Fig. 6, smv). State 0: two setae. **State 1**: more than two setae. This character has been used to identify members of the *asychis* species group (Hayat 1998). Only species within the *asychis* group have only two setae on the submarginal vein; all other *Aphelinus* species have more than two setae.

5: Forewing, ventral surface of costal cell, number of setae (Fig. 6, cc). **State 0**: one line of setae. **State 1**: two or more lines of setae. **State 2**: setae not arranged in lines.

6: Forewing, linea calva. State 0: completely closed by a line of setae on dorsal surface running parallel to posterior wing margin (Fig. 7A). **State 1**: open posteriorly (Fig. 7B). **State 2**: partly closed by one or two setae (Fig. 7C).

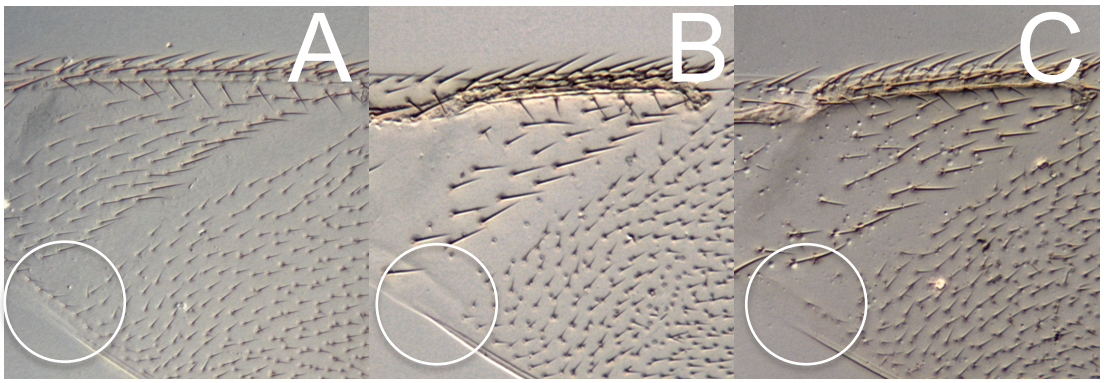

Figure 7: *Aphelinus* forewings, bases**,** dorsal view. A: linea calva completely closed by line of setae; B: linea calva open; C: linea calva partly closed by one or two setae.

7: Forewing, brachyptery. State 0: no brachypterous specimens known. **State 1**: brachypterous and non-brachypterous specimens known. **State 2**: all specimens brachypterous.

8: Forewing, color. State 0: forewing hyaline or subhyaline. **State 1**: forewing distinctly infuscated.

9: Shape of F1 in female (Fig. 8). State 0: wider than long. **State 1**: subquadrate. **State 2**: 1.2-2.0x longer than wide. **State 3**: more than 2.0x longer than wide.

10: Shape of F2 in female (Fig. 8). State 0: wider than long. **State 1**: subquadrate. **State 2**: 1.2-2.0x longer than wide. **State 3**: more than 2.0x longer than wide.

11: Shape of F3 in female (Fig. 8). **State 0**: wider than long. **State 1**: subquadrate. **State 2**: 1.2-2.0x longer than wide. **State 3**: more than 2.0x longer than wide.

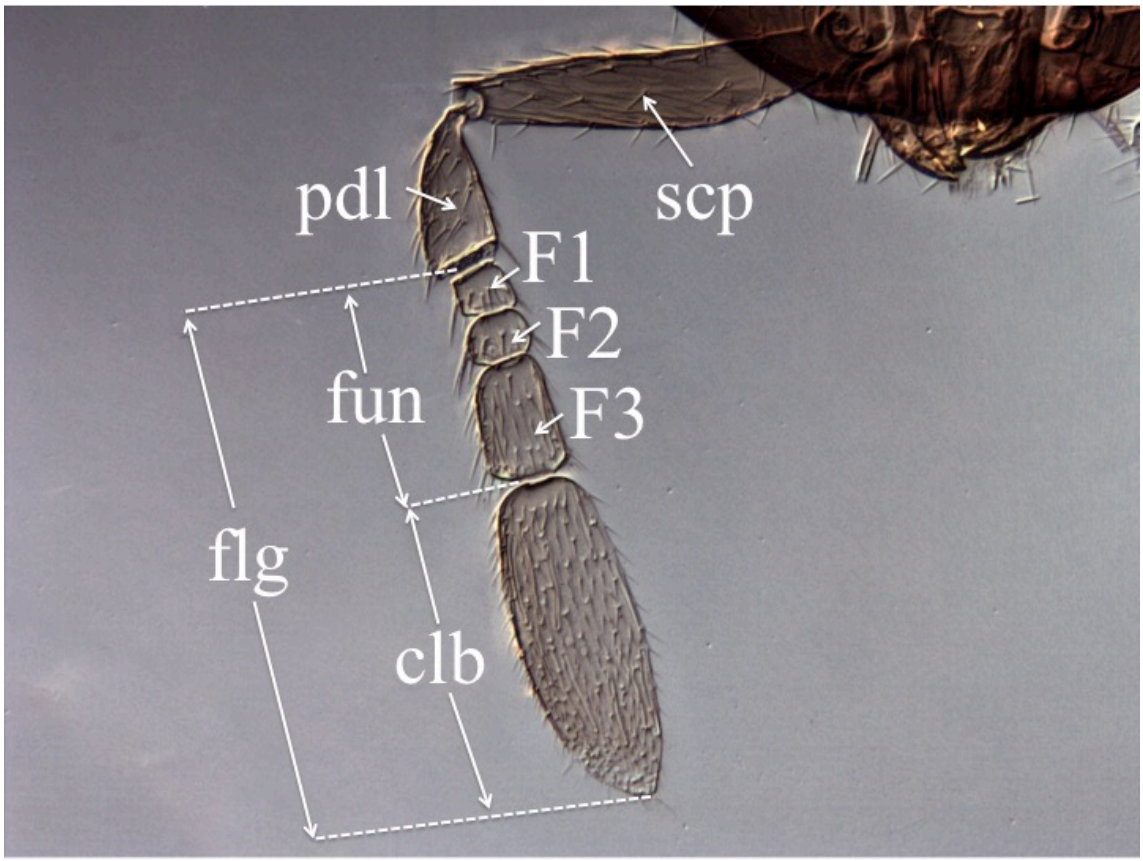

Figure 8: *Aphelinus* antenna, lateral view. Abbreviations: scp = scape; pdl = pedicel; flg = flagellum; fun = funicle; F1 = funicle segment 1; F2 = funicle segment 2; F3 = funicle segment 3; clb = club

12: Relative length of female F1 and F2. State 0: F1 shorter than F2. **State 1**: F1 and F2 subequal. **State 2**: F1 longer than F2.

13: Relative length of female F2 and F3. State 0: F2 shorter than F3. **State 1**: F2 and F3 subequal. **State 2**: F2 longer than F3.

14: Funicle segments 1-3 in female. State 0: one or more segments not longer than wide. **State 1**: all segments longer than wide, usually length at least 1.25x width.

15: Antennae color in female. State 0: all segments dark brown or black. **State 1**: all segments tan or yellowish-brown. **State 2**: all segments white, yellow, or pale. **State 3**: F1-F3 and club contrastingly lighter than pedicel and scape.

16: Club shape in female (Fig. 8). State 0: less than 2.0x longer than wide. **State 1**: between 2.0-3.0x longer than wide. **State 2**: more than 3.0x longer than wide.

17: Head color. State 0: head largely yellow. **State 1**: head largely yellow with occiput brown. **State 2**: head dark brown to black. **State 3**: head mostly brown or black, face yellow.

18: Mesosoma color. State 0: mesosoma >50% yellow to white. **State 1**: mesosoma <50% yellow.

19: Ovipositor length (Fig. 9). State 0: shorter than mesotibia. **State 1**: subequal to mesotibia length. **State 2**: 1-1.5x length of mesotibia. **State 3**: >1.5x length of mesotibia.

20: Shape of F1 in male. State 0: wider than long. **State 1**: subquadrate. **State 2**: 1.2-2.0x longer than wide. **State 3**: more than 2.0x longer than wide.

21: Shape of F2 in male. State 0: wider than long. **State 1**: subquadrate. **State 2**: 1.2-2.0x longer than wide. **State 3**: more than 2.0x longer than wide.

22: Shape of F3 in male. State 0: wider than long. **State 1**: subquadrate. **State 2**: 1.2-2.0x longer than wide. **State 3**: more than 2.0x longer than wide.

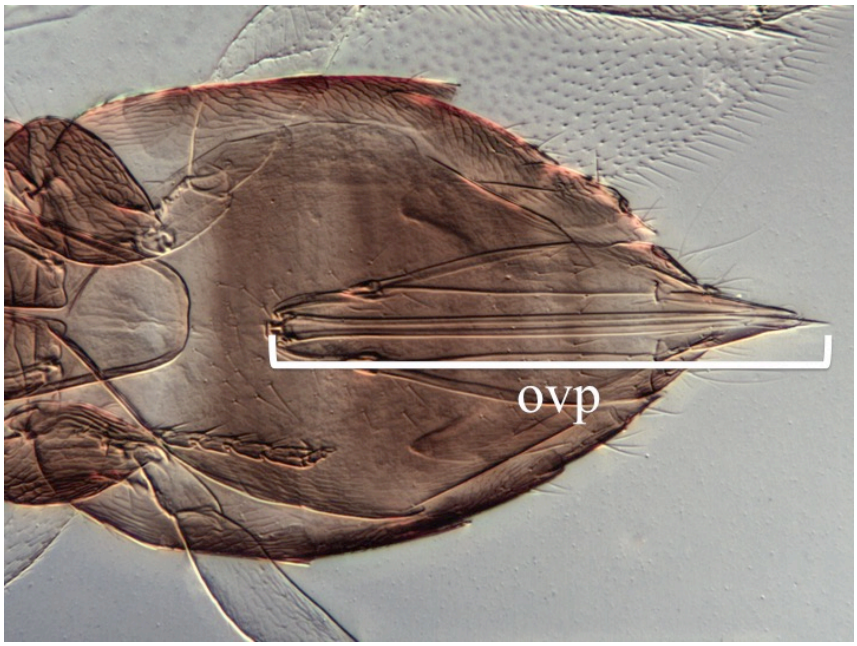

Figure 9: *Aphelinus* female, metasoma, ventral view. Abbreviation: ovp = length of ovipositor

23: Relative length of male F1 and F2. State 0: F1 shorter than F2. **State 1**: F1 and F2 equal. **State 2**: F1 longer than F2.

24: Relative length of male F2 and F3. State 0: F2 shorter than F3. **State 1**: F2 and F3 equal. **State 2**: F2 longer than F3.

25: Funicle segments 1-3 in male. State 0: one or more segments not longer than wide. **State 1**: all segments longer than wide, usually length at least 1.25x width.

26: Antennae color in male. State 0: all segments dark brown or black. **State 1**: all segments tan or yellowish-brown. **State 2**: all segments white, yellow, or pale. **State 3**:

F1-F3 and club contrastingly lighter than pedicel and scape. **State 4:** pedicel, F1-F3, and club contrastingly lighter than scape.

27: Club shape in male. State 0: less than 2.0x longer than wide. **State 1**: between 2.0-3.0x longer than wide. **State 2**: more than 3.0x longer than wide.

28: Number of gland pores on male scape. State 0: 0 pores. **State 1**: 1 pore. **State 2**: 2 pores. **State 3**: 3 pores. **State 4**: 4 pores. **State 5**: 5 pores. **State 6**: >5 pores.

29: Conformation of cuticle surrounding gland pore on male scape. State 0: no gland pores present. **State 1**: pore openings not raised above surface of surrounding cuticle (Fig. 10A). **State 2**: pore openings located on distinctly raised areas, truncated (Fig. 10D). **State 3**: pore openings located on distinctly raised areas, rounded on top (Fig. 10C). **State 4**: pore openings located in recessed area along distinctly raised, crenulate ridge (Fig. 10B).

30: Location of gland pores on male scape. State 0: no gland pores present. **State 1**: most proximal gland in basal third of scape. **State 2**: most proximal gland in apical third of scape. **State 3**: most proximal gland in middle third of scape.

31: Carina delimitation around gland pores on male scape. State 0: no gland pores present. **State 1**: carina completely surrounds pores (Fig. 11A). **State 2**: carina at proximal end of pores only (Fig. 11B). **State 3**: no carina around pores (Fig. 11C).

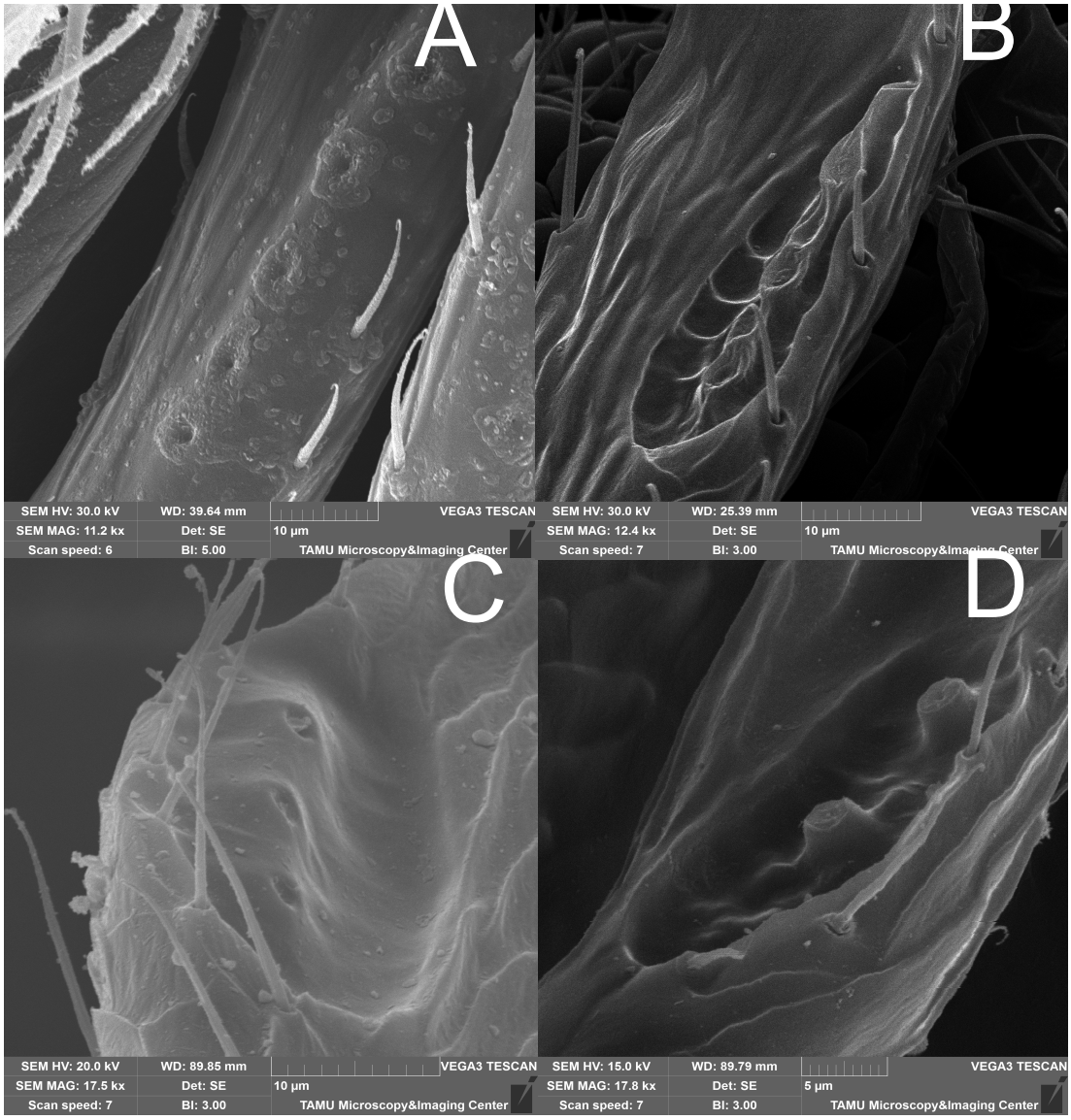

Figure 10: *Aphelinus* male scapes, ventral view. A = not raised, opening on continuous convex ridge; B = high points on continuous ridge; C = raised, conical, rounded on top; D = raised, conical, flat on top.

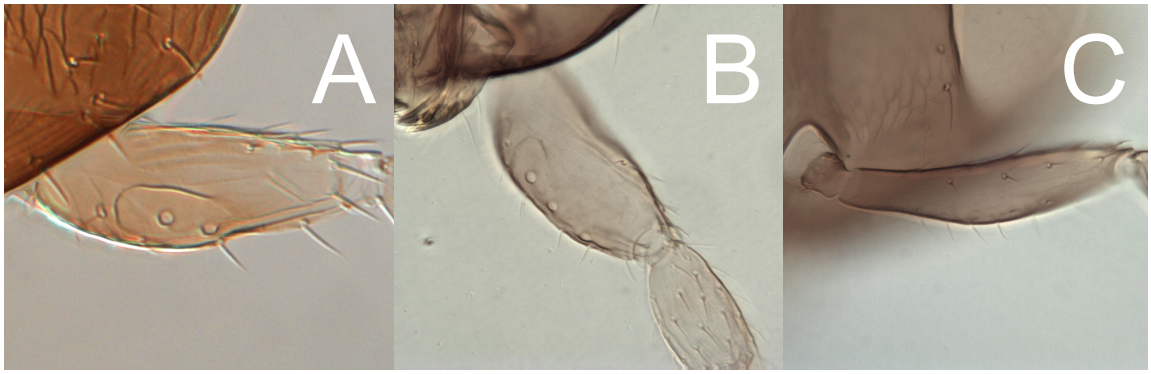

Figure 11: States of carina on *Aphelinus* male scapes, lateroventral view. A = pores completely surrounded by carina (due to image stacking carina not as visible on right side as it is in actuality); B = carina at proximal end of pores only; C = no carina around pores

32: Phallobase length (Fig. 14). State 0: anterior end in basal third. **State 1**: anterior end far in distal third of metasoma. **State 2**: anterior end in middle third of metasoma.

33: Phallobase shape. State 0: more or less an oval. **State 1**: lyre-shaped, narrowing in anterior third and then widening again.

34: Posterior-most sternum in male, internal surfaces (Fig. 12). State 0: without internal, longitudinal sclerotized surfaces (Fig. 12A). **State 1**: with internal, longitudinal sclerotized surfaces (Fig. 12B).

35: Posterior-most sternum in male (Fig. 13). State 0: posterior margin more or less transverse. **State 1**: posterior margin somewhat emarginate, at midline emargination about 1/3 to 1/2 length of sclerotized folds on either side (Fig. 13A). **State 2**: posterior margin strongly emarginate, at midline emargination 2/3 length of lateral sclerotized folds, or more (Fig. 13B).

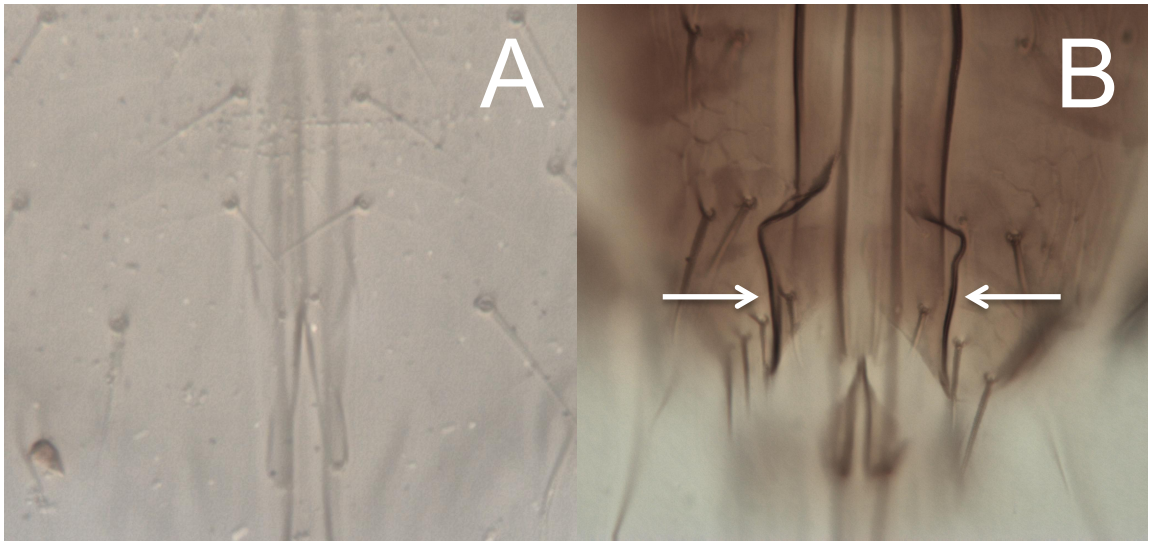

Figure 12: *Aphelinus* male sterna, ventral view. A: without internal, longitudinal sclerotized surfaces; B: with internal, longitudinal sclerotized surfaces (see arrows).

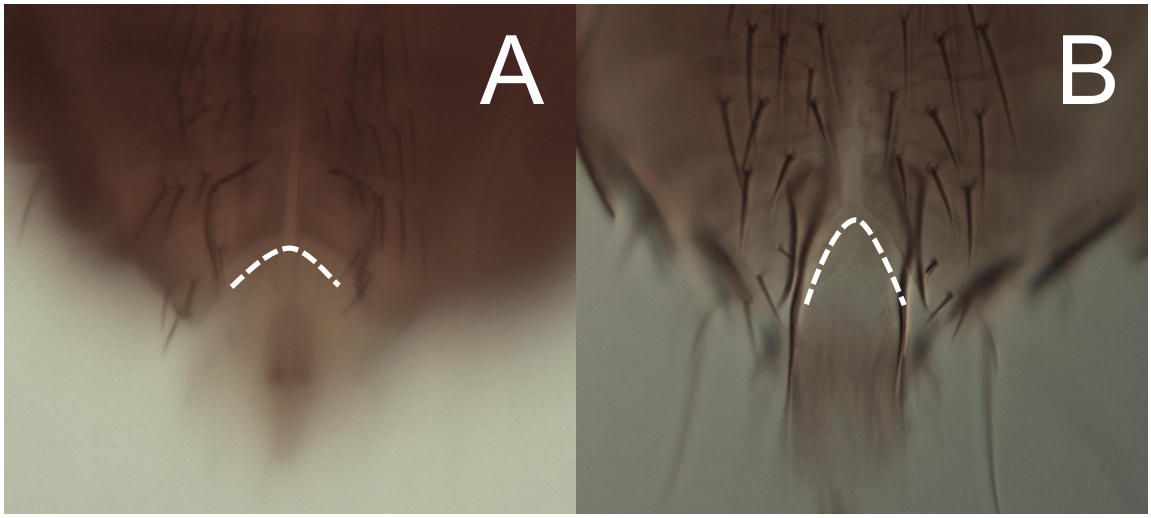

Figure 13: *Aphelinus* male sterna, ventral view. A: somewhat emarginate; B: strongly emarginate.

36: Digiti length (Fig. 14, dig). State 0: long, length >3x width. **State 1**: intermediate, length about 2x width. **State 2**: short, about 1x width.

37: Digiti, number of apical denticles (Fig. 14, dnt). State 0: one. **State 1**: two. **State 2**: three.

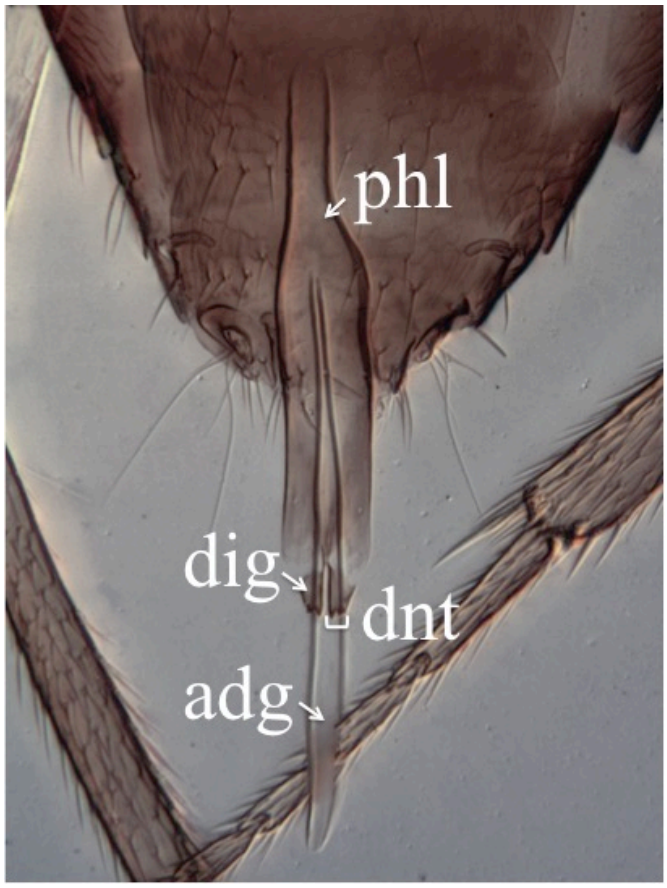

Figure 14: *Aphelinus* male genitalia, ventral view. Abbreviations: phl = phallobase; dig = digiti; dnt = denticles, adg = aedeagus.

Character Analysis

The above characters were coded in mx across all 14 sequenced species of *Aphelinus* and the outgroup *Aphytis melinus*. The results were exported as a Nexus file and opened in PAUP*. The tree file from the maximum likelihood analysis with E-INS-i alignment was opened and linked to the above Nexus file in PAUP*. Character diagnostics (CI and RI) were calculated for each character. The Nexus file and tree file were then opened and linked in Mesquite. The Trace Character History with Parsimony Ancestral States tool was used to provide most parsimonious reconstructions of character state changes.

Results

The CI and RI values calculated by PAUP* are reported in Table 12. Five characters (8, 13, 14, 24, 25) are constant, and the CI and R.I values are thus reported as n/a. 37 trees (one tree per character) were visualized in Mesquite, and those that had an RI >0.667 are shown (Figs. 15 – 20, 22 – 24). One character with CI=1, RI=0/0 (Fig. 21) is also shown and later discussed.

Table 12: CI and RI values calculated in PAUP* for each morphological character.

Character #	Character	CI	RI
1	Forewing, basal cell, number of setae	1	0/0
2	Forewing, basal cell/linea calva interspace, number of setae	0.667	0.667
3	Forewing, basal cell/linea calva interspace, arrangement of setae	0.75	0.8
4	Forewing, submarginal vein, number of setae	0.5	0
5	Forewing, ventral surface of costal cell, number of setae	1	1
6	Forewing, linea calva	0.333	0.5
7	Brachyptery	1	0/0
8	Forewing, color	n/a	n/a
9	Shape of F1 in female	0.5	0.5
10	Shape of F2 in female	0.5	0.5
11	Shape of F3 in female	0.333	0
12	Relative size of F1 compared to F2 in female	1	0/0
13	Relative size of F2 compared to F3 in female	n/a	n/a
14	Funicle segments 1-3 in female	n/a	n/a
15	Antennae color in female	1	0/0
16	Club shape in female	0.333	0.333
17	Head color	1	1
18	Mesosoma color	1	1
19	Ovipositor length	0.667	0
20	Shape of F1 in male	1	1
21	Shape of F2 in male	0.5	0.5
22	Shape of F3 in male	0.667	0
23	Relative size of F1 compared to F2 in male	1	0/0
24	Relative size of F2 compared to F3 in male	n/a	n/a
25	Funicle segments 1-3 in male	n/a	n/a
26	Antennae color in male	0.6	0.6
27	Club shape in male	0.333	0
28	Number of gland pores on male scape	0.8	0
29	Conformation of cuticle surrounding gland pore on male scape	1	0/0
30	Location of gland pores on male scape	1	0/0
31	Carina delimitation around gland pores on male scape	1	1
32	Phallobase Length	0.333	0
33	Phallobase shape	0.25	0.4
34	Posterior-most sternum in male, internal surfaces	1	1
35	Posterior-most sternum in male	0.667	0
36	Digiti length	1	1
37	Digiti, number of apical denticles	1	0/0

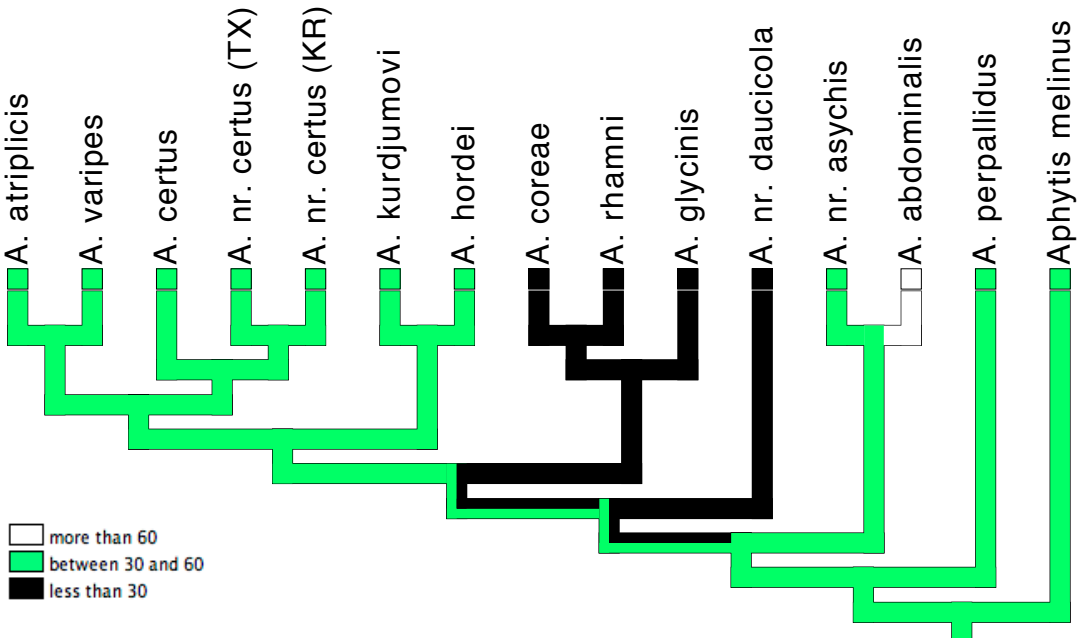

Figure 15: Character 2: forewing, basal cell/linea calva interspace, number of setae. CI=0.667, RI=0.667.

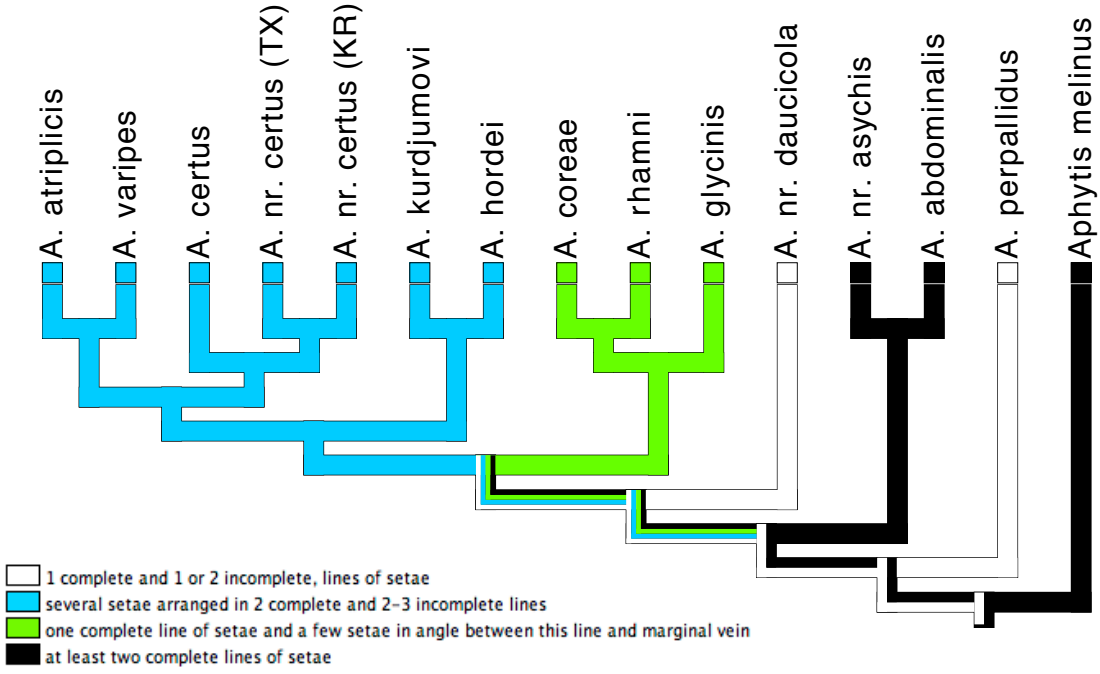

Figure 16: Character 3: forewing, basal cell/linea calva interspace, arrangement of setae. CI=0.75, RI=0.8.

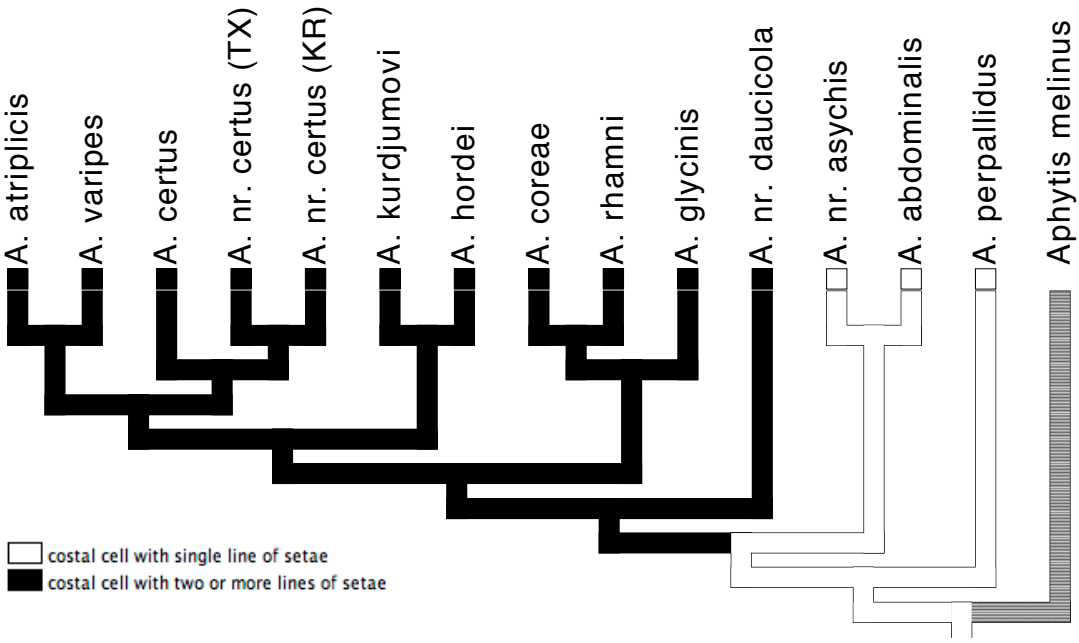

Figure 17: Character 5: Forewing, ventral surface of costal cell, number of setae. CI=1, RI=1.

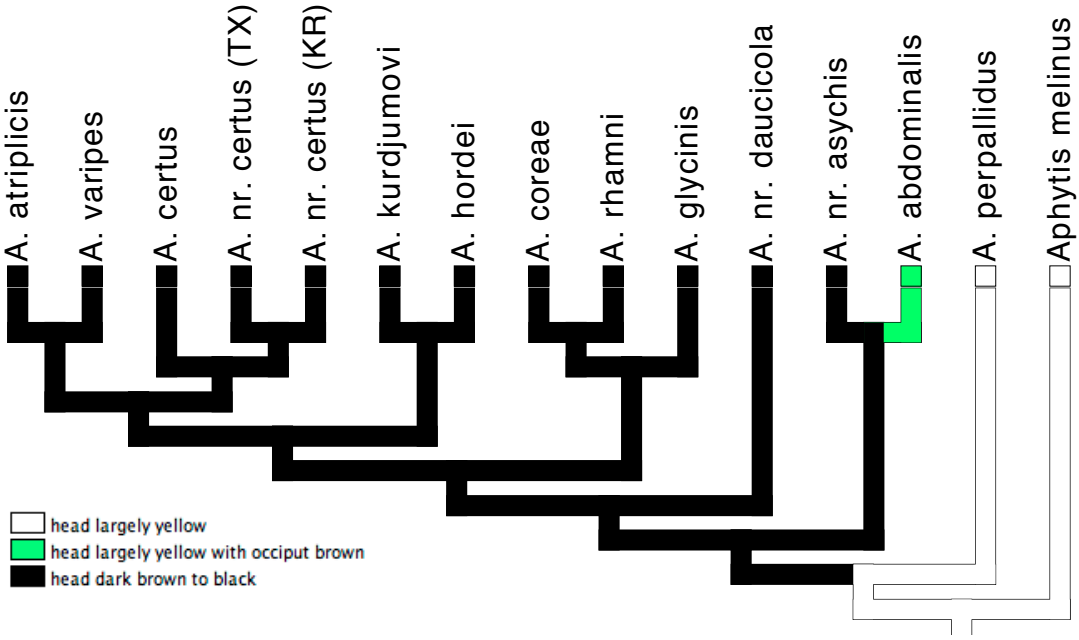

Figure 18: Character 17: Head color. CI=1, RI=1.

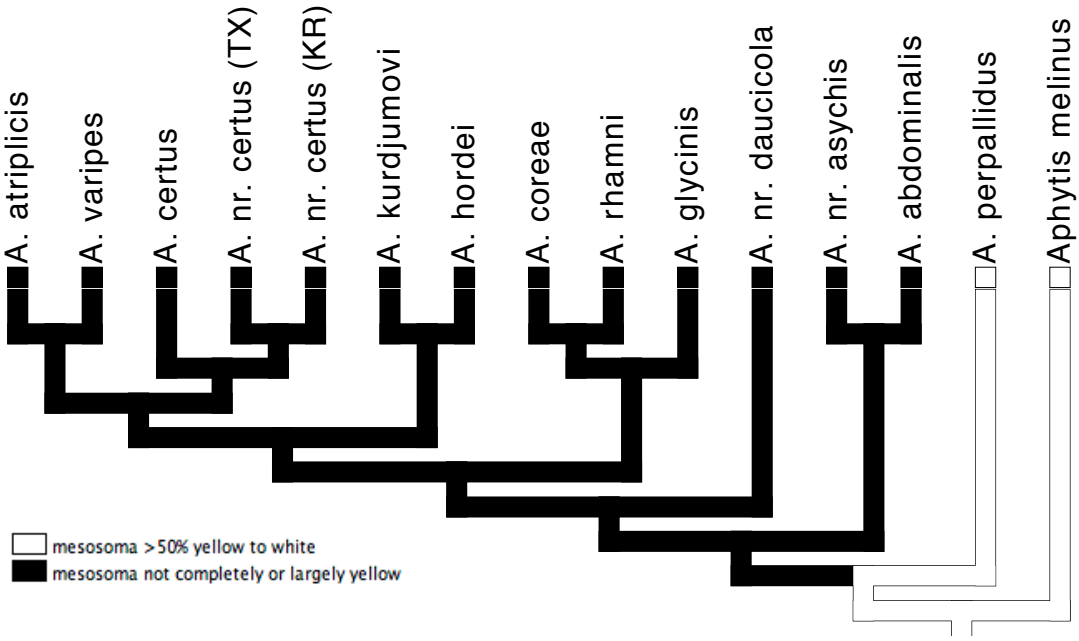

Figure 19: Character 18: Mesosoma color. CI=1, RI=1.

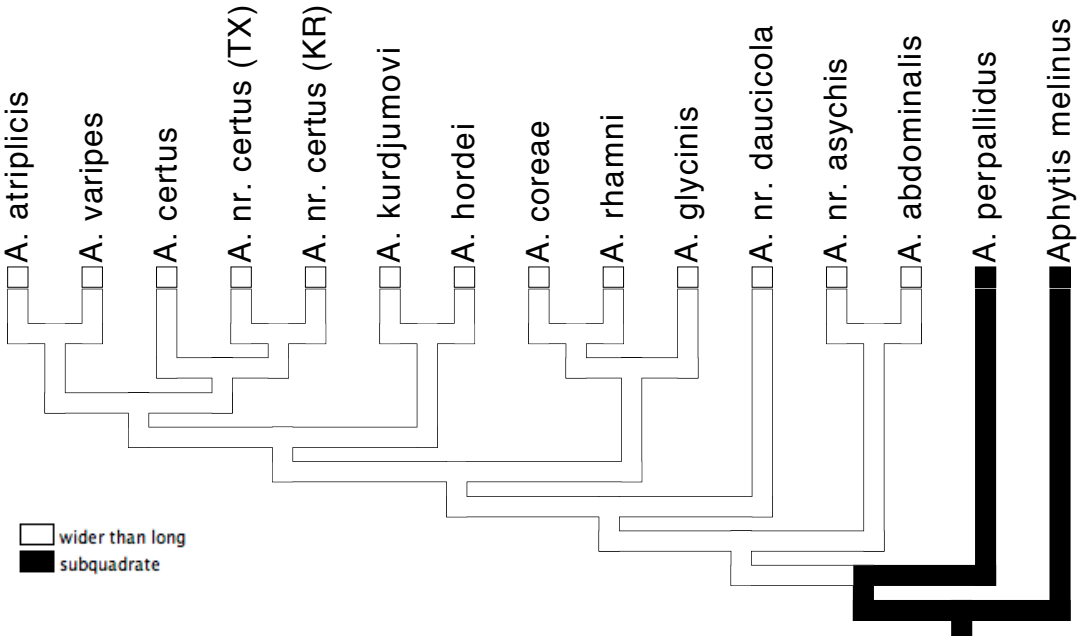

Figure 20: Character 20: Shape of F1 in male. CI=1, RI=1.

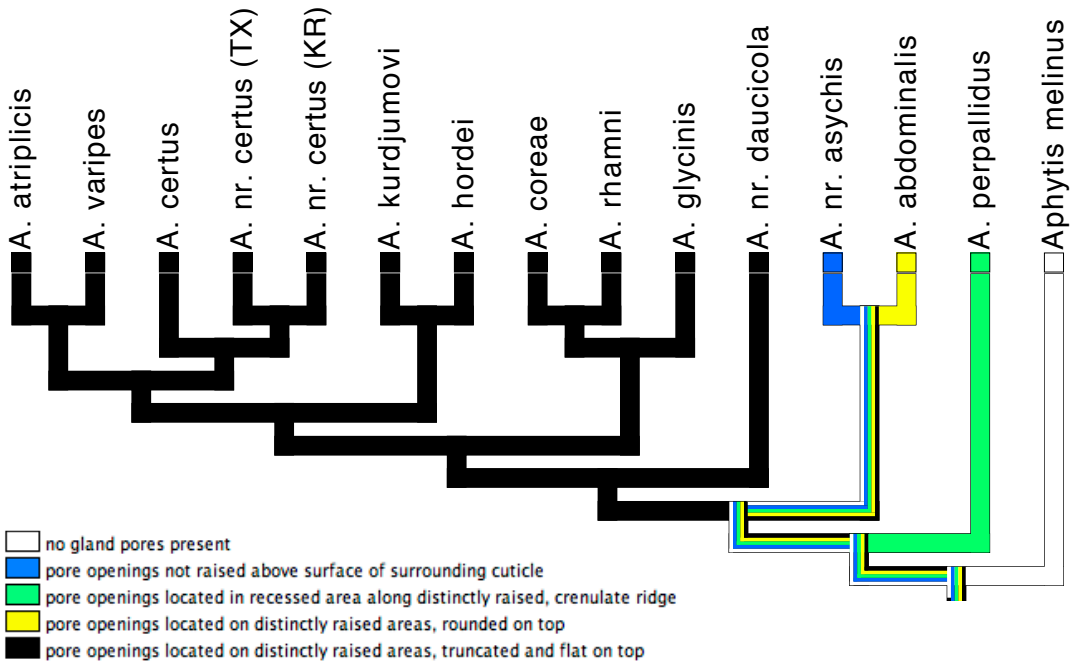

Figure 21: Character 29: Conformation of cuticle surrounding gland pores on male scape. CI=1, RI=0/0.

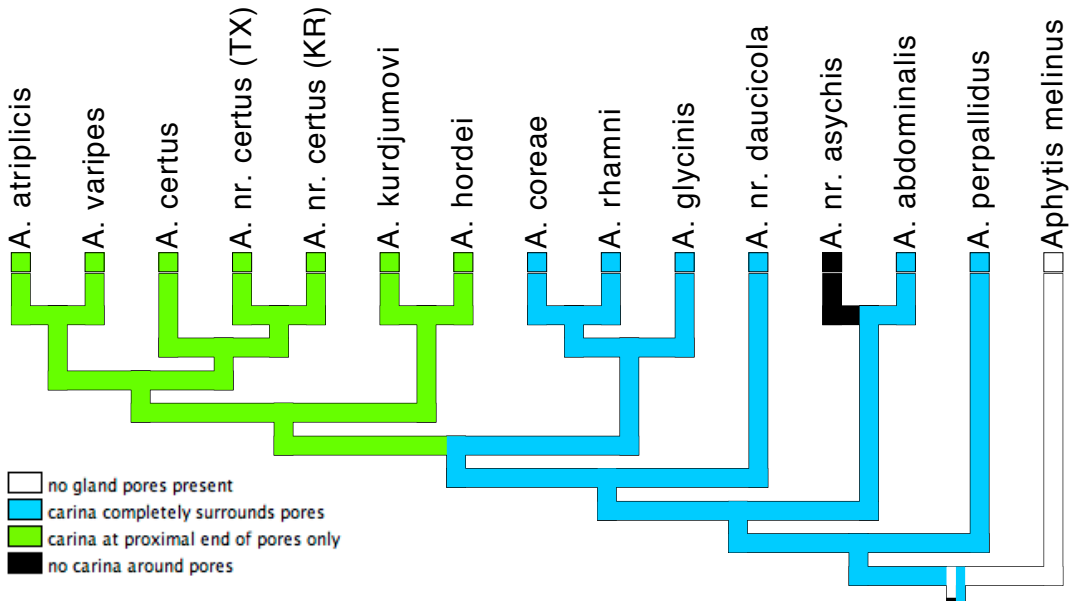

Figure 22: Character 31: Carina delimitation around gland pores on male scape. CI=1, RI=1.

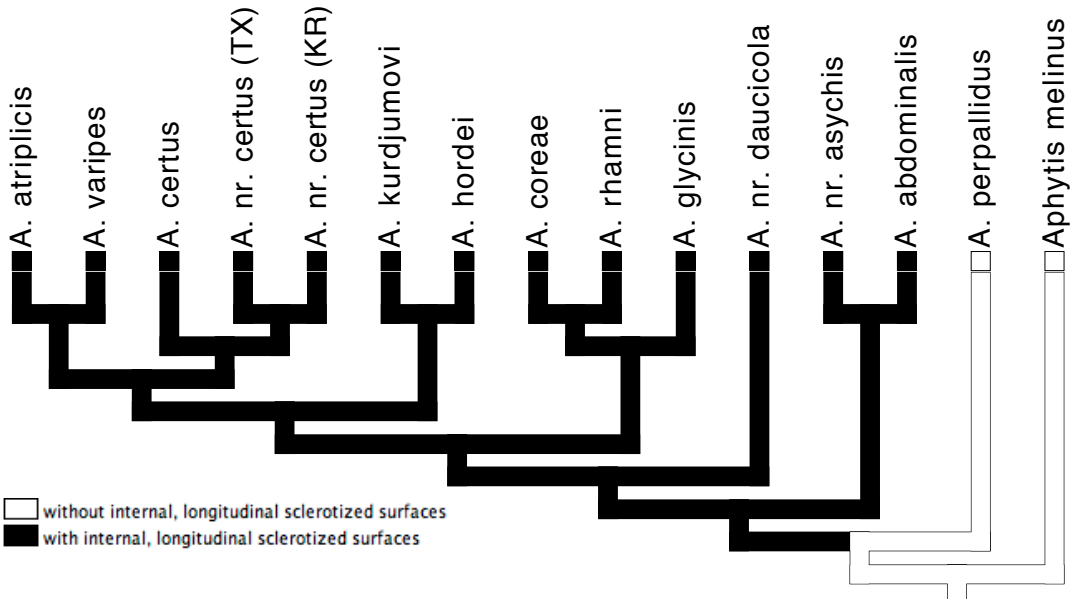

Figure 23: Character 34: Posterior most sternum in male, internal surfaces. CI=1, RI=1.

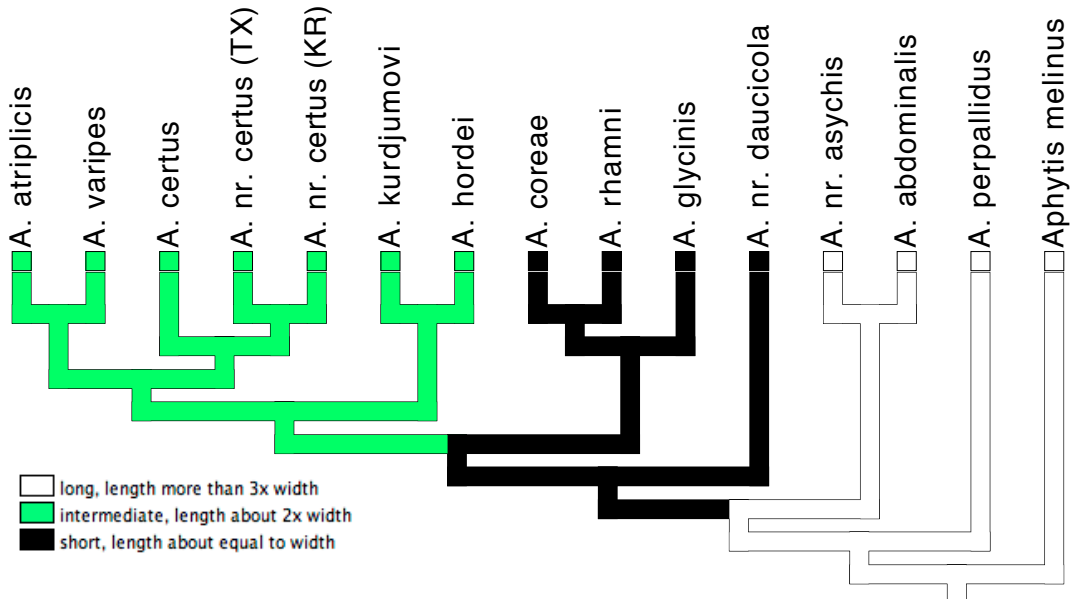

Figure 24: Character 36: Digiti length. CI=1, RI=1.

Discussion

The results of the optimization of the morphological characters on to the maximum likelihood tree showed that some characters have little or no phylogenetic value (characters 4, 11, 19, 22, 27, 29, 33, 36) and some are autapomorphies (characters 1, 7, 12, 13, 23, 30, 31, 38). Nine appeared to have phylogenetic value (RI >0.667) and are discussed below.

The plesiomorphic condition for character 2 (Fig. 15), the number of setae in the interspace between the basal cell and the linea calva on the forewing, appears to be 30-60 setae. There is a decrease in number of setae in the *mali* and *daucicola* group. An increase in number of setae was observed independently in *A. abdominalis*, which has more than 60 setae. *Aphelinus abdominalis* specimens tend to be large in overall body size, so this condition may be size related.

The changes in arrangement of setae in the interspace between the basal cell and the linea calva (character 3) appear to correlate with character 2, the number of setae in this area. The *mali* group has one complete line of setae with few setae in angle between that line and marginal vein and the *daucicola* group has one complete and one or two incomplete lines of setae. Both of those groups have a decrease in the number of setae as discussed above, whereas the remaining taxa, which were coded to have more than 30 setae, have at least two lines of setae proximad to linea calva. Characters 2 and 3 appear to be related, not independent.

In character 5 (Fig. 17), the plesiomorphic condition is clearly costal cell with single line of setae on ventral surface. There are more setae arranged in more than one line in the non-basal groups.

For character 17 (Fig. 18), head color, the plesiomorphic condition is yellow. There appears to be a shift in *A. abdominalis*, where the head is brown and the occiput or parts of the face are yellow and the apomorphic condition is dark brown to black head, with no yellow in more derived taxa.

Character 18, mesosoma color, suggests that mesosoma largely (>50%) yellow is plesiomorphic. The non-basal groups have mesosoma not largely (<50%) yellow.

The plesiomorphic condition of character 20, shape of F1 in males, is subquadrate. It is interesting to note that the shape of F1 in females was not reported to be phylogenetically valuable.

The plesiomorphic condition of character 31 (Fig. 22), carina delimitation around gland pores on male scape, is the carina completely surrounding gland pores. There is an apomorphic transition in *varipes* group in having the carina at the proximal end only. There is a reversion in *A. asychis* where there is no carina around pores.

Although character 29 had RI <0.667, this character shows the importance of broad taxon sampling, and is therefore discussed. For character 29 (Fig. 21), the parsimony optimization in PAUP* and Mesquite assumes that state 5 (pore openings located on distinctly raised areas, truncated and flat on top) is basal and every other state is autapomorphic. However, it is more reasonable to assume the basal state is state 0 (no gland pores present on male scape) as in *Aphytis melinus,* and that state 5 is a

synapomorphy. The parsimony reconstruction at the base of the tree appears to be an artifact of having only a single outgroup and single terminal taxa representing species groups at the base of the tree.

Characters 29 and 31 clearly illustrate why it is important to investigate evolution of morphology using a robust phylogeny. Without a phylogeny and looking at the morphological states themselves, it would be tempting to place *A. asychis* as basal to remaining *Aphelinus*, as the courtship behavior (discussed in Chapter III) and the area that consists of the gland pores are so drastically different in *A. asychis*. The gland pore character system appears much simpler in the *asychis* group compared to other *Aphelinus*. However, as discussed in characters 29 and 30, the states of *A. asychis* are not the plesiomorphic states but rather are reversions to a simple external morphology.

The plesiomorphic condition of character 34 (Fig. 23), the internal surfaces of the posterior most sternum in male, is internal surfaces without longitudinal sclerotized surfaces. There is an apomorphic transition to internal surfaces with longitudinal sclerotized surfaces.

The plesiomorphic condition of character 36 (Fig. 24) is long digiti (digitus length >3x width). There are two fundamental shifts, one being with *mali* and *daucicola* group with short digiti, where the length is about equal to the width, and two being the *varipes* group with intermediate digiti, where the length is about 2x width.

Conclusion

Wing characters, specifically the number and arrangement of setae in the interspace between the basal cell and linea calva and the number of setae on the ventral surface of

the costal cell, were observed to be taxonomically important in diagnosing species groups, corresponding with what has been found in previous work. The carina delimitation around gland pores on the male scape, internal surfaces of the posterior-most sternum in males and digiti length were shown to be taxonomically useful.

To further understand these morphological patterns, future work should include broader taxon sampling in the species groups that were not well represented and the species groups not represented at all.

CHAPTER V

REVISION OF THE *APHELINUS ASYCHIS* WALKER, 1839 (HYMENOPTERA: APHELINIDAE) SPECIES GROUP

Introduction

The current taxonomy of the *Aphelinus asychis* species group is summarized in Table 13, with the two currently valid species within this group being *A. asychis* and *A. semiflavus*.

Aphelinus asychis Walker was described in 1839 from British and Irish material. Graham (1976) designated one of the three syntypes (in BMNH) as a lectotype. *Aphelinus affinis* Förster, 1841, *Aphelinus brachyptera* Kurdjumov, 1913, *Aphelinus brevicalcar* Thomson, 1876, *Aphelinus dubia* Kurdjumov, 1913, *Aphelinus euthria* Walker, 1839, and *Myina affinis* Förster, 1841 are currently considered junior synonyms of *A. asychis* (Graham 1976).

Aphelinus semiflavus Howard, 1908 (holotype in NMNH), was originally collected near Fort Collins, Colorado, parasitizing *Myzus persicae.* Girault (1917) treated *A. brevipennis* as a junior synonym of *A. semiflavus*.

There has been a lot of confusion over whether or not *A. asychis* and *A. semiflavus* are two different species. Ferrière (1965) and Nikol'skaya and Yasnosh (1966) synonymized *A. semiflavus* with *A. asychis*. Mackauer and Finlayson (1967) argued that they should remain separate because they seem to differ in host ranges and

could possibly be different geographic strains. *Aphelinus semiflavus* has since been treated as a valid species separate from *A. asychis* by several researchers (Raney 1971; Raney et al. 1973; Ro & Long, 1997). However, distinguishing between the two species has been difficult. For example, during the biological control project of *Therioaphis trifolii*, the spotted alfalfa aphid, in the United States in the 1950's, *A. asychis* was initially recorded as *A. semiflavus* in publications on this project (Hagen and van den Bosch 1968; Clausen 1978).

Further evidence is necessary to determine whether these two nominal taxa are one species, are races of one species with different host ranges, or are two distinct cryptic species.

Table 13: Current taxonomic structure of *Aphelinus asychis* species group.

Current valid species of *A. asychis* group	***Aphelinus asychis* Walker, 1839**		
	Synonyms:	*Aphelinus affinis*	Förster, 1841
		Aphelinus brachyptera	Kurdjumov, 1913
		Aphelinus brevicalcar	Thomson, 1876
		Aphelinus dubia	Kurdjumov, 1913
		Aphelinus euthria	Walker, 1839
		Myina affinis	Förster, 1841
	***Aphelinus semiflavus* Howard, 1908**		
	Synonym:	*Aphelinus brevipennis*	Girault, 1917
Putative new species of *A. asychis* group	New species 1 - Kazakhstan New species 2 - China		

Synapomorphies

The *Aphelinus asychis* group differs from other *Aphelinus* species groups by the following traits:

1. Submarginal vein with only 2 [not 3 or more] setae (Hayat 1998).
2. Oviposition probing/penetration site on host dorsal [not ventral] (de Farias & Hopper, 1999).

Biological Control

Aphelinus asychis is common in both the Old World and New World and it is an important parasitoid of aphids (ca. 60 documented aphid hosts). It has been used in the biological control of at least six different aphid species (Noyes 2016; Kalina & Stary 1976). In addition to the work on control of *Therioaphis trifolii*, the spotted alfalfa aphid, mentioned above, *A. asychis* was also the focus of work on biological control programs of *Schizaphis graminum*, the greenbug, during the 1970's and 1980's (Cate et al. 1973; Johnson et al. 1979; Summy et al. 1979) and *Diuraphis noxia,* the Russian wheat aphid, (Prokrym et al. 1998; Brewer et al. 2001) during the 1990's.

During foreign exploration for natural enemies of the Russian wheat aphid in the 1990's, *A. asychis* was found in Europe, Asia, northern Africa, and South America, where it parasitized *Diuraphis* spp. (Hopper et al. 1996; Gonzales et al. 1994). A major factor that impedes the success of biological control programs is the delayed recognition of cryptic species. Testing for reproductive compatibility is one way to discover cryptic species. Kazmer et al. (1996) tested seven lab cultures of *A. asychis* that were collected during foreign exploration for interculture reproductive compatibility. They examined all

possible crosses (49) of the seven lab cultures. Three completely and reciprocally reproductively incompatible groups – from the Mediterranean basin, Kazakhstan, and China – were discovered. These were also reflected in clusters from phenetic analysis of 61 RAPD loci banding patterns. These may represent cryptic species. Further work is needed to understand the nature and relationships of these three groups among each other and among other species in the *A. asychis* species complex, and this is one of the three objectives of this study, see below.

Research Objectives

1. Determine whether *A. asychis* and *A. semiflavus* are one species, are races of one species with different host ranges, or are two distinct cryptic species.
2. Code morphological characters for all available material of species in the *A. asychis* group, including representatives of cultures from Kazmer et al (1996).
3. Using morphologic data, determine if new species exist and if existing synoyms are correctly placed.

Materials and Methods

Specimen Preparation

Specimens used in this study were killed in 95% ethanol and stored in 95% ethanol in freezers. Most were then critical point dried using a Samdri 790 CPD unit. Critical-point-dried specimens were then card mounted with Franklin International's water soluble Titebond Liquid Hide Glue. Selected specimens were slide mounted following Noyes (1982) protocol. All card-mounted and slide-mounted specimens were assigned individual barcode accession numbers (e.g., TAMUIC X0852885, USNM ENT 4532898

etc.). Label data for type specimens are reported verbatim, where | signifies a new line on a label and || separates different labels.

Figures

Images for figures were acquired using digital imaging and image-stacking. Specimens photographed for coloration were removed from alcohol storage, placed on a layer of water-based, water-soluble jelly in small watch glass, submerged in alcohol, and photographed using a Leica M205 FA stereomicroscope and Leica applications suite software. Slide-mounted specimens were photographed using an Olympus BH2 microscope with DIC illumination and Image-Pro Plus Software. Zerene Stacker was used for all image stacking. Adobe Photoshop CS6, Adobe Lightroom 6.0, and Adobe InDesign CS6 were used for final modifications to images and layout of plates.

Database Management

All images were deposited in Morphbank and in mx, a web-based content management database system (Yoder et al. 2006). Morphological codings were conducted in mx. The mx system is open source, with further documentation available at http://mx.phenomix.org

Measurements

Measurements from slide mounts were taken using an eyepiece reticle in a Zeiss standard 16 microscope. Measurements from card mounts were taken using an eyepiece reticle in a Leica MZ16 microscope.

Head

The length of the head was measured from the anterior to the posterior margin in dorsal view (Fig. 25, A). The frontovertex length was measured in dorsal view from the dorsal margin of the scrobal impression to the occiput (Fig. 25, G). Both were measured at their widest points. The posterior ocellar diameter (Fig. 25, E), distance from posterior ocelli to eye margin, (Fig. 25, C) and distance from posterior ocelli to occipital margin (Fig. 25, F) were measured as illustrated in Figure 25. The widths of each antennal segment (scape, pedicel, F1, F2, F3, and club) were measured at their widest points. The lengths of each antennal segment were measured from proximal to distal end.

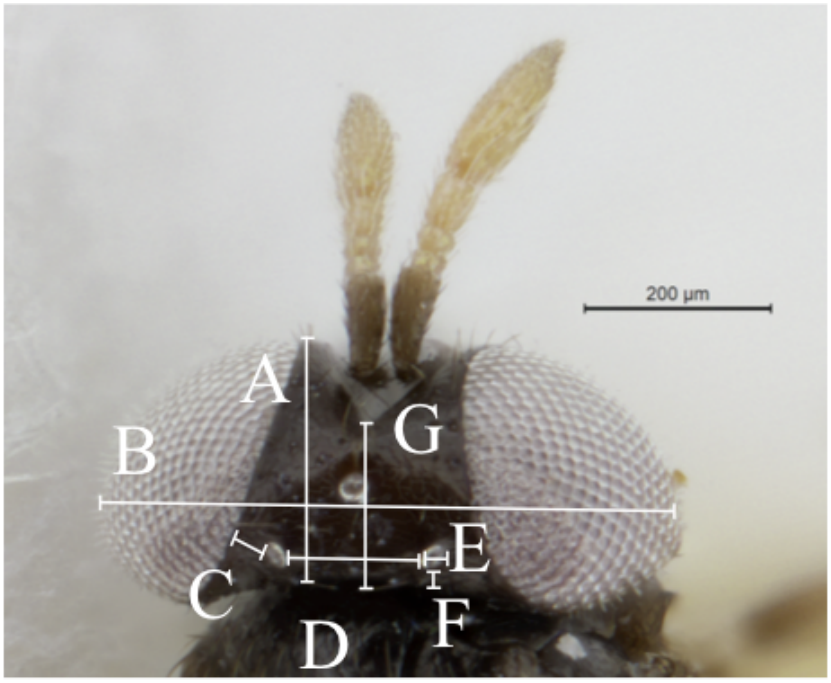

Figure 25: *Aphelinus* n. sp. 2, female, head, dorsal view. A: length; B: width; C: posterior ocellus to eye margin distance; D: posterior interocellar distance; E: posterior ocellus diameter; F: posterior ocellus to occipital margin distance; G: frontovertex length.

Meso/Metasoma length

Meso/metasoma length of specimens was measured from the anterior margin of the pronotum to the apex of the epiproct using slide-mounted specimens. The lengths of the mesosoma, the midlobe of mesoscutum, and the scutellum were measured from their anterior to posterior margins along the midline and widths were measured at their widest points.

Wings

Forewing measurements are shown in Figure 26; hind wing measurements follow those of the forewing.

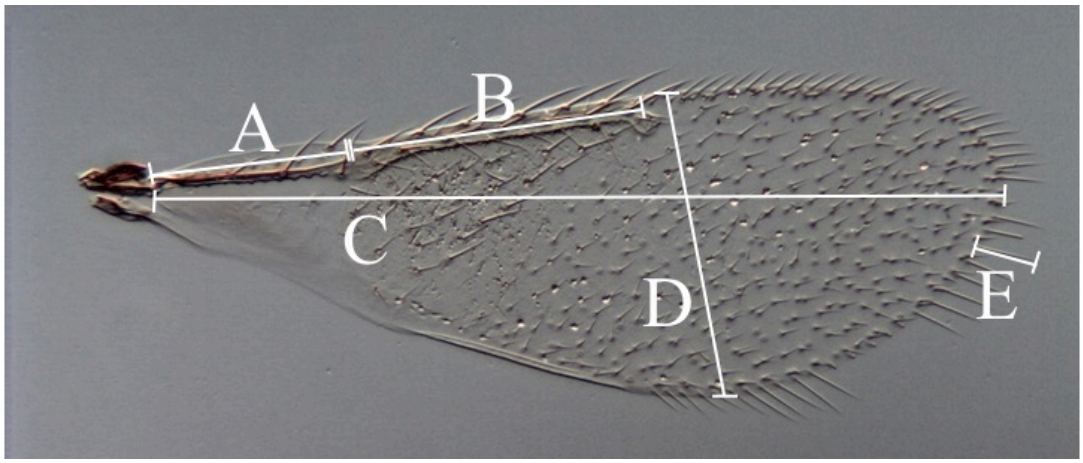

Figure 26: *Aphelinus* n. sp. 1, female, forewing, dorsal view. A: costal cell length; B: marginal vein length; C: overall length; D: overall width; E: longest marginal seta length.

Ovipositor and Male Genitalia

Ovipositor length was measured as illustrated in Figure 27. The length of the phallobase was measured from the anterior margin of the genital capsule to the posterior

end of the digiti (Fig. 14, phl). The width of the phallobase was measured at its widest point (Fig 14, phl). The length of the digitus was measured between its most anterior to most posterior points, and its width was measured at its widest point (Fig. 14, dig).

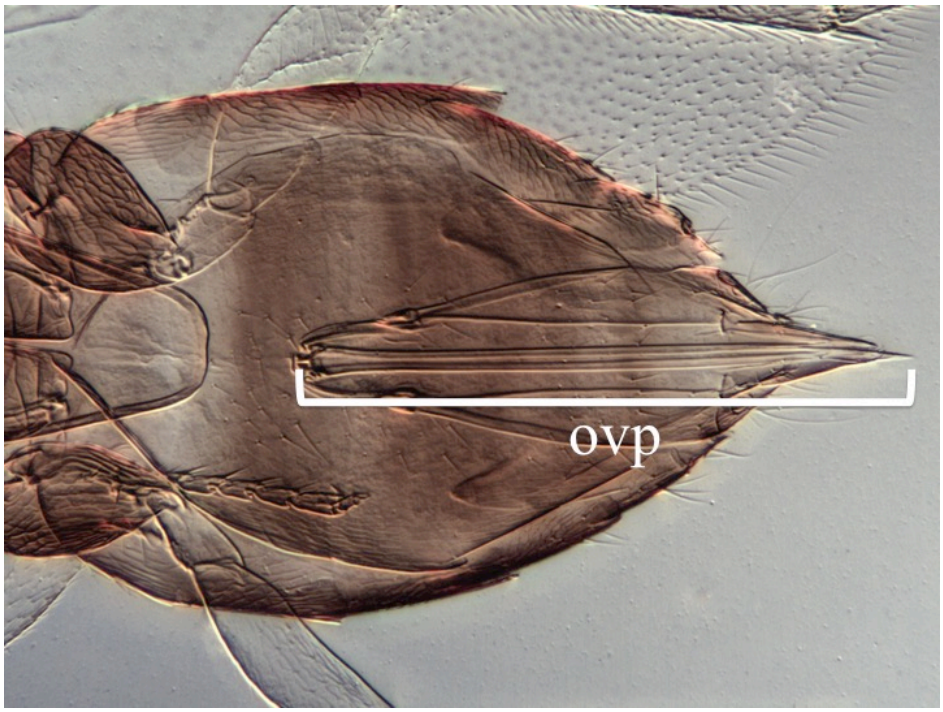

Figure 27: *Aphelinus* female, metasoma, ventral view. Abbreviation: ovp = ovipositor

Results

Following Hayat (1998) I consider a submarginal vein with only two setae to be diagnostic for the *A. asychis* group. In females, F1 and F2 are subquadrate, and F3 is 1.2-2.0x longer than wide. In males, F1 and F2 are wider than long, and F3 is >3.0x longer

than wide. Brachypterous wings are also common in this group, particularly in males. There is marked sexual dimorphism, particularly in antennal proportions and coloration, which is not found in other *Aphelinus* species.

Taxonomy

Aphelinus *n. sp. 1*

Diagnosis. Female. Legs with procoxa yellow [not brown], mesocoxae and metacoxae brown [not yellow]; all femora and all tibiae yellow [not brown at base with apex yellow or pale]; radicle and basal portion of scape yellowish white, apical portion of scape and pedicel brown [not entirely brown]; F1, F2, F3, and club yellow [not brown]; tip of club dusky [club not entirely yellow]. Male. Similar except all antennal segments yellowish brown [antennal segments uniform in color], scape with five minute pores on convex ridge and with most proximal pore at midpoint of scape (Fig. 28).

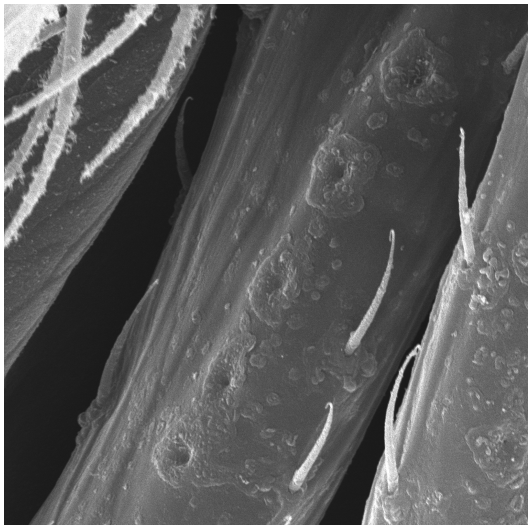

Figure 28: *Aphelinus* n. sp. 1, male, scape, ventral view. Note the five linearly arranged exocrine gland pores.

Description: Female (Figs. 29B, D, F and 30B, D – F).

Color (Fig. 29B, D, F). Head and mesosoma dark brown; radicle and basal portion of scape yellowish white; apical portion of scape and pedicel brown; F1, F2, F3, and club yellow; tip of club dusky; legs with procoxa yellow, mesocoxae and metacoxae brown; all femora and tibiae yellow; metasoma yellow from base to apex, lateral margins of metasoma darker than mesal area except in basal quarter.

Body length. 0.57-0.88 mm (n=3; slide mounts) (Holotype 0.77 mm).

Head (Figs. 29B and 30B). Width 1.15-1.3x head length in anterior view; frontovertex width 0.35-0.39x head width and 1.08-1.43x frontovertex length; posterior ocelli diameter 0.6x posterior ocelli to eye margin distance and 1.5x posterior ocelli to occipital margin distance; antenna as in Figure 30B with scape length 5.0-5.88x scape width; pedicel length 1.5-1.88x pedicel width; F1 and F2 subquadrate, length of both

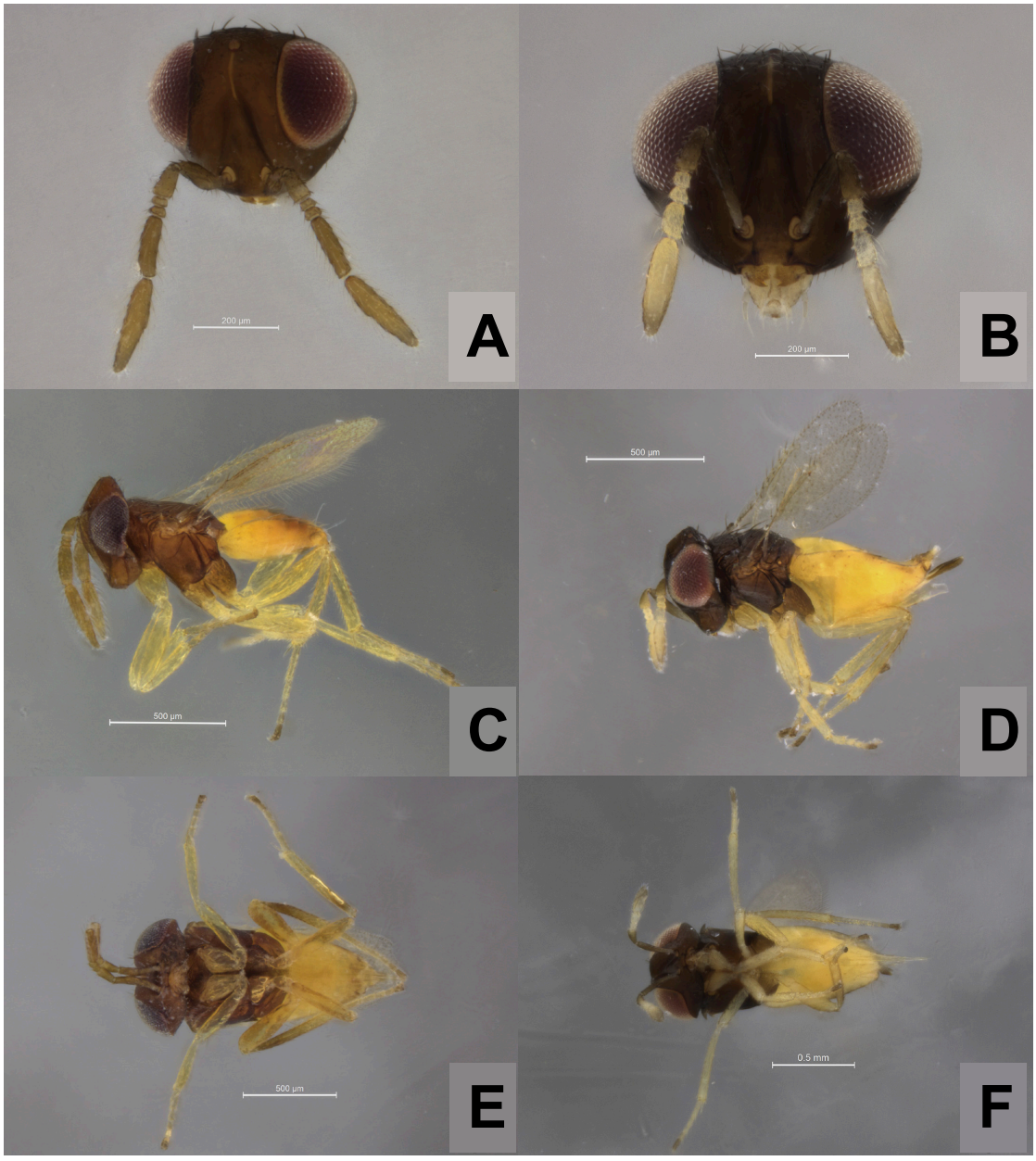

Figure 29: *Aphelinus* n. sp. 1, paratype specimens in 95% ethanol. A: male, antennae and face, anterior view (TAMUIC X0856562); B: female, antennae and face, anterior view (TAMUIC X0856563); C: male, habitus, lateral view (TAMUIC X0856562); D: female, habitus, lateral view (TAMUIC X0856563); E: male, habitus, ventral view (TAMUIC X0856562); F: female, habitus, ventral view (TAMUIC X0856563).

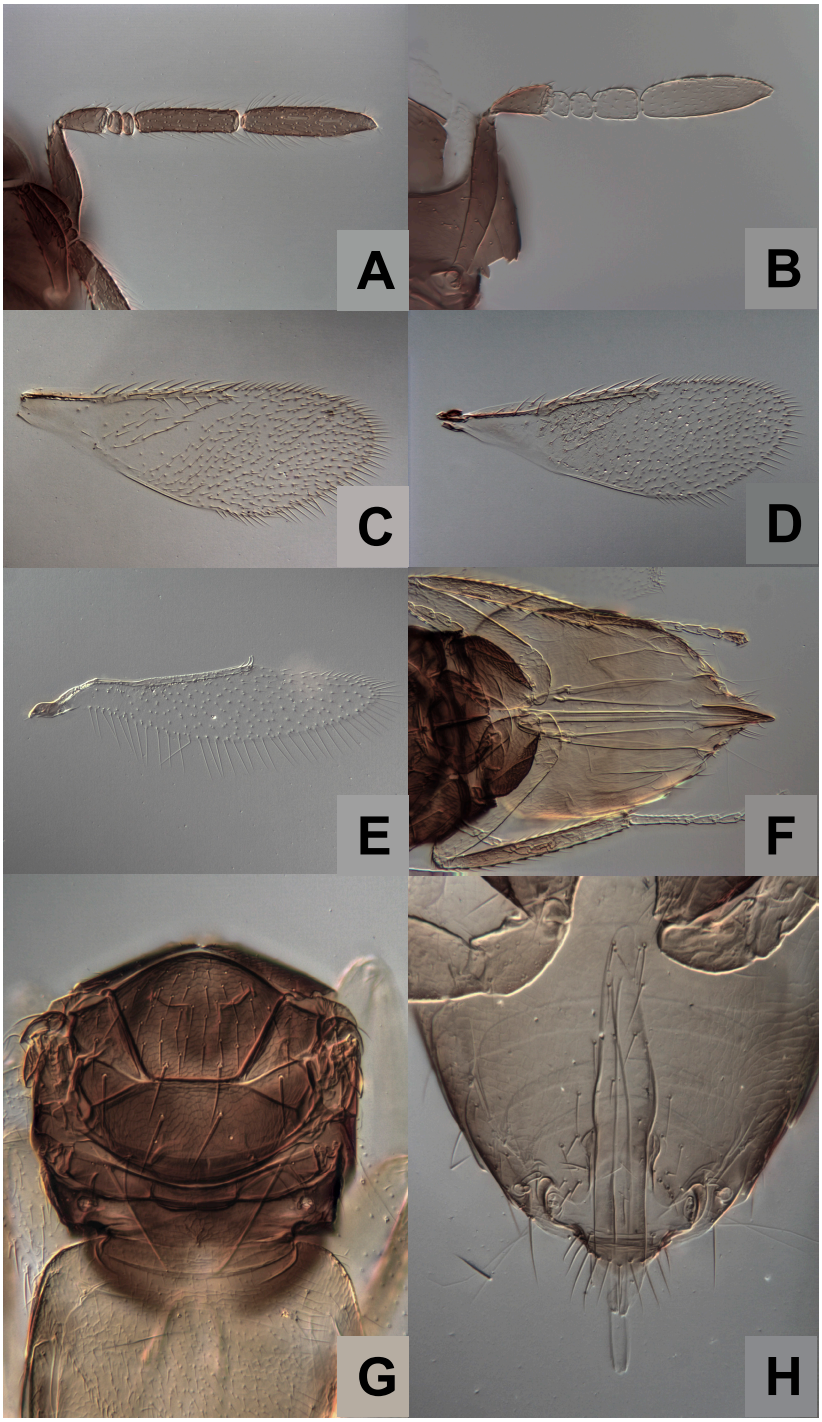

Figure 30: *Aphelinus* n. sp. 1, slide-mounted paratypes. A: male, antenna, lateral view (TAMUIC X0852885); B: female, antenna, lateral view (TAMUIC X0852877); C: male, forewing, dorsal view (TAMUIC X0852885); D: female, forewing, dorsal view (TAMUIC X0852875); E: female, hind wing, dorsal view (TAMUIC X0852869); F: female, metasoma, ventral view (TAMUIC X0852880); G: female, mesosoma, dorsal view (TAMUIC X0852880); H: male, genitalia, ventral view (TAMUIC X0852885).

0.92-1x width; F3 length 1.44-1.76x F3 width; club length 3.08-3.25x club width and 2.47-3x F3 width, with 8 longitudinal sensilla.

Mesosoma (Figs. 29G, and 30D, F). Midlobe of mesoscutum length 0.67-0.73x midlobe width, with two pairs of long setae (one pair lateral and one pair posterior) and 31-33 short setae; side lobes of mesoscutum each with one pair of long setae and one pair of short setae; scutellum with two pairs of long setae (one pair anterior and one pair posterior); mesotibial spur length 0.73-0.80x mesobasitarsus length; metatibial spur length 0.47-0.49x metabasitarsus length.

Forewing (Fig. 30D). Length 2.47-2.78x forewing width, longest marginal seta 0.14-0.17x forewing width; costal cell 0.76-0.80x marginal vein length, with one line of 6-7 setae on ventral surface and 1-2 dorsal setae in apical quarter; submarginal vein with two setae; marginal vein with two rows of 12-18 large dorsal setae, one row of 7-11 small dorsal setae, and one row of 7-10 ventral setae; interspace between basal cell and linea calva with 18-33 setae arranged in two complete lines and two incomplete lines; linea calva closed with 2-3 setae at its posterior end, setae bordering linea calva proximally are arranged uniformly and evenly to posterior margin of wing.

Hind wing (Fig. 30E). Length 3.69-4.50x hind wing width; longest marginal seta 0.31-0.53x hind wing width.

Metasoma (Figs. 29F, and 30D, F). Length 1.13-1.14x mesosoma length; ovipositor length 1.27-1.31x mesotibia length and 1.16-1.20x metatibia length; third valvula length 0.35-0.36x ovipositor length.

Description: Male (Figs. 29A, C, E and 30A, C, H). Similar to female except:

Color (Fig. 29A, C, E). All antennal segments yellowish brown; metasoma yellow at base darkening gradually to light brown at apex.

Head (Figs. 29A and 30A). Antenna with scape length 4.89x scape width, with five pores along midline of single continuous convex ridge on ventral surface (Fig. 28); pores small, approximately same diameter as base of adjacent setae, pedicel length 1.7x pedicel width; length of F1 and F2 both 0.53x their width; F3 length 4.35x F3 width; club length 4.64x club width and 1.38x F3 length.

Metasoma (Fig. 29E and 30C, H). Length 0.96x mesosoma length; phallobase length (including digiti) 6.06x phallobase width; digiti length 5.14x digiti width.

Holotype (USNM). Female, card mounted. Label data: "Texas: Brazos Co. | College Station | TAMU Lab Culture | 15.xii.1992 T92/051 | ex: *Diuraphis noxia* | on wheat || T92/051 orig. collection | P.R. of China | Ningxia | 21.vi.1992 | Keith Hopper coll. | ex. *Diuraphis* | *agropyromophaga* || TAMUIC X0852864".

Paratypes (USNM, TAMU, BMNH). 30 card mounts (9 female, 21 male). 10 card mounts (2 female, 8 male) from original material with label data reading "P.R. China: Pingluo | Ningxia 19.xi.1992 | T92/051 orig. mat. | Keith Hopper | ex. *Diuraphis*" (TAMUIC accession numbers: females: X0852882, X0852886; males: X0852878 to -79, X0852883, X0852887, X0852889 to -92). 10 card mounts (7 female, 3 male) from F1 progeny with the same label data as holotype (TAMUIC accession numbers: females: X0852864 to -67, X0852870, X0852873, X0852876; males: X0852874, X0852871, X0852863). 10 (all male) card mounts, voucher specimens from non-destructive DNA extraction, with same label data as original material (TAMUIC accession numbers:

X0856046 to -55). 7 slide mounts (5 female, 2 male). 3 slide mounts from original material with same label data as above (females: X0852880, X0852888; male: X0852885). 4 slide mounts from F1 progeny, same label data as above (females: X0852869, X0852875, X0852877; male: X0852868).

Other material examined. CHINA: Harbin: 3 males, 5 females. TAMUIC X0853040 to -47 (TAMU). JAPAN: Honshu: 2 females. CNCHYMEN 019042 and CNCHYMEN 019033 (CNC).

Hosts. The original material was collected from *Diuraphis agropyromophaga* in the field in China. In lab culture, *Diuraphis noxia* on wheat was used as the host.

Distribution. Northern China and Japan.

Discussion. The most notable distinction of the type series specimens from China, Pingluo from other *A. asychis* specimens examined is the presence of yellow procoxae, yellow femora, and yellow tibiae. In all other *asychis* group species, all coxae are brown, and femora and tibiae are patterned with brown. The China, Harbin series exhibits the same leg-pattern coloration as the type series. I am treating the China, Harbin series as conspecific, noting that the head and metasoma are much darker, almost black, and the antennal club is darker at apex than in China, Pingluo. There is one specimen from the Japan, Honshu series that exhibits same leg coloration patterns as the type series of China, Pingluo, however the other specimens in this series resemble *asychis*.

Aphelinus *n. sp. 2*

Diagnosis. Female. Legs with all coxae brown [not with procoxae yellow], profemur and mesofemur light brown with apex yellow or pale [not entirely yellow or dark brown with apex yellow or pale], metafemur yellow [not light or dark brown with apex yellow or pale], protibia and mesotibia yellow [not dark brown with apex yellow or pale], metatibia light brown with apex yellow [not entirely yellow or dark brown with apex yellow or pale]. Male. Similar except all antennal segments are yellowish brown [antennal segments not without uniformity in color], scape with five minute pores on convex ridge and with proximal most pore at midpoint of scape.

Description: Female (Figs. 31B, D, F and 32B, D – F).

Color (Fig. 31B, D, F). Head and mesosoma dark brown; radicle and basal portion of scape yellowish white, apical portion of scape and pedicel brown, and F1, F2, F3, and club yellow, tip of club dusky; legs with all coxae brown, profemur and mesofemur light brown with apex yellow or pale, metafemur yellow, protibia and mesotibia yellow, metatibia light brown with apex yellow [not entirely yellow or dark brown with apex yellow or pale].; metasoma yellow from base to apex, lateral margins of metasoma darker than mesal area except in basal quarter.

Body length. 0.81-0.91 mm (n=3; slide mounts) (Holotype 0.7 mm).

Head (Figs. 31B and 32B). Width 1.14-1.22x head length in anterior view; frontovertex width 0.53-0.57x head width and 1.91-2.63x frontovertex length; posterior ocelli diameter 0.6-0.75x posterior ocelli to eye margin distance and 1.5x the posterior ocelli to occipital margin distance; antenna as in Figure 31B with scape length 5.8-7.25x

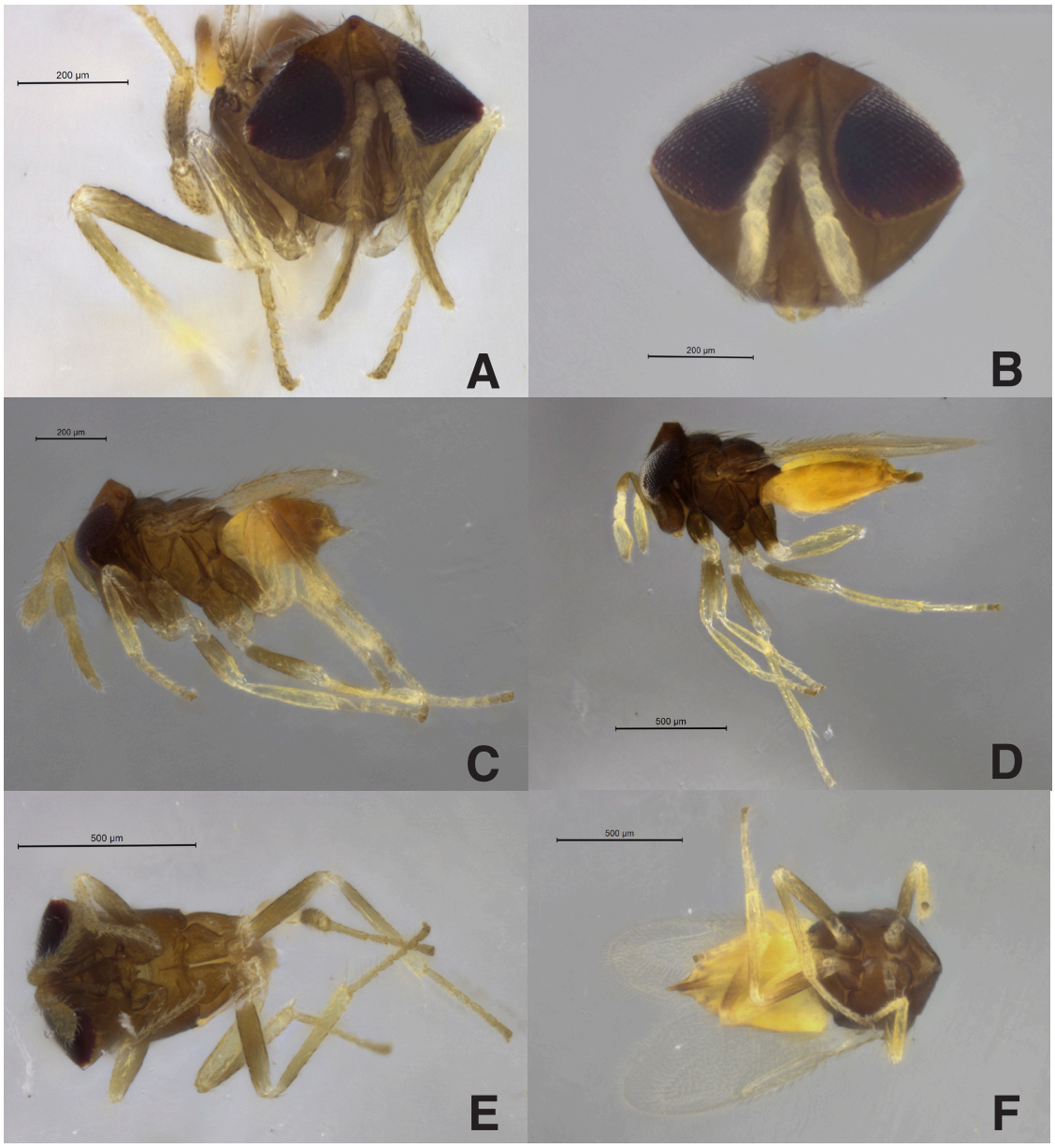

Figure 31: *Aphelinus* n. sp. 2, paratype specimens in 95% ethanol. A: male, antennae and face, anterior view (TAMUIC X0853050); B: female, antennae and face, anterior view (TAMUIC X0856403); C: male, habitus, lateral view (TAMUIC X0856401); D: female, habitus, lateral view (TAMUIC X0856400); E: male, habitus, ventral view (TAMUIC X0853050); F: female, habitus, ventral view (TAMUIC X0856403).

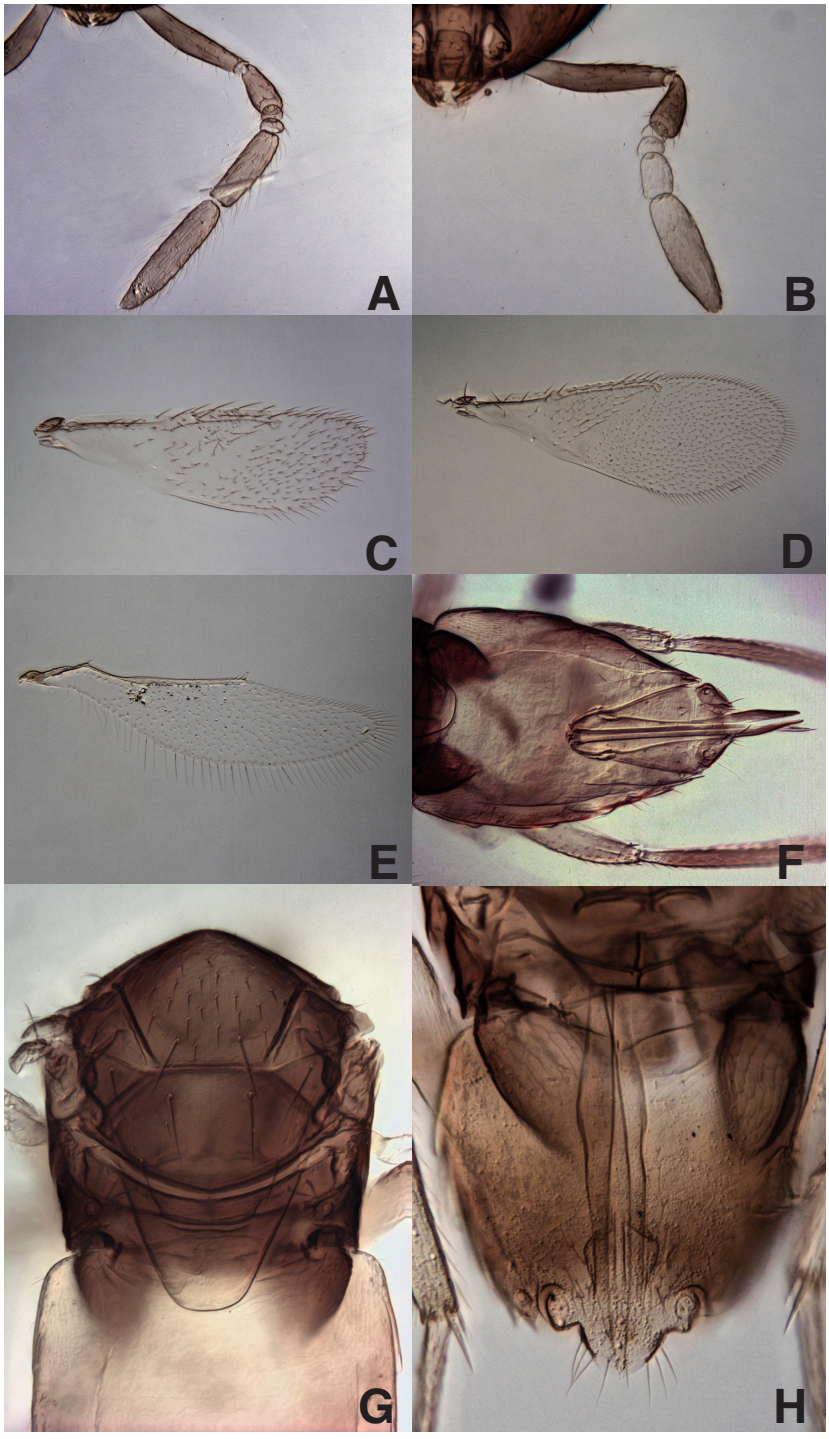

Figure 32: *Aphelinus* n. sp. 2, slide-mounted paratypes. A: male, antenna, lateral view (TAMUIC X0856044); B: female, antenna, lateral view (TAMUIC X0855782); C: male, forewing, dorsal view (TAMUIC X0856072); D: female, forewing, dorsal view (TAMUIC X0616386); E: female, hind wing, dorsal view (TAMUIC X0852956); F: female, metasoma, ventral view (TAMUIC X0616386); G: female, mesosoma, dorsal view (TAMUIC X0852880); H: male, genitalia, ventral view (TAMUIC X0856075).

scape width, pedicel length 1.8-2.2x pedicel width, F1 and F2 subquadrate, length of both 1x width, F3 length 1.4-1.6x F3 width, and club length 2.86-3.67x club width and 2.75-3.14x F3 width, with 8 longitudinal sensilla.

Mesosoma (Figs. 31D,F and 32G). Midlobe of mesoscutum length 0.75-0.76x midlobe width with two pairs of long setae (one pair lateral and one pair posterior) and 34-35 short setae; side lobes of mesoscutum each with one pair of long setae and one pair of short setae; scutellum with two pairs of long setae (one pair anterior and one pair posterior); mesotibial spur length 0.69-0.83x mesobasitarsus length, metatibial spur length 0.44-0.6x metabasitarsus length.

Forewing (Fig. 32D). Length 2.28-2.41x forewing width, longest marginal seta 0.12-0.16x forewing width; costal cell 0.63-0.7x length of marginal vein, with one line of 6-7 setae on ventral surface and 1-2 dorsal setae in apical quarter; submarginal vein with two setae; marginal vein with two rows of 14-15 large dorsal setae, one row of 7-8 small dorsal setae, and one row of 8-10 ventral setae; interspace between basal cell and linea calva with 30-33 setae arranged in three complete lines and two incomplete lines; linea calva closed with 2-3 setae at its posterior end, setae bordering linea calva proximally arranged uniformly and evenly to posterior margin of wing.

Hind wing (Fig. 32E). Length 4.6x hind wing width, longest marginal seta 0.67x hind wing width.

Metasoma (Figs. 31D, F and 32F). Length 1.42x mesosoma length; ovipositor length 1.6x mesotibia length and 1.33x metatibia length; third valvula length 0.31-0.41x ovipositor length.

Description: Male (Figs. 31A, C, E and 32A, C, H). Similar to female except:

Color (Fig. 31A, C, E). All antennal segments yellowish brown; metasoma yellow at base darkening gradually to light brown at apex.

Head (Figs. 31A and 32A). Antenna with scape length 5.2-7.5x scape width with five pores along midline of single continuous convex ridge on ventral surface, pores small, approximately same diameter as base of adjacent seta, pedicel length 2-2.2x pedicel width, F1 length and F2 length both 0.6x width, F3 length 2.8-3.33x F3 width, club length 3.43-4.33x club width and 1.63-1.71x F3 length.

Metasoma (Fig. 31C, E and 32H). Length 0.81-0.9x mesosoma length; phallobase length (including digiti) 5.11-6.38x phallobase width; digiti length 4.67-5x digiti width.

Holotype (USNM). Female, card mounted. Label data: "Texas: Brazos Co. | College Station | TAMU Lab Culture | coll. 23.vii.1991 || ex: *Diuraphis* | *noxia* | on wheat: | T91/061 || T91/061 orig. collection: | U.S.S.R. Dmitrievka | 16-17.v.1991 || S. Halbert coll. | ex. *Diuraphis* | *noxia* on grass || TAMUIC X0852959".

Paratypes (USNM, TAMU, BMNH). 41 card mounts (38 female, 3 male). 19 card mounts (18 female, 1 male) with the same label data as holotype (TAMUIC accession numbers: females: X0852952 to -58, X0852961 to -64, X0852966 to -72; male: X0852965). 15 card mounts (all female) with label data reading "USSR: Kazakhstan | Dmitrievka | Ex: Russian Wheat Aphid || On: Wheat | 16-17.v.1991 | S. Halbert T91-061" (TAMUIC accession numbers: X0855626 to -39, X0855641). 7 card mounts (5 females, 2 males) of voucher specimens from non-destructive DNA

extraction, with label data reading “KAZAKHSTAN | Dmitrevka | 13.v.1991 | Popraski & Halbert | EPL-92-6B || DNA extracted | BIIRL 2014” (TAMUIC accession numbers: females: X0856043, X0856045, X0856074, X0856076, X0856078; males: X0856041, X0856077). 12 slide mounts (6 female, 6 male) with the same label data as holotype. (females: X0616386, X0852956, X0856782, X0855779, X0855781, X0855772; males: X0856042, X0856044, X0856072, X0856073, X0856075, X0855780)

Other material examined. None.

Hosts. The original material was collected from *Diuraphis noxia* in the field in Dmitrievka, Kazakhstan. In lab culture, *Diuraphis noxia* on wheat was used as the host.

Distribution. The collection of type material is only known from Dmitrievka, Kazakhstan.

Discussion. The most notable distinction of the type series from Kazakhstan, Dmitrievka from other *A. asychis* series examined is the presence of yellow mesotibia, and profemur, mesofemur, and metatibia light brown at base and yellow at apex. *Aphelinus asychis* specimens have mesotibia, metatibia, profemur, and mesofemur dark brown at base and yellow at apex. *Aphelinus semiflavus* have mesotibia, profemur, and mesofemur yellow, and metatibia brown at base and yellow at apex.

Aphelinus asychis *Walker 1839*

Aphelinus asychis Walker 1839, lectotype designation by Graham (1976).

Aphelinus euthria Walker 1839, synonymy and lectotype designation by Graham (1976).

Myina affinis Förster 1841, synonymy and lectotype designation by Graham (1976).

Aphelinus affinis (Förster 1841): Dalla Torre (1898).

Aphelinus brevicalcar Thomson 1876, lectotype designation by Graham (1976).

Aphelinus brachyptera Kurdjumov 1913, synonymy and lectotype designation by Graham (1976).

Aphelinus dubia Kurdjumov 1913, synonymy and lectotype designation by Graham (1976).

Diagnosis. Female. Legs with all coxae brown [not with procoxae yellow], profemur and mesofemur dark brown with apex yellow or pale [not entirely yellow or light brown with apex yellow or pale], metafemur yellow [not light or dark brown with apex yellow or pale], protibia yellow [not dark brown with apex yellow or pale], mesotibia and metatibia dark brown with apex yellow [not entirely yellow or light brown with apex yellow or pale]. Male. Similar except all antennal segments are yellowish brown [antennal segments not without uniformity in color], scape with five minute pores on convex ridge and with proximal most pore at midpoint of scape.

Description: Female (Figs. 33, B, D, F and 33B, D – G).

Color (Fig. 33B, D, F). Head and mesosoma dark brown; radicle and basal portion of scape yellowish white, apical portion of scape and pedicel brown, and F1, F2,

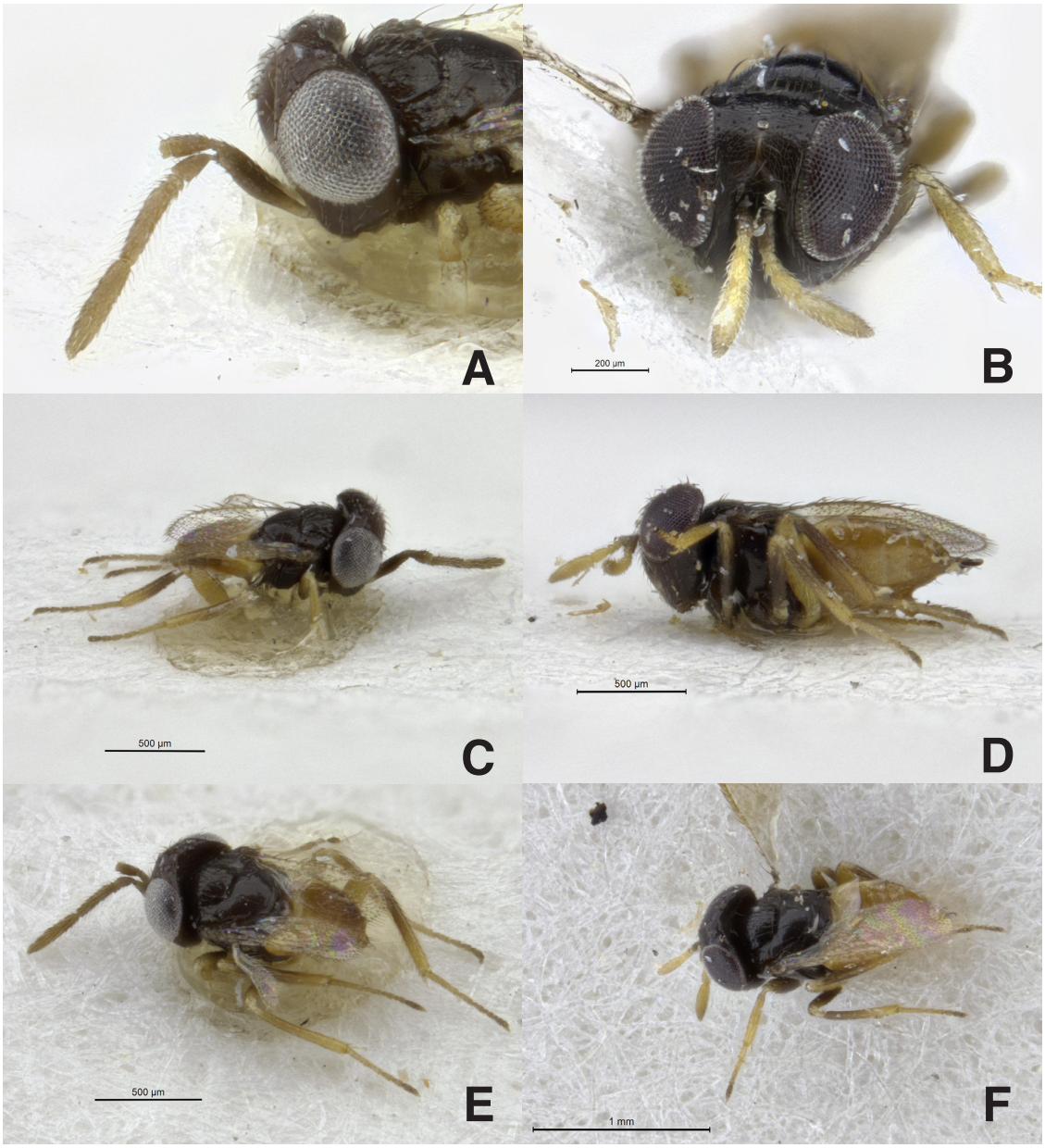

Figure 33: *Aphelinus asychis*, card-mounted specimens. A: male, antennae and face, anterior view (BMNH 1038770); B: female, antennae and face, anterior view (BMNH 1038772); C: male, habitus, lateral view (BMNH 1038770); D: female, habitus, lateral view (BMNH 1038772); E: male, habitus, ventral view (BMNH 1038770); F: female, habitus, ventral view (BMNH 1038772).

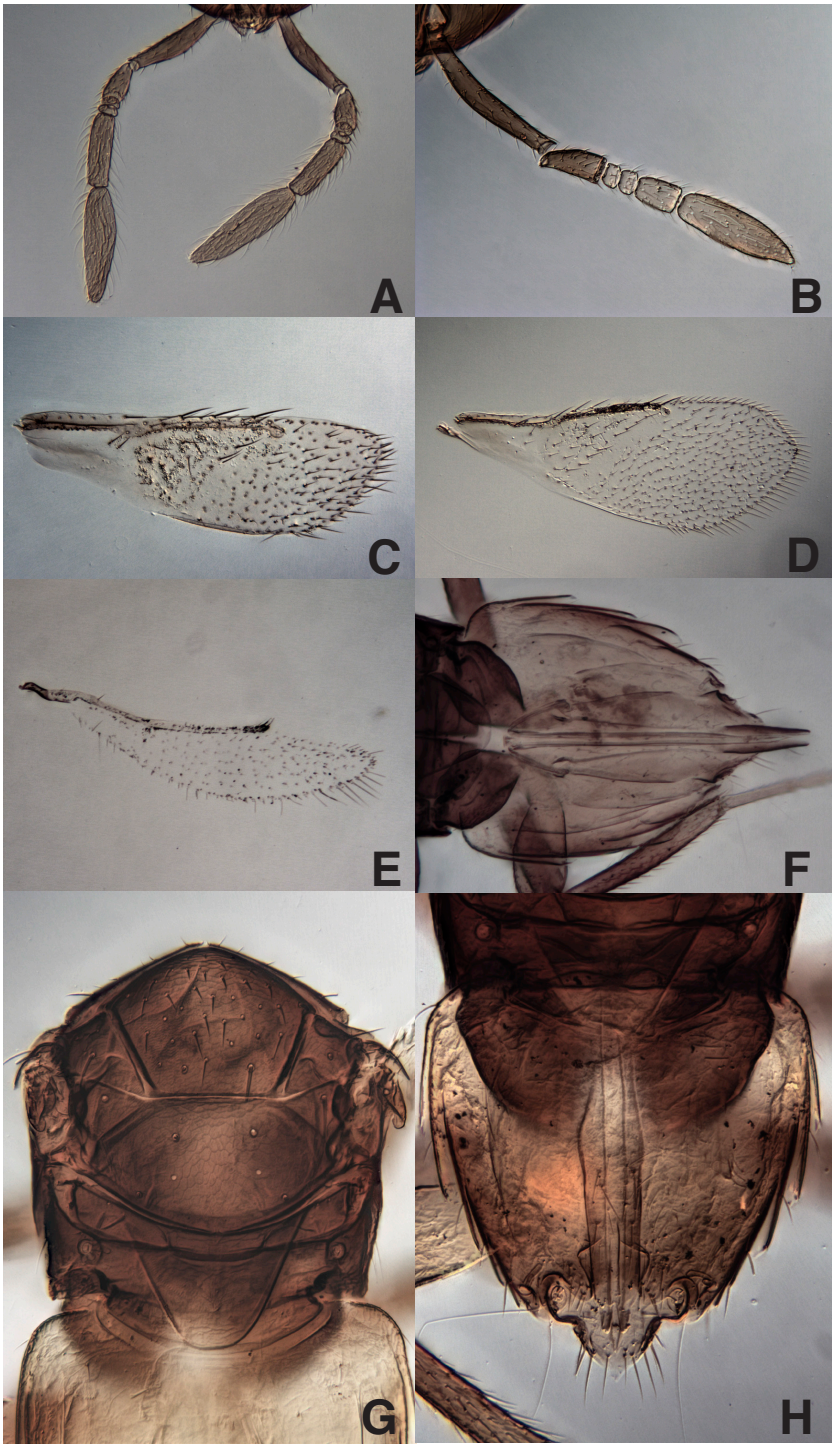

Figure 34: *Aphelinus asychis*, slide mounted specimens. A: male, antenna, lateral view (TAMUIC X0856568); B: female, antenna, lateral view (TAMUIC X0856569); C: male, forewing, dorsal view (TAMUIC X0856303); D: female, forewing, dorsal view (TAMUIC X0856301); E: female, hind wing, dorsal view (TAMUIC X0856301); F: female, metasoma, ventral view (TAMUIC X0856301); G: female, mesosoma, dorsal view (TAMUIC X0856301); H: male, genitalia, ventral view (TAMUIC X0856303).

F3, and club yellow, tip of club dusky; legs with all coxae brown, profemur and mesofemur dark brown with apex yellow or pale, metafemur yellow, protibia yellow, mesotibia and metatibia dark brown with apex yellow; metasoma yellow from base to apex, lateral margins of metasoma darker than mesal area except in basal quarter.

Body length. 0.86-0.92 mm (n=2; slide mounts).

Head (Figs. 33B and 34B). Width 0.76-1.13 head length in anterior view; frontovertex width 0.47-0.53x head width and 1.4-2.63x frontovertex length; posterior ocelli diameter 0.5x posterior ocelli to eye margin distance and 1.5x posterior ocelli to occipital margin distance; antenna as in Figure 32, B with scape length 6.45-6.55x scape width, pedicel length 1-92-2.08x pedicel width, F1 and F2 subquadrate, length of both 1.06-1.11x width, F3 length 1.31-1.54x F3 width, and club length 2.89-3.17x club width and 2.75-3.35x F3 width, with 8 longitudinal sensilla.

Mesosoma (Figs. 33D, F and 34G). Midlobe of mesoscutum length 0.66-0.79x midlobe width with two pairs of long setae (one pair lateral and one pair posterior) and 29 short setae; side lobes of mesoscutum each with one pair of long setae and one pair of short setae; scutellum with two pairs of long setae (one pair anterior and one pair posterior); mesotibial spur length 0.62-0.64x mesobasitarsus length, metatibial spur length 0.6-0.8x metabasitarsus length.

Forewing (Fig. 34D). Length 2.83x forewing width, longest marginal seta 0.2x forewing width; costal cell length 0.74x marginal vein length, with one line of 5 setae on ventral surface and 1 dorsal setae in apical quarter; submarginal vein with two setae; marginal vein with two rows of 10 large dorsal setae, one row of 5 small dorsal setae,

and one row of 7 ventral setae; interspace between basal cell and linea calva with 25 setae arranged in three complete line and one incomplete lines; linea calva closed with three setae at its posterior end, setae bordering linea calva proximally are arranged uniformly and evenly to posterior margin of wing.

Hind wing (Fig. 34E). Length 4.4x hind wing width, longest marginal seta 0.53x hind wing width.

Metasoma (Figs. 33D, F and 34F). Length 1-79-2.04x mesosoma length; ovipositor length 1.22-1.34x mesotibia length and 0.97-1.24x metatibia length; third valvula length 0.22-0.27x ovipositor length.

Description: Male (Figs. 33A, C, E and 34A, C, H). Similar to female except:

Color (Fig. 33A, C, E). All antennal segments yellowish brown; metasoma yellow at base darkening gradually to light brown at apex.

Head (Figs. 33A and 34A). Antenna with scape length 4.69-4.75x scape width with five pores along midline of single continuous convex ridge on ventral surface, pores small, approximately same diameter as base of adjacent seta, pedicel length 1.8-1.86x pedicel width, F1 length 0.59-0.62x F1 width, F2 length 0.54-0.62x F2 width, F3 length 3.47-3.69x F3 width, club length 0.59-0.68x club width and 1.52-1.58x F3 length.

Metasoma (Fig. 33C, E and 34H). Length 1.13-1.35x mesosoma length; phallobase length (including digiti) 5.38-7x phallobase width; digiti length 3.6-4.5x digiti width.

Type material.

Aphelinus asychis Walker 1839, lectotype female (BMNH, examined). Card-mounted. Label data: "*A. asychis* | Walker || *Aphelinus* | *asychis* | LECTOTYPE | M. de V. Graham | det. 1974 || B.M.N.H. TYPE | HYM | 5.2881".

Aphelinus euthria Walker 1839, lectotype female and paralectotype female **(**BMNH, examined**)**. Three paralectotype females.

Myina affinis Förster 1841, lectotype female (NHMV, examined). Card-mounted. Label data: "*Myina affinis* | Förster | Lectotype ♀|| *M. affinis* Förster || Collect. G. Mayr". Paralectotype female (NHMV, examined). Card-mounted. Label data: "*M. affinis* | Förster, Type || Collect. | G. Mayr".

Aphelinus brevicalcar Thomson 1876, lectotype female (LUZN, examined). Card-mounted. Label data: "*Aphelinus brevicalcar* | Lectotype ♀. Thomas. | M. de V. Graham || Lectotype || Type No. 1574:1".

Aphelinus brachyptera Kurdjumov 1913, lectotype female (NHMV, examined). Card-mounted. Label data: "*Aphelinus brachyptera* | (Först. MS). | Lectotype | M. de V. Graham || *A. brachyptera* | Förster Type || Collect. G. Mayr || 182".

Aphelinus dubia Kurdjumov 1913, lectotype female (NHMV, examined). Mounted on minuten pin on block. Label data: "*Aphelinus* | (Föst. MS.) K | Lectotype || *M. dubia* | Förster, Type || Collect. | G. Mayr". Paralectotypes, five females. Mounted on minuten pins on block. Label data as lectotype.

Other material examined. AUSTRALIA:Australian Capital Territory: 1 sex unknown, 3 males, 17 females. ANIC 64571-64591 (ANIC). BRAZIL: 57 females.

TAMU-ENTO X0852695-X0852751 (TAMU). CANADA: 16 females, 1 mixed series, 1 unknown. CNCHYMEN 122773-122774, 122777, 122805, 122828, 122830, 122832-122833, 122835-122839, 122843, 122849, 122891, 122893, 122897 (CNC). CANADA:Nova Scotia: 1 sex unknown. CNCHYMEN 122825 (CNC). CANADA:Ontario: 1 male, 2 sex unknowns, 4 females. CNCHYMEN 122728 (EMEC); TAMU-ENTO X0854432 (TAMU); CNCHYMEN 18232, 122727, 122738-122740 (CNC). CHILE: 7 males, 29 females. TAMU-ENTO X0852752-X0852753, X0852784-X0852793, X0852834-X0852837, X0852839-X0852844, X0852846-X0852847, X0852849-X0852854, X0852856-X0852861 (TAMU). EGYPT: 1 male, 3 females. BMNH(E) 1039587-1039590 (BMNH). FRANCE: 52 males, 1 mixed series, 8 sex unknowns, 3 unknowns, 81 females. EMEC 749093 (EMEC); BMNH(E) 1039558, 1039562, 1039575; ANIC 64736-64746, 64749-64765, 64772-64779 (ANIC); TAMU-ENTO X0616384-X0616385, X0852794-X0852803, X0852893-X0852917, X0852947, X0853323-X0853325, X0855642-X0855645, X0855777-X0855778, X0856082-X0856095, X0856301-X0856304, X0856306-X0856307, X0856319, X0856321-X0856322, X0856325, X0856327-X08563278, X0856330, X0856333, X0856337-X0856345, X0856568-X0856569, X0856625, X0856674 (TAMU); CNCHYMEN 19026 (CNC); UCRC 75231-75232, 326836, 326868, 326870 (UCRC); USNM 1212186-1212195, 1212272 (USNM). GERMANY: 2 males, 2 females. USNM 763812, 1119640-1119642 (USNM). INDIA: 1 sex unknown, 20 females. BMNH(E) 1039638 (BMNH); USNM 1119615, 1119620-1119631, 1119633-1119634, 1119637, 1119639, 1212205, 1212213-1212214 (USNM). ISRAEL: 7 males, 1 mixed series, 3 sex

unknowns, 15 females. UCRC 300205, 300211, 300225 (UCR); EMEC 749000, 749098-749099; UCRC 300206-300208, 300210, 300212-300224, 300226-300227, 326859 (UCRC). ITALY: 9 males, 2 sex unknowns, 19 females. BMNH(E) 1039570, 1039574, 1038774; X0856351, X0856358-X0856360, X0856362-X0856368, X0856564-X0856567, X8056361 (TAMU); CNCHYMEN 19045 (CNC); USNM 1212200-1212204, 1212206-1212209, 1212435 (USNM). JAPAN: 4 females, 5 males. CNCHYMEN 19030, 19032-19033, 19035-19036, 19038, 19040-19042 (CNC). MOROCCO: 5 males, 1 sex unknown, 15 females. TAMU-ENTO X0856308-X0856311, X0856313-X0856318, X0856320, X0856323- X0856324, X0856326, X0856329, X0856331-X0856332, X0856334-X0856336 (TAMU). NEPAL: 1 female. BMNH(E) 1039267 (BMNH). PAKISTAN: 20 males, 3 sex unknowns, 8 females. TAMU-ENTO X0852974-X0853002, X0854532, X0854632, X0854732 (TAMU). SOUTH AFRICA: 9 males, 5 females. ANIC 65020-65021, 65023-65029, 65032-65034 (ANIC); USNM 1119565, 1119573 (USNM). SPAIN: 6 males, 12 females. BMNH(E) 1039559, 1039561, 1039565-1039566, 1039568-1039569; TAMU-ENTO X0616389, X0616411, X0852950, X0856305, X0856346-X0856350, X0856352, X0856781 (TAMU); USNM 1212437 (USNM). SWEDEN: 4 males, 6 females. BMNH(E) 1039571-1039573, 1039578, 1039581-1039586 (BMNH). TURKEY: 2 females. BMNH(E) 1039563-1039564 (BMNH). UNITED KINGDOM: 2 males, 6 females. BMNH(E) 1038770-1038773, 1039560, 1039636-1039637 (BMNH); USNM 1212436 (USNM). USA:California: 1 female, 1 male. UCRC 75429, 75431 (UCRC); USA:California:Alameda Co.: 1 male, 1 unknown, 9 females. EMEC 749077-749079,

749081, 749083-749087, 749089, 749732 (EMEC). USA:Colorado: 3 males, 4 females. USNM 1119605-1119608, 1119612-1119614 (USNM). USA:Colorado:Larimer Co.: 2 females. USNM 1119578-1119579 (USNM). USA:Florida:Alachua Co.: 2 females. CNCHYMEN 122771, 122813 (CNC). USA:Hawaii: 3 females. USNM 1212218-1212220 (USNM).USA:Kansas:Riley Co.: 2 females. USNM 1119500, 1119580 (USNM). USA:Maine:Aroostook Co.: 1 female. USNM 1119576 (USNM). USA:Maryland:Prince George's Co.: 1 female. USNM 1119577 (USNM). USA:Maryland:Wicomico Co.: 1 female. USNM 1119599 (USNM). USA:Minnesota: 1 sex unknown, 1 female. USNM 1212238-1212239 (no date) (USNM). USA:Missouri:Wayne Co.: 1 unknown, 23 females. CNCHYMEN 122780-122782, 122783-122801, 122804, 122809-122811 (CNC). USA:Ohio:Franklin Co.: 5 females. USNM 1119610-1119611, 1119617-1119619 (USNM). USA:Oklahoma: 6 males, 2 mixed series, 18 females. EMEC 749510, 749578-749582, 749589, 749617, 749619, 749621-749635, 749664 (EMEC); TAMU-ENTO X0616388 (TAMU). USA:Oklahoma:Payne Co.: 5 mixed series, 1 female. USNM 1119550-1119553, 1212245, 1212438 (USNM). USA:Texas: 7 males, 1 sex unknown, 2 females. TAMU-ENTO X0852918-X0852925, X0853732, X0852938, (TAMU). Country not specified: 8 males, 9 females. UCRC 13848, 13996 (UCR); ANIC 64766-64771, 64780-64781, 65065-65067 (ANIC); EMEC 749618, 749620, 749636 (EMEC); USNM 1119589 (USNM).

Distribution. Old World and some New World populations, discussed below.

Discussion. The most notable distinction of *A. asychis* specimens is leg coloration as described in the Diagnosis. I am treating collections from Spain, Morocco, and Italy as conspecific, noting that the metafemora are dark brown [not yellow]. I am also treating the collection from England, Sussex as conspecific, noting that the profemora and mesofemora are yellow [not dark brown with apex yellow or pale]. I am treating the population from Hawaii, Hoda and India, Bangalore as conspecific, noting that the protibia are brown [not yellow].

Numerous populations of *A. asychis* were found in North America. The population from Texas, Randall Co. is presumed to be recovered from biological control program release of *A. asychis* against the Russian wheat aphid in that area. The population from Missouri, Wayne Co. was collected from malaise trap and one specimen from Florida was collected by a flight interception trap, both in the late 1980's. The populations from Oklahoma, Stillwater were from a lab culture of *A. asychis* for *Schizaphis graminum* biological control work. The two specimens collected from Kansas, Manhattan from spotted alfalfa aphid in a greenhouse is most likely part of agricultural research at Kansas State University. The series from California, Alameda Co. 1962 is from the UC Insectary and was possibly being research as candidate for biological control agent against yellow clover aphid or other aphid pests.

However, in a few cases, *A. asychis* was found in North America before any documented biological control releases. An *A. asychis* specimen was collected in Florida in 1952, however it does not have any associated host data. Two specimens from Maryland, one from *Myzus persicae* and one from strawberry aphids were collected in

1962 and 1950, respectively. One specimen from Maine in 1958 was collected from a *Capitophorus* aphid mummy. Two specimens from Colorado were collected from *Myzus persicae* mummies, once in 1940 and once in 1988. This record is especially interesting as it is close to the type locality and host of *A. semiflavus*. The specimens from Minnesota, Ohio, and California (UCRC 75429 and 75431) did not have collecting date or host information.

The female lectotype and paralectotype of *affinis* Förster was examined (NHMV, Vienna). They are point-mounted specimens in good condition. I concur with Graham (1976) that *affinis* Förster is a junior synonym of *asychis* Walker. The lectotype of *brachyptera* Kurdjumov (NHMV, Vienna) was examined. It is a brachypterous female mounted on a minuten pin through the mesosoma. I concur with Graham (1976) that *brachyptera* Kurdjumov is a junior synonym of *asychis* Walker. The lectotype female of *brevicalcar* Thomson (LUZN, Sweden) was examined. It is a card-mounted female in reasonably good condition. I concur with Graham (1976) that *brevicalcar* Thomson is a junior synonym of *asychis* Walker.

The type material of *dubia* Kurdjumov (NHMV, Vienna) which consists of a female lectotype and five female paralectotypes, mounted together on a small wooden block on minuten pins, and a second pin with a wooden block bearing five additional female paralectotypes, was examined. A red dot next to one pin identifies the lectotype. The specimens are dirty and in poor condition and the minuten pins are rusting. Although I note some color variation in the metasoma of these specimens, I concur with Graham (1976) that *dubia* Kurdjumov is a junior synonym of asychis Walker. The

lectotype female and paralectotype females of *euthria* Walker (BMNH, London) was examined. The lectotype and one paralectotype are mounted on the same card and are in poor condition (lectotype is missing all of the metasoma). Three additional paralectotypes individually card mounted and are in reasonably good condition. I concur with Graham (1976) that *euthria* Walker is a junior synonym of *asychis* Walker.

Aphelinus semiflavus *Howard 1908*

Aphelinus semiflavus Howard 1908.

Aphelinus brevipennis Girault 1917, synonymy by Gahan 1924.

Diagnosis. Female. Legs with all coxae brown [not with procoxae yellow], profemur, mesofemur, metafemur, protibia, mesotibia entirely yellow [not light or dark brown at base and yellow or pale at apex] and metatibia light brown with apex yellow [not entirely yellow or dark brown with apex yellow or pale]. Male. Similar except all antennal segments are yellowish brown [antennal segments not without uniformity in color], scape with five minute pores on convex ridge and with proximal most pore at midpoint of scape.

Description: Female (Figs. 35B, D, F and 36B, D – G).

Color (Fig. 35B, D, F). Head and mesosoma dark brown; radicle and basal portion of scape yellowish white, apical portion of scape and pedicel brown, and F1, F2, F3, and club yellow, tip of club dusky; legs with all coxae brown, profemur, mesofemur, metafemur, protibia, mesotibia entirely yellow and metatibia light brown with apex

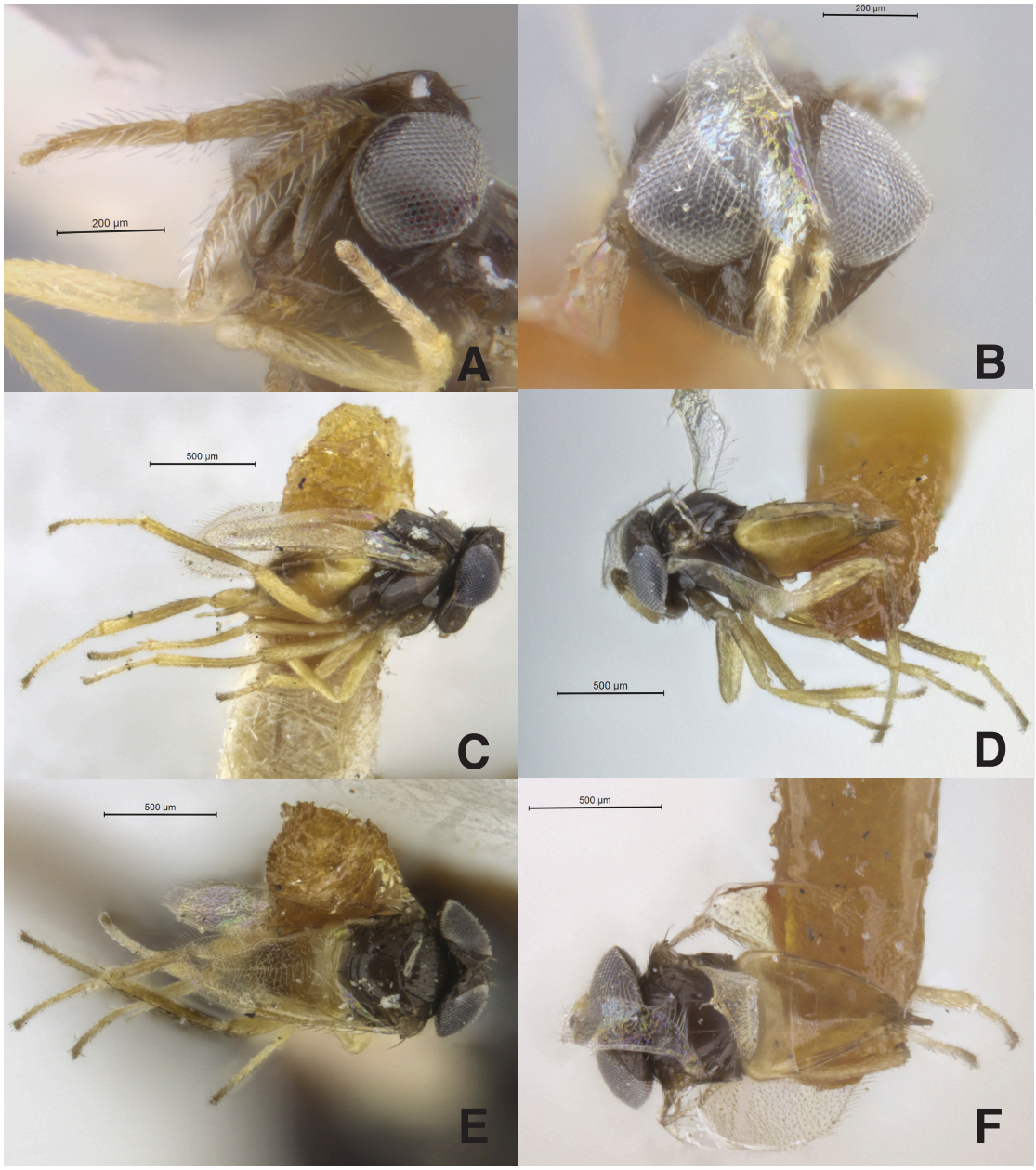

Figure 35: *Aphelinus semiflavus*, point-mounted specimens. A: male, antennae and face, anterior view (UCRC ENT 326803); B: female, antennae and face, anterior view (paralectotype); C: male, habitus, lateral view (USNMNH 2076436); D: female, habitus, lateral view (paralectotype); E: male, habitus, ventral view (USNMNH 2076436); F: female, habitus, ventral view (paralectotype).

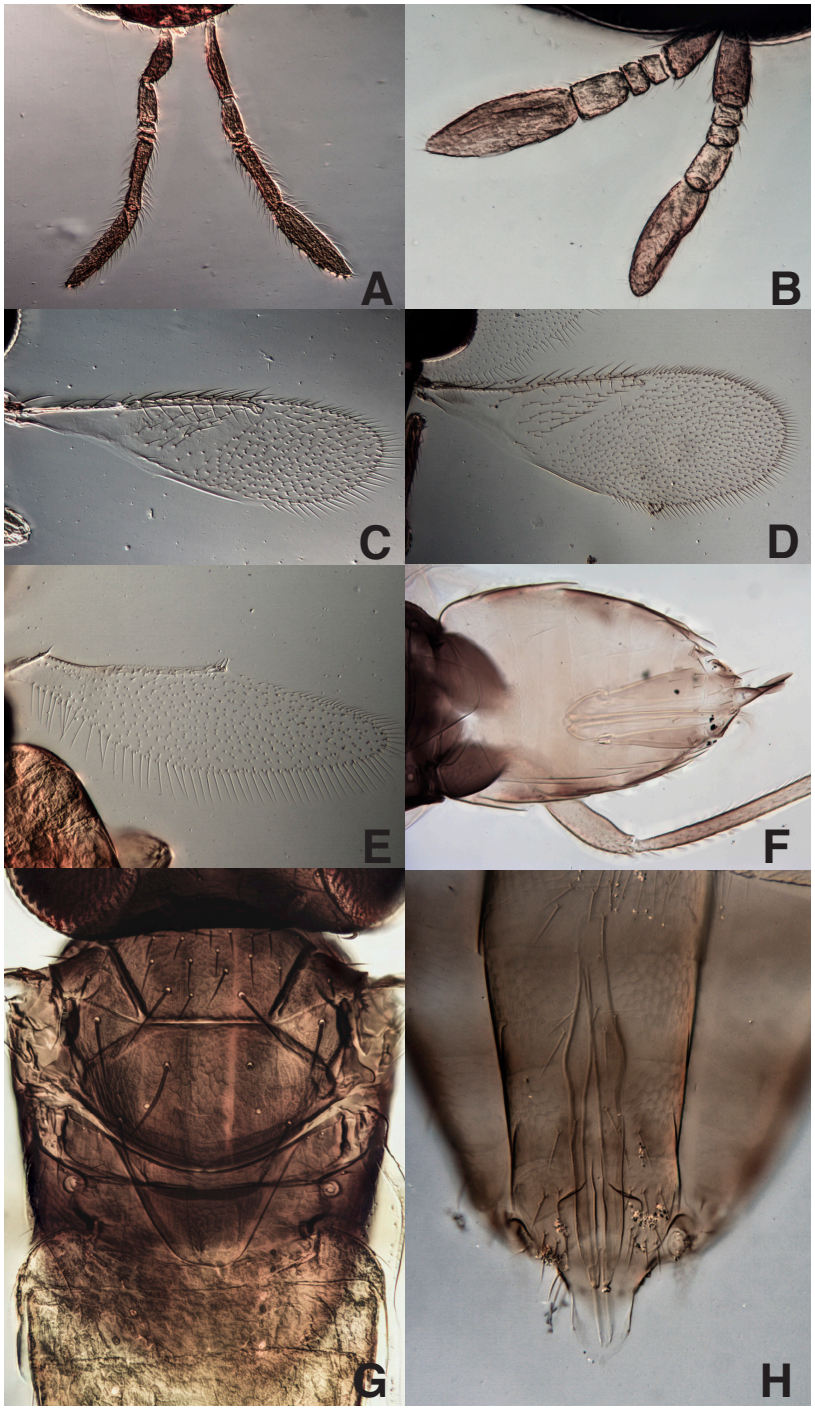

Figure 36: *Aphelinus semiflavus*, slide-mounted specimens. A: male, antenna, lateral view (paralectotype); B: female, antenna, lateral view (paralectotype); C: male, forewing, dorsal view (paralectotype); D: female, forewing, dorsal view (paralectotype); E: female, hind wing, dorsal view (paralectotype); F: female, metasoma, ventral view (UCRC 326827); G: female, mesosoma, dorsal view (paralectotype); H: male, genitalia, ventral view (UCRC 326826).

yellow; metasoma yellow from base to apex, lateral margins of metasoma darker than mesal area except in basal quarter.

Body length. 0.83-1.04 mm (n=3; slide mounts) (Paralectotypes 0.5-0.63 mm).

Head (Figs. 35B and 36B). Width 1.19-1.31x head length in anterior view; frontovertex width 0.43-0.52x head width and 3.14-3.67x frontovertex length; posterior ocelli diameter 0.5x posterior ocelli to eye margin distance and 1.5x posterior ocelli to occipital margin distance; antenna as in Figure 34, B with scape length 6.8-7x scape width, pedicel length 2-2.25x pedicel width, F1 and F2 subquadrate, length of both 0.91-1.13x width, F3 length 1.5-1.91x F3 width, and club length 3.18-4.43x club width and 2.62-2.92x F3 width, with 8 longitudinal sensilla.

Mesosoma (Figs. 35D, F and 36G). Midlobe of mesoscutum length 0.74-0.76x midlobe width with two pairs of long setae (one pair lateral and one pair posterior) and 30-31 short setae; side lobes of mesoscutum each with one pair of long setae and one pair of short setae; scutellum with two pairs of long setae (one pair anterior and one pair posterior); mesotibial spur length 0.6-0.65x mesobasitarsus length, metatibial spur length 0.37-0.45x metabasitarsus length.

Forewing (Fig. 36D). Length 2.33-2.81x forewing width, longest marginal seta 0.09-0.13x forewing width; costal cell length 0.61-0.67x marginal vein length, with one line of 10-12 setae on ventral surface and 1-2 dorsal setae in apical quarter; submarginal vein with two setae; marginal vein with two rows of 14-17 large dorsal setae, one row of 7-13 small dorsal setae, and one row of 7-10 ventral setae; interspace between basal cell and linea calva with 31-40 setae arranged in three complete line and one to two

incomplete lines; linea calva closed with 3 setae at its posterior end, setae bordering linea calva proximally are arranged uniformly and evenly to posterior margin of wing.

Hind wing (Fig. 36E). Length 3.54-3.74x hind wing width, longest marginal seta 0.23-0.33x hind wing width.

Metasoma (Figs. 35D, F and 36F). Length 2x mesosoma length; ovipositor length 0.87x mesotibia length and 1.24x metatibia length; third valvula length 0.27x ovipositor length.

Description: Male (Figs. 35A, C, E and 36A, C, H). Similar to female except:

Color (Fig. 35A, C, E). All antennal segments yellowish brown; metasoma yellow at base darkening gradually to light brown at apex.

Head (Figs. 35A and 36A). Antenna with scape length 6.4x scape width with five pores along midline of single continuous convex ridge on ventral surface, pores small, approximately same diameter as base of adjacent seta, pedicel length 1.67-2.2x pedicel width, F1 length 0.6x F1 width, F2 length 0.55-0.6x F2 width, F3 length 4.2-4.4x F3 width, club length 6.2x club width and 1.48x F3 length.

Metasoma (Fig. 35C, E and 36H). Length 1.33x mesosoma length; phallobase length (including digiti) 6x phallobase width; digiti length 4.5x digiti width.

Type material examined.

Aphelinus semiflavus Howard 1908, lectotype female (USNM, examined). Label data: “Type | No. 12031 | USNM || Aphelinus n.sp. | near mali || Myzus persicae | Ft. Collins, Colo. | C.B. Gillette | det. July 15, 1908”. The slide containing the lectotype has 3 female and 2 male specimens under one cover slip. The female specimen in the lowest

middle portion of the slide is herein designated lectotype, and the slide has been labeled accordingly. Paralectotypes. (USNM, examined). Two females and two males on same slide, data as lectotype. Two females, one male, one sex unknown, on cardmounts with label data reading as "*Myzus persicae* | Fort Collins, CO || C. B. Gillette | Det. July, 15, 08 || Type | No. 12031| U.S.N.M.".

Aphelinus brevipennis Girault 1918, lectotype female. (USNM, examined). Slide-mounted parts: "Aphelinus | brevipennis | Girault | female type || 19801". Point mount: "Ohio || 1693 || 19801". The female lectotype designated herein is mounted on a point, and parts consisting of an antenna, a forewing, a hind wing, a midleg and a hindleg were dissected by Girault and mounted on a slide. Paralectotype male (USNM). Point-mounted. Label data: "Ohio || 1704 || 19801".

Other material examined. CANADA: 2 sex unknowns, 18 females, 8 males. CNCHYMEN 18213-18219, 122831, 122834, 122842, 122844-122847, 122850-122860, 122867, 122894-122895 (CNC). CANADA:Nova Scotia: 5 males. CNCHYMEN 122822-122824, 122826-122827 (CNC). FRANCE: 1 male. UCRC 326865 (UCRC).INDIA: 1 unknown, 2 sex unknowns. USNM 1119632, 1119636, 1119638 (USNM). KOREA: 5 females, 16 males. TAMU-ENTO X0856593-X0856613 (TAMU). MEXICO: 3 males. TAMU-ENTO 616387, X0853003, X0853005 (TAMU). SPAIN: 1 male. CNCHYMEN 19028 (CNC). USA:California: 1 unknown, 3 sex unknowns, 57 females, 26 males, 2 mixed seriess. UCRC 326827, 326863, 326887 (UCR); UCRC 14057, 326787, 326798, 326803, 326822-326826, 326828-326829, 326832-326833, 326838, 326840, 326842-326843, 326845-326850, 326853, 326855,

326860-326861, 326866, 326869, 326874-326877, 326879, 326881-326883 (UCRC); EMEC 749011-749021, 749024-749027, 749029, 749032-749034, 749036-749039, 749041-749046, 749048, 749080, 749088, 749511, 749513-749514, 749517, 749562, 749567-749568, 749574, 749577, 749601, 749607, 749611-749616 (EMEC). USA:California:Alameda Co.: 3 females, 1 male. ANICDatabaseNo 64521 (ANIC); EMEC 749082, 7490022-7490023 (EMEC). USA:California:Fresno Co.: 1 unknown. USNM 1119584 (USNM). USA:California:Kern Co.: 11 females, 7 males. EMEC 749028, 749047, 749049, 749512, 749561, 749590-749597, 749602-749605, 749637 (EMEC). USA:California:Los Angeles Co.: 2 sex unknowns, 1 female. USNM 1212283-1212284 (USNM); EMEC 749563 (EMEC). USA:California:Monterey Co.: 2 males. EMEC 749030-749031 (EMEC). USA:California:Orange Co.: 3 females, 3 males. UCRC 326831, 326834-326835, 326837 (UCR); UCRC 326803, 326830 (UCRC). USA:California:Riverside Co.: 1 unknown, 1 sex unknown, 16 females, 6 males, 1 mixed series. UCRC 326864 (UCR); UCRC 13843-13845, 326839, 326871, 326886, UCRC 13994, UCRC 13995 (UCRC); EMEC 749035, 749040, 749560, 749572, 749575-749576, 749583-749588, 749600, 749608-749610 (EMEC). USA:California:Santa Barbara Co.: 1 female. CNCHYMEN 122848 (CNC). USA:California:Santa Clara Co.: 1 female, 1 male. EMEC 749090, 749092 (EMEC). USA:California:Sonoma Co.: 1 male. EMEC 749091 (EMEC). USA:California:Tulare Co.: 1 female. BMNH(E) 1039253 (BMNH). USA:Colorado:Delta Co.: 1 mixed series. UCRC 13847 (UCRC). USA:Colorado:Larimer Co.: 2 sex unknowns, 1 female, 11 males. USNM 121228, 1119635, 1119643, 1212226-1212236 (USNM). USA:Florida: 1

male. CNCHYMEN 122814 (CNC). USA:Florida:Palm Beach Co.: 1 female. USNM 1119593 (USNM). USA:Georgia:Clarke Co.: 2 females, 5 males. CNCHYMEN 122803, 122806-122808, 122819-122821 (CNC). USA:Kansas:Riley Co.: 2 females, 1 male, 1 mixed series. USNM 763852, 1119509, 1119581, 1119601 (USNM). USA:Maine:Aroostook Co.: 2 females. USNM 1119572, 1119575 (USNM). USA:Maine:Penobscot Co.: 2 mixed series. USNM 763837, 763862 (USNM). USA:Maryland: 1 female. CNCHYMEN 122802 (CNC). USA:Massachusetts:Barnstable Co.: 4 females, 1 male. USNM 1212210-1212211, 1212215-1212217 (USNM). USA:Minnesota: 1 mixed series. USNM 763857 (USNM). USA:Montana: 1 females. TAMU-ENTO X0616383 (TAMU). USA:New Jersey:Morris Co.: 1 female, 1 male. EMEC 749569, 749571 (EMEC). USA:New Jersey:Ocean Co.: 1 female. EMEC 749570 (EMEC). USA:New Mexico: 1 male. USNM 1212244 (USNM). USA:New Mexico:Dona Ana Co.: 2 females, 1 male. USNM 1212222-1212224 (USNM). USA:New York:Onondaga Co.: 1 sex unknown. USNM 1119570 (USNM). USA:New York:Tompkins Co.: 7 females, 2 males. USNM 763827, 1119595-1119598, 1119602-1119604 (USNM); UCRC 13846 (UCRC). USA:North Carolina:Jackson Co.: 2 females. CNCHYMEN 122816-122817 (CNC). USA:Ohio:Franklin Co.: 2 unknowns, 3 females, 4 males. USNM 763832, 1119582-1119583, 1119587-1119588, 1119590-1119592, 1119616 (USNM). USA:Oregon:Lane Co.: 1 female. USNM 1212237 (USNM). USA:Pennsylvania: 1 female. USNM 1119571 (USNM). USA:South Carolina:Pickens Co.: 1 male. UCRC 13992 (UCRC). USA:Texas: 2 females. TAMU-ENTO X0852937, X0852939 (TAMU). USA:Texas:Brazos Co.: 1 female. TAMU-

ENTO X0852940 (TAMU). USA:Texas:Carson Co.: 2 females. TAMU-ENTO X0852928-X0852929 (TAMU). USA:Virginia: 3 females. TAMU-ENTO X0852934, X0852936 (TAMU); CNCHYMEN 122818 (CNC). Country not specified: 5 females, 1 male, 1 mixed series. USNM 763817, 763822, 763842, 763847, 763867 (USNM); UCRC 326685 (UCR); EMEC 398444 (EMEC).

Distribution. New World, with few populations in Old World, discussed below.

Discussion. There has been confusion in that past on whether or not *A. asychis* and *A. semiflavus* are two separate species. Based on the material examined, leg coloration patterns are clearly different among the two. Regarding the New World populations examined, I am treating most North American populations as *semiflavus*, noting that in the Mexico and Canada Winnipeg populations, the metatibia are yellowish brown [not dark brown at base with apex pale].

The India, Bangalore and Iran, Dezful populations are being treated as sp. nr. *semiflavus*, noting that the India population has midtibia and midfemora with brown [not yellow] and the Dezful, Iran population has legs like semiflavus except one female with brown [not yellow] on midtibia and midfemora.

There is one series from Virginia with one specimen that we are treating as ? *semiflavus*, noting that the forefemora and foretibia and brown [not yellow].

Future work should use molecular data to determine whether populations of *A. semiflavus* in Old World vs. New World are in fact one species, are races of one species with different host ranges, or are two distinct cryptic species.

I have examined the holotype and allotype of *brevipennis* Girault and agree with the conclusion of Gahan 1924 that it is a junior synonym of *semiflavus* Howard. Although Ferrière (1965), Nikol'skaya and Yasnosh (1966), and Yasnosh (1978) treated *semiflavus* as a junior synonym of *asychis* Walker, for reasons discussed above I consider it to be a distinct and valid species.

Other Potential New Species

There are two additional potentially new species, but there is not enough material to describe them. The first potential new species is from Canada, Harrow which has leg coloration like *asychis*, but includes a brown metafemora [not yellow]. There are two other Canadian series with one specimen in each series that also has this leg coloration.

The second potential new species from England, Dorking, represented by a single specimen, has leg coloration with all segments very dark brown.

CHAPTER VI

CONCLUSIONS

The phylogenetic analyses conducted in this thesis help lay a preliminary phylogenetic framework for the classification of *Aphelinus*. It was found (1) that *A. perpallidus* is sister taxon to all other included *Aphelinus* species (supporting its differentiation at subgenus rank) (2) that *A. abdominalis* and *A. asychis* are members of a clade that is sister group to other included *Aphelinus* sp.; (3) that the *varipes* and *mali* groups are monophyletic (but the latter is weakly supported in maximum likelihood analysis); and (4) that the placement of *A.* nr. *daucicola* is unstable. Although taxon sampling is not complete, the number of *Aphelinus* taxa included in this thesis included representatives of species groups and subgenera that before had not been included in studies of the genus (i.e., *abdominalis* group, *Mesidia* subgenus). To further develop this phylogenetic framework, future work should broaden in taxon sampling, particularly by including more representatives from the *daucicola*, *abdominalis, asychis,* and *nepalensis* species groups of subgenus *Aphelinus*; additional taxa from subgenus *Mesidia*; and further outgroups.

In developing the morphological character set for investigating evolution of morphology in *Aphelinus*, a survey of the modified structures on male scapes was conducted. This study serves as a first step in understanding the interesting and modified structures on *Aphelinus* male scapes. From this, we can begin to understand mate selection strategies in this group, as well as add to the knowledge base of sex glands in

parasitic Hymenoptera, from which information regarding *Aphelinus* was lacking. In addition to sexual selection and taxonomy, morphologically distinctive components of the male scape suggests that they may also be useful for phylogenetic inferences within *Aphelinus*, and may have broad phylogenetic signal across the genus. This was tested in Chapter IV, and it was discovered that the carina delimitation character has strong phylogenetic signal (CI=1 RI=1). Future SEM work should include additional representatives from each species group and other *Aphelinus* subgenera. Future TEM work is needed to investigate whether or not the glandular complex in *Aphelinus* is consistent with the type I secretory cells documented in other chalcidoid taxa.

While investigating evolution of morphological characters in *Aphelinus*, wing characters, specifically the number and arrangement of setae in the interspace between the basal cell and linea calva and the number of setae on the ventral surface of the costal cell, were observed to be taxonomically important in diagnosing species groups, corresponding with what has been found in previous work. The internal surfaces of the posterior-most sternum in males and digiti length were also shown to have phylogenetic signal and be taxonomically useful. To further understand the evolution of morphological characters in *Aphelinus*, future work should include broader taxon sampling in the species groups and subgenera that were not well represented and the species groups and subgenera that were not represented at all.

Through the development of a morphological character set, a revision of the *Aphelinus asychis* species group was conducted. It was determined that the two existing valid species within the *asychis* group, *A. asychis* and *A. semiflavus*, are in fact two

distinct cryptic species and were redescribed. After coding morphological characters for all available material of species in the *A. asychis* group, including representatives of cultures from Kazmer et al (1996), two new species (one from China and one from Kazakhstan) were described.

In summary, the comprehensive and robust classification of *Aphelinus,* and specifically of the *Aphelinus asychis* species group, will greatly facilitate the use of species in this group in biological control programs against important agricultural pests. The clarification of *Aphelinus* species names will also aid in studies of parasitoid speciation, host switching, and mate recognition. The revision and associated digital electronic products will benefit both specialists in parasitoid taxonomy and biological control researchers.

LITERATURE CITED

Altschul SF, Gish W, Miller W, Myers EW, Lipman DJ. 1990. Basic local alignment search tool. *Journal of Molecular Biology* **215**(3): 403-410.

Amornsak W, Cribb B, Gordh G. 1998. External morphology of antennal sensilla of *Trichogramma australicum* Girault (Hymenoptera: Trichogrammatidae). *International Journal of Insect Morphology and Embryology* **27**(2): 67-82.

Arce Gomez S, Rumiatto M. 1989. Evaluation of the biological control of *Schizaphis graminum* (Rondani, 1852) by exotic introduced parasites. *Documentos, Unidade de Execução de Pesquisa de Âmbito Estadual de Dourados, EMBRAPA, Brazil* **39**: 163-164.

Ashmead WH. 1888. Descriptions of some unknown parasitic Hymenoptera in the collection of the Kansas State Agricultural College received from Prof. EA Popenoe. *Bulletin of the Kansas Agricultural Experiment Station* **3**: i-viii.

Askar S, El-Hussieni M. 2015. Biological aspects of the aphid parasitoid *Aphelinus albipodus* (Hayat & Fatima) (Hymenoptera: Aphelinidae) parasitizing mealy plum aphid *Hyalopterus pruni* (Geoffroy) (Homoptera, Aphidoidea). *Egyptian Journal of Biological Pest Control* **25**(3): 619-623.

Bin F, Vinson SB. 1986. Morphology of the antennal sex-gland in male *Trissolcus basalis* (Woll.) (Hymenoptera: Scelionidae), an egg parasitoid of the green stink bug, *Nezara viridula* (Hemiptera: Pentatomidae). *International Journal of Insect Morphology and Embryology* **15**(3): 129-138.

Bin F, Wäckers F, Romani R, Isidoro N. 1999. Tyloids in *Pimpla turionellae* (L.) are release structures of male antennal glands involved in courtship behaviour (Hymenoptera: Ichneumonidae). *International Journal of Insect Morphology and Embryology* **28**(1): 61-68.

Boucek Z, Graham MdV. 1978. British check-list of Chalcidoidea (Hymenoptera): taxonomic notes and additions. *Entomologist's Gazette* **29**(4): 225-235.

Brewer MJ, Nelson DJ, Ahern RG, Donahue JD, Prokrym DR. 2001. Recovery and range expansion of parasitoids (Hymenoptera: Aphelinidae and Braconidae) released for biological control of *Diuraphis noxia* (Homoptera: Aphididae) in Wyoming. *Environmental Entomology* **30**(3): 578-588.

Campbell B, Heraty J, Rasplus J, Chan K, Steffen-Campbell J, Babcock C. 2000. Molecular systematics of the Chalcidoidea using 28S-D2 rDNA. In *Hymenoptera—Evolution, Biodiversity and Biological Control*, pp. 59-73. CSIRO Publishing, Collingwood, Australia.

Carver M. 1980. A new species of *Aphelinus* [*prociphili*] Dalman (Hymenoptera: Chalcidoidea: Encyrtidae) [parasite of the pemphigine aphid, *Prociphilus fraxinifolii*]. *Proceedings of the Entomological Society of Washington* **82**: 536-540.

Cate R, Eikenbary R, Morrison R. 1977. Preference for and effect of greenbug parasitism and feeding by *Aphelinus asychis*. *Environmental Entomology* **6**(4): 547-550.

Cate RH, Archer RD, Eikenbary KJ, Starks RD, Morrison. 1973. Parasitization of the greenbug by *Aphelinus asychis* and the effect of feeding by the parasitoid on aphid mortality. *Environmental Entomology* **2**(4): 549-554.

Christiansen-Weniger P. 1994. Morphological observations on the preimaginal stages of *Aphelinus varipes* (Hymenoptera: Aphelinidae) and the effects of this parasitoid on the aphid *Rhopalosiphum padi* (Homoptera: Aphididae). *Entomophaga* **39**(3-4): 267-274.

Clausen CP. 1956. Biological control of insect pests in the continental United States. *United States Department of Agriculture Technical Bulletin.* **1139**: 1-151.

-. 1978. *Introduced Parasites and Predators of Arthropod Pests and Weeds: a World Review*. Agriculture Handbook 480, USDA, Washington, D.C., 545 pp.

Conesa A, Götz S, Garcia-Gomez JM, Terol J, Talon M, Robles M. 2005. Blast2GO: a universal tool for annotation, visualization and analysis in functional genomics research. *Bioinformatics* **21**: 3674-3676.

Dahms E. 1973. Courtship behaviour of *Melittobia australica* Girault, 1912, (Hymenoptera: Eulophidae). *Memoirs of the Queensland Museum* **16**: 411-414.

-. 1984a. An interpretation of the structure and function of the antennal sense organs of *Melittobia australica* (Hymenoptera: Eulophidae) with the discovery of a large dermal gland in the male scape. *Memoirs of the Queensland Museum* **21**(2): 361-377.

-. 1984b. Revision of the genus *Melittobia* (Chalcidoidea: Eulophidae) with the description of seven new species. *Memoirs of the Queensland Museum* **21**: 271-336.

Dalla Torre K. 1898. Catalogus Hymenopterorum hucusque descriptorum systematicus et synonymicus. In *Chalcididae et Proctotrupidae*, Vol V, p. 221, Lepzig.

De Santis L. 1948. Estudio monográfico de los afelínidos de la República Argentina (Hymenoptera, Chalcidoidea). *Revista del Museo de La Plata (Nueva Serie)* **5**: 23–280.

Elliott N, Burd J, Armstrong J, Walker C, Reed D, Peairs F. 1995. Release and recovery of imported parasitoids of the Russian wheat aphid in eastern Colorado. *Southwestern Entomologist* **20**(2): 125-129.

Evans G, Schauff M, Kokyokomi M, Yokomi R. 1995. A new species of *Aphelinus* (Hymenoptera: Aphelinidae) that parasitizes the spirea aphid, *Aphis spiraecola* patch (Homoptera: Aphididae). *Proceedings of the Entomological Society of Washington* **97**: 17–21.

Ferrière C. 1965. *Hymenoptera Aphelinidae d'Europe et du Bassin Méditerraneéen. Faune de l'Europe et du Bassin Méditerraneéen.* Masson et Cie èditeurs, Paris.

Ferry-Graham LA, Bolnick DI, Wainwright PC. 2002. Using functional morphology to examine the ecology and evolution of specialization. *Integrative and Comparative Biology* **42**(2): 265-277.

Florey P, Humphries C, Kitching I, Scotland R, Siebert D, Williams M. 1992. *Cladistics. A practical course in systematics.* Clarendon Press, Oxford.

Gahan AB. 1925. Some new parasitic Hymenoptera with notes on several described forms. *Proceedings of the United States National Museum* **65**: 1-23.

Gerling D, Roitberg B, Mackauer M. 1990. Instar-specific defense of the pea aphid, *Acyrthosiphon pisum*: Influence on oviposition success of the parasite *Aphelinus asychis* (Hymenoptera: Aphelinidae). *Journal of Insect Behavior* **3**(4): 501-514.

Gibson GA, Huber JT, Woolley JB. 1997. *Annotated keys to the genera of Nearctic Chalcidoidea (Hymenoptera)*. NRC Research Press.

Girault A. 1911. A new aphid-infesting *Aphelinus* which is not black. *Entomologist* **44**: 178.

-. 1913a. Australian Hymenoptera Chalcidoidea-IV. The family Eulophidae with descriptions of new genera and species. *Memoirs of the Queensland Museum*. **2**: 140-296

-. 1913b. *A few new chalcidoid Hymenoptera from Queensland, Australia*. Wisconsin Natural History Society.

-. 1915. Australian Hymenoptera Chalcidoidea VII - The family Encyrtidae with descriptions of new genera and species. *Memoirs of Queensland Museum* **4**: 1-184.

-. 1929. Description of a case of lunacy in Homo and of new six-legged articulates. Published privately, Brisbane, 4pp.

-. 1932. New lower Hymenoptera from Australia and India. Published privately, Brisbane, 6pp.

Goodpasture C. 1975. Comparative courtship behavior and karyology in *Monodontomerus* (Hymenoptera: Torymidae). *Annals of the Entomological Society of America* **68**(3): 391-397.

Gordh G, DeBach P. 1978. Courtship behavior in the *Aphytis lingnanensis* group, its potential usefulness in taxonomy, and a review of sexual behavior in the parasitic Hymenoptera (Chalcidoidea: Aphelinidae). *Hilgardia* **46**(2): 37-75.

Graham MWRDV. 1976. The British species of *Aphelinus* with notes and descriptions of other European Aphelinidae (Hymenoptera). *Systematic Entomology* **1**(2): 123-146.

Guerrieri E, Pedata P, Romani R, Isidoro N, Bin F. 2001. Functional anatomy of male antennal glands in three species of Encyrtidae (Hymenoptera: Chalcidoidea). *Journal of Natural History* **35**(1): 41-54.

Hagen KS, van den Bosch R. 1968. Impact of pathogens, parasites, and predators on aphids. *Annual Review of Entomology* **13**(1): 325-384.

Haldeman S. 1851. *Eriophilus mali*. *Pennsylvania Farm Journal* **1**: 130-131.

Hayat M. 1972. The species of *Aphelinus* Dalman, 1820 [Hymenoptera: Aphelinidae] from India. *Entomophaga* **17**(1): 49-58.

Hayat M. 1983. The genera of Aphelinidae (Hymenoptera) of the world. *Systematic Entomology* **8**(1): 63-102.

-. 1990. Taxonomic studies on *Aphelinus* (Hymenoptera: Aphelinidae). II. A new subgenus from India, with comments on *Mesidia* and *Mesidiopsis*. *Oriental Insects* **24**: 253-257.

-. 1991a. Taxonomic studies on *Aphelinus* (Hymenoptera: Aphelinidae). III. Notes on *A. japonicus* Ashmead and *A. howardii* Ashmead. *Entomon* **16**(3): 179-181.

-. 1991b. Taxonomic studies on *Aphelinus* (Hymenoptera: Aphelinidae). IV. A new and three known species from Nepal. *Entomon* **16**(3): 183-186.

-. 1998. Aphelinidae of India (Hymenoptera: Chalcidoidea): a taxonomic revision. *Memoirs on Entomology, International* **13**: 1-416

Hayat M, Fatima K. 1992. Taxonomic studies on *Aphelinus* (Hymenoptera: Aphelinidae). V. Description of a new species and further records from *A. gossypii* with a new synonymy. *Entomon* **17**(1-2): 103-107.

Heimpel GE, Ragsdale DW, Venette R, Hopper KR, Rutledge CE, Wu Z. 2004. Prospects for importation biological control of the soybean aphid: anticipating potential costs and benefits. *Annals of the Entomological Society of America* **97**(2): 249-258.

Hennessey R. 1981a. Setal patterns of the wings of *Aphelinus*, *Mesidia*, and *Mesidiopsis* (Hymenoptera: Aphelinidae), their value as taxonomic characters. *Entomophaga* **26**(4): 363-374.

-. 1981b. At-rest setal wing coupling and restraining mechanisms in the Encyrtidae and Aphelinidae (Hymenoptera: Chalcidoidea). *Annals of the Entomological Society of America* **74**(2): 172-176.

Heraty J, Burks R, Cruaud A, Liljeblad J, Munro J, Mottern J, Murray E, Triapitsyn S, George J, Rasplus J, Gibson G, Delvare G, Janšta P, Gumovsky A, Huber J, Woolley J, Dal Molin A, Krogmann L, Heydon S, Polaszek A, Schmidt S,

Darling D, Gates M, Baur H, Pinto J, van Noort S, & Yoder M. 2013. A phylogenetic analysis of the megadiverse Chalcidoidea (Hymenoptera). *Cladistics* **29**(5): 466-542.

Heraty JM, Woolley JB, Hopper KR, Hawks DL, Kim J-W, Buffington M. 2007. Molecular phylogenetics and reproductive incompatibility in a complex of cryptic species of aphid parasitoids. *Molecular Phylogenetics and Evolution* **45**(2): 480-493.

Hopper K, Coutinot D, Chen K, Kazmer D, Mercadier G, Halbert S, Miller R, Pike K, Tanigoshi L. 1998. Exploration for natural enemies to control Diuraphis noxia (Homoptera: Aphididae) in the United States. *Response model for an introduced pest—the Russian wheat aphid Thomas Say Publications in Entomology, Entomological Society of America, Lanham, MD*: 167-182.

Hopper KR, Woolley JB, Hoelmer K, Wu K, Qiao G-X, Lee S. 2012. An identification key to species in the *mali* complex of *Aphelinus* (Hymenoptera, Chalcidoidea) with descriptions of three new species. *Journal of Hymenoptera Research* **26**: 73-96.

Howard L. 1908. Upon the aphis-feeding species of *Aphelinus*. *Entomological News* **19**(8): 365-367.

-. 1914. Concerning some Aphelininae. *Proceedings of the Entomological Society of Washington* **16**(2): 79-85.

-. 1917. A new aphis-feeding *Aphelinus*. *Proceedings of the Biological Society of Washington* **30**: 77.

Huang J. 1994. *Systematic studies on Aphelinidae of China (Hymenoptera: Chalcidoidea)*. Chongqing Publishing House.

ICZN. 1999. *International Code of Zoological Nomenclature*. Fourth Edition. The International Trust for Zoological Nomenclature, London, UK. 306 pp.

Isidoro N, Bin F. 1995. Male antennal gland of *Amitus spiniferus* (Brethes) (Hymenoptera: Platygastridae), likely involved in courtship behavior. *International Journal of Insect Morphology and Embryology* **24**(4): 365-373.

Isidoro N, Bin F, Colazza S, Vinson S. 1996. Morphology of antennal gustatory sensilla and glands in some parasitoid Hymenoptera with hypothesis on their role in sex and host recognition. *Journal of Hymenoptera Research* **5**: 206-239.

Isidoro N, Bin F, Romani R. 1999. Diversity and function of male antennal glands in Cynipoidea (Hymenoptera). *Zoologica Scripta* **28**(1-2): 165-174.

Japoshvili G, Abrantes I. 2006. *Aphelinus* species (Hymenoptera: Aphelinidae) from the Iberian Peninsula, with the description of one new species from Portugal. *Journal of Natural History* **40**(13-14): 855-862.

Johnson J, Eikenbary R, Holbert D. 1979. Parasites of the greenbug and other graminaceous aphids: identity based on larval meconia and features of the empty aphid mummy. *Annals of the Entomological Society of America* **72**(6): 759-766.

Kazmer DJ, Maiden K, Ramualde N, Coutinot D, Hopper KR. 1996. Reproductive compatibility, mating behavior, and random amplified polymorphic DNA variability in some *Aphelinus asychis* (Hymenoptera: Aphelinidae) derived from the Old World. *Annals of the Entomological Society of America* **89**(2): 212-220.

Kim JW, Heraty J. 2012. A phylogenetic analysis of the genera of Aphelininae (Hymenoptera: Aphelinidae), with a generic key and descriptions of new taxa. *Systematic Entomology* **37**(3): 497-549.

Li C, Zhang S. 2004. A new species and a new record of *Aphelinus* Dalman (Hymenoptera: Aphelinidae) from China. *Entomotaxonomia* **27**(1): 69-73.

Liao D, Li X, Pang X, Chen T. 1987. *Economic insect fauna of China*., Vol 34, *Hymenoptera: Chalcidoidea* (1). Beijing: Science Press.

Mackauer M. 1972. The aphid-attacking genera of Aphelinidae (Hymenoptera), including the description of a new genus. *The Canadian Entomologist* **104**(11): 1771-1779.

Michener CD. 1970. *Systematics in support of biological research*. National Academies.

Munro JB, Heraty JM, Burks RA, Hawks D, Mottern J, Cruaud A, Rasplus J-Y, Jansta P. 2011. A molecular phylogeny of the Chalcidoidea (Hymenoptera). *PLoS One* **6**(11): e27023.

Nikolskaya M, Yasnosh V. 1966. *Aphelinidae of the European part of USSR and Caucasus* (Chalcidoidea: Aphelinidae). Asc of USSR. Nauka.

Nikolskaya MN. 1952. The chalcid fauna of the USSR (Chalcidoidea). *Opred Faune* **44**: 1-575.

Noirot C, Quennedey A. 1974. Fine structure of insect epidermal glands. *Annual Review of Entomology* **19**(1): 61-80.

Noyes J. 2016. Universal Chalcidoidea Database. World Wide Web electronic publication. http://www.nhm.ac.uk/chalcidoids

Pedata P, Isidoro N. 1993. Evidence of male sex glands on the antenna of *Encarsia asterobemisiae* Viggiani et Mazzone (Hymenoptera: Aphelinidae). *Bollettino del Laboratorio di Entomologia Agraria "Filippo Silvestri"* **50**: 271-280.

Prinsloo G, Neser O. 1994. The southern African species of *Aphelinus* Dalman (Hymenoptera: Aphelinidae), parasitoids of aphids (Homoptera: Aphidoidea). *Journal of African Zoology* **108**(2): 143-162.

Prokrym D, Pike K, Nelson D. 1998. Biological control of *Diuraphis noxia* (Homoptera: Aphididae): implementation and evaluation of natural enemies. *Response Model for an Introduced Pest—The Russian Wheat Aphid Thomas Say Publications in Entomology, Entomological Society of America, Lanham, MD*: 183-208.

Raney, H.G. 1970, Host-parasite interactions between *Aphelinus asychis* (Walker), an imported parasite, and three aphid species of sorghums. (Doctoral dissertation, Oklahoma State University, 72pp.)

Rhoades J. 2015. A comparative study of courtship behaviors across the genus *Aphelinus* (Aphelinidae, Hymenoptera) and their role in speciation. (Master of Science thesis, University of Delaware, 50pp).

Romani R, Isidoro N, Bin F. 1999. Further evidence of male antennal glands in Aphelinidae: the case of *Aphytis melinus* DeBach (Hymenoptera: Aphelinidae). *Journal of Hymenoptera Research* **8**(1): 109-155.

Romani R, Rosi MC, Isidoro N, Bin F. 2008. The role of the antennae during courtship behaviour in the parasitic wasp *Trichopria drosophilae*. *Journal of Experimental Biology* **211**(15): 2486-2491.

Sacchetti P, Belcari A, Romani R, Isidoro N, Bin F. 1999. External morphology and ultrastructure of male antennal glands in two diapriids (Hymenoptera: Diapriidae). *Entomological Problems* **30**(1): 63-71.

Sell P, Kuo-Sell H. 1989. Well-tried and new beneficial organisms. Practical knowledge obtained in biological pest control in ornamental cultivation under glass and possibilities for its development. *Deutscher Gartenbau* **43**(42): 2548-2553.

Shrestha G, Skovgård H, Steenberg T, Enkegaard A. 2015. Preference and life history traits of *Aphelinus abdominalis* (Hymenoptera: Aphelinidae) when offered different development stages of the lettuce aphid *Nasonovia ribisnigri* (Hemiptera: Aphididae). *BioControl* **60**(4): 463-471.

Simão FA, Waterhouse RM, Ioannidis P, Kriventseva EV, Zdobnov EM. 2015. BUSCO: assessing genome assembly and annotation completeness with single-copy orthologs. *Bioinformatics*. **31**(19): 3210-3212.

Smith AB. 1998. What does palaeontology contribute to systematics in a molecular world? *Molecular Phylogenetics and Evolution* **9**(3): 437-447.

Stanke M, Morgenstern B. 2005. AUGUSTUS: a web server for gene prediction in eukaryotes that allows user-defined constraints. *Nucleic Acids Research* **33**: W465-W467.

Starks K, Burton R, Teetes G, Wood Jr E. 1976. Release of parasitoids to control greenbugs on sorghum. United States Department of Agriculture, ARS-S-91. 12 p.

Suck HB, Seo MJ, Kang EJ, Yoon KS, Yu YM, Yasunaga-Aoki C, Youn YN. 2012. Laboratory studies of *Aphelinus asychis*, a potential biological control agent for *Myzus persicae*. *Journal of the Faculty of Agriculture, Kyushu University* **57**(2): 431-439.

Summy K, Gilstrap F, Corcoran S. 1979. Parasitization of greenbugs and corn leaf aphids in west Texas. *Southwestern Entomologist* **4**: 176-180

Thomson, CG. 1876. *Skandinaviens Hymenoptera*. 1–192. H. Ohlsson, Lund.

Timberlake P. 1924. Descriptions of new chalcid-flies from Hawaii and Mexico (Hymenoptera). *Proceedings of the Hawaiian Entomological Society* **5**(3): 395-417

van den Assem J, Den Bosch HI, Prooy E. 1982. *Melittobia* courtship behaviour: a comparative study of the evolution of a display. *Netherlands Journal of Zoology* **32**(4): 427-471.

van den Assem J, Gijswijt M, Nubel BK. 1980. Observations on courtship-and mating strategies in a few species of parasitic wasps (Chalcidoidea). *Netherlands Journal of Zoology* **30**(2): 208-227.

Wiens JJ. 2000. *Phylogenetic Analysis of Morphological Data*. Smithsonian Institute Press, Washington D.C.

Wu Z, Hopper KR, O'Neil RJ, Voegtlin DJ, Prokrym DR, Heimpel GE. 2004. Reproductive compatibility and genetic variation between two strains of *Aphelinus albipodus* (Hymenoptera: Aphelinidae), a parasitoid of the soybean

aphid, *Aphis glycines* (Homoptera: Aphididae). *Biological Control* **31**(3): 311-319.

Yasnosh V. 1963. New species of the genus *Aphelinus* Dalm.(Hymenoptera, Chalcidoidea) in the fauna of the USSR. *Entomotogicheskoye Obozreniye* **42**: 178-185.

-. 1978. Hymenoptera II. Chalcidoidea 15. Aphelinidae. *Opredeliteli po faune SSSR*: 1-494.

-. 2002. Annotated check list of the Aphelinidae (Hymenoptera: Chalcidoidea), parasitoids of aphids (Homoptera: Aphidoidea) in Georgia. *Proceedings of the Institute of Zoology, Georgian Academy of Sciences* **21**: 169-172.

Yoder M, Mikó I, Seltmann K, Bertone M, Deans A. 2010. A Gross Anatomy Ontology for Hymenoptera. *PLoS ONE* **12:** (e15991).

Zehavi A, Rosen D. 1988. A new species of *Aphelinus* (Hymenoptera: Aphelinidae) from Israel, with notes on the mali group. *Israel Journal of Entomology* **22**: 101-108.

APPENDIX

Appendix A.

The table of genes used in Chapter II listed by their gene number in *A. atriplicis* (assigned randomly by AUGUSTUS) and associated annotation (from BLAST2GO). Of the 110 genes used, the annotations of 104 are listed below. The annotations of the other 6 genes that are unknown are listed as "N/A".

gene number in *A. atriplicis*	**gene name**
g10145.t1	protein pfc0760c-like
g10490.t1	cox assembly mitochondrial protein homolog
g10494.t1	kynurenine formamidase
g1062.t1	transmembrane protein 205
g1069.t1	PREDICTED: uncharacterized protein LOC100680226
g10785.t1	protein af-9
g10787.t1	probable 39s ribosomal protein mitochondrial
g11144.t1	protein tipin homolog
g11189.t1	39s ribosomal protein mitochondrial
g11210.t1	PREDICTED: uncharacterized protein LOC100678319 isoform X2
g11211.t1	ribosomal l1 domain-containing protein cg13096
g11236.t1	cd2 antigen cytoplasmic tail-binding protein 2 homolog isoform x1
g11585.t1	nadh dehydrogenase
g11913.t1	riboflavin kinase
g12108.t1	zinc finger 1
g12166.t1	cell wall protein rbr3
g12238.t1	protein fam114a2 isoform x1
g12268.t1	transmembrane protein 194a
g12453.t1	---NA---
g12495.t1	uncharacterized protein LOC100187594
g12540.t1	---NA---
g13958.t1	nucleoside diphosphate-linked moiety x motif mitochondrial-like isoform x1
g14034.t1	60s ribosomal protein l7
g14062.t1	upf0687 protein c20orf27 homolog

g14561.t1	transmembrane protein 135-like
g14608.t1	protein c19orf12 homolog
g14697.t1	protein aatf
g1480.t1	transient receptor potential protein
g14869.t1	complex iii assembly factor lyrm7
g14923.t1	serologically defined colon cancer antigen 3 homolog isoform x2
g15144.t1	28s ribosomal protein mitochondrial
g15241.t1	f-box only protein 9
g15496.t1	synaptonemal complex protein 1-like isoform x1
g15536.t1	PREDICTED: uncharacterized protein LOC105363622
g16720.t1	zinc finger protein 830 isoform x4
g16809.t1	PREDICTED: uncharacterized protein LOC103315804
g16838.t1	polycystic kidney disease protein 1-like 3
g16953.t1	PREDICTED: uncharacterized protein LOC105194478 isoform X2
g17203.t1	beta-sarcoglycan isoform x5
g17272.t1	---NA---
g17276.t1	nabaecin-1 precursor
g17348.t1	n-alpha-acetyltransferase 30 isoform x3
g17368.t1	PREDICTED: uncharacterized protein LOC100677826 isoform X4
g17885.t1	glucose-6-phosphate isomerase
g17937.t1	---NA---
g18181.t1	protein sgt1 homolog ecdysoneless
g18260.t1	actin-binding rho-activating
g18426.t1	mitochondrial import inner membrane translocase subunit tim21
g18654.t1	integrator complex subunit 1
g1866.t1	---NA---
g19011.t1	PREDICTED: mucin-17-like
g19109.t1	ribosome-binding factor mitochondrial isoform x1
g1915.t1	ribosome maturation protein sbds
g19284.t1	brca1-a complex subunit abraxas-like isoform x1
g19404.t1	transmembrane protein 223 isoform x1
g20192.t1	39s ribosomal protein mitochondrial
g20361.t1	e3 ubiquitin-protein ligase hakai
g20430.t1	fumarylacetoacetate hydrolase domain-containing protein 2a isoform x3
g21216.t1	bromodomain-containing protein 8
g21279.t1	protein asterix
g21350.t1	tryptophan--trna cytoplasmic

g22960.t1	pyroglutamyl-peptidase 1
g23015.t1	probable gpi-anchored adhesin-like protein pga55
g2452.t1	orexin receptor type 1-like isoform x1
g2718.t1	protein phosphatase 1 regulatory subunit 21 isoform x1
g2901.t1	methyltransferase-like protein 13 isoform x3
g2928.t1	probable trna (guanine -n)-dimethyltransferase
g2973.t1	PREDICTED: uncharacterized protein C20orf24 homolog
g3015.t1	facilitated trehalose transporter tret1-like
g3102.t1	transmembrane protein 147
g3512.t1	transmembrane protein 104 homolog isoform x2
g3597.t1	cdgsh iron-sulfur domain-containing protein 2 homolog
g3621.t1	necap-like protein cg9132-like
g3630.t1	PREDICTED: uncharacterized protein LOC100121379 isoform X1
g3688.t1	protein serac1
g3739.t1	glucosidase 2 subunit beta-like
g3888.t1	probable 28s ribosomal protein mitochondrial isoform x3
g4490.t1	mediator of dna damage checkpoint protein 1-like
g5025.t1	claspin homolog
g5341.t1	PREDICTED: uncharacterized protein LOC100118472, partial
g5426.t1	enolase-phosphatase e1
g5591.t1	spindle and kinetochore-associated protein 1-like
g6078.t1	probable gpi-anchored adhesin-like protein pga55
g6085.t1	PREDICTED: uncharacterized protein LOC103315870
g6144.t1	protein cip2a isoform x1
g6148.t1	---NA---
g6181.t1	PREDICTED: uncharacterized protein LOC105364806
g6500.t1	low quality protein: lysine-specific demethylase phf2-like
g6736.t1	choline o-acetyltransferase
g6922.t1	uncharacterized protein LOC100313523
g6931.t1	nuclear pore glycoprotein p62
g6980.t1	aristaless-related homeobox protein
g7360.t1	udp- c:betagal beta- -n-acetylglucosaminyltransferase-like protein 1
g7423.t1	glutathione s-transferase c-terminal domain-containing protein homolog
g7427.t1	PREDICTED: uncharacterized protein LOC105365715
g753.t1	integrator complex subunit 10
g7603.t1	golgi resident protein gcp60
g7612.t1	conserved oligomeric golgi complex subunit 1

g770.t1	ribosomal protein mitochondrial
g7953.t1	tubulin-specific chaperone c
g8183.t1	adenylate kinase isoenzyme 6
g8468.t1	coiled-coil domain-containing protein 40
g8848.t1	PREDICTED: uncharacterized protein LOC105368263
g9037.t1	micronuclear linker histone poly isoform x3
g9122.t1	sid1 transmembrane family member 1-like
g9302.t1	b-cell lymphoma leukemia 11a
g9394.t1	maestro heat-like repeat-containing protein family member 1 isoform x1
g9407.t1	grpe protein homolog mitochondrial isoform x1
g9502.t1	autophagy-related protein 2 homolog a isoform x2
g9851.t1	PREDICTED: uncharacterized protein LOC100679849

Appendix B

Table of partitioning scheme found by PartionFinder used in maximum likelihood analysis in Chapter II.

Subset	Best Model	Subset Partitions	Subset Sites
1	JTT+G+F	geneg10787, geneg11210, geneg11585, geneg12540, geneg14869, geneg16838, geneg16953, geneg17276, geneg1866, geneg19284, geneg19404, geneg21216, geneg22960, geneg23015, geneg5025, geneg6181, geneg6500, geneg8848	1-607, 608-847, 1384-2452, 3645-3928, 3929-4367, 11544-11734, 12525-14600, 14601-15544, 19115-19246, 21213-21618, 25376-25502, 26601-27709, 28366-28571, 39073-39473, 45138-46135, 46136-47862, 52733-53328, 60188-60398
2	JTT+G+F	geneg14034, geneg17885, geneg21279, geneg21350, geneg2718, geneg2973, geneg3102, geneg3597, geneg3621, geneg6931, geneg7953, geneg8183	848-1273, 1274-1383, 8726-9284, 20620-20877, 40393-40569, 40570-41010, 44222-44531, 56164-56434, 56435-56569, 57076-57304, 57551-57675, 58896-59351
3	VT+G+F	geneg10490, geneg12108, geneg12495, geneg1915, geneg20430	2453-2916, 21619-22634, 24841-25168, 29701-30240, 59913-60187
4	JTT+G+F	geneg20361, geneg1062, geneg12166, geneg12453, geneg14608, geneg1480, geneg15536, geneg17203, geneg17368, geneg17937, geneg2452, geneg3630, geneg6980, geneg9851	2917-3464, 8494-8725, 9285-11279, 12167-12524, 16435-16685, 19821-19960, 22635-22740, 23972-24840, 32182-32416, 43843-44221, 55403-56163, 59352-59912, 60399-60649, 61046-61396

5	JTT+G+F	geneg10494, geneg11189, geneg13958, geneg14062, geneg15144, geneg18260, geneg19109, geneg20192, geneg3739, geneg3888, geneg5426, geneg5591, geneg7360, geneg7603, geneg770	3465-3644, 4368-4752, 7619-7849, 18249-18645, 20410-20619, 20878-21212, 27710-28135, 29381-29700, 41929-42438, 43486-43842, 50680-51000, 51001-52311, 53414-53631, 53632-54686, 61397-61506
6	HIVb+G+F	geneg1069, geneg15496, geneg19011, geneg7427	4753-5242, 16686-17792, 42439-42920, 60650-61045
7	JTT+G+F	geneg14923, geneg17348, geneg18654, geneg6922, geneg753, geneg9394, geneg9502	5243-7362, 11280-11543, 18646-19114, 32417-34581, 34820-36486, 44532-44977, 61507-62141
8	JTT+G+F	geneg11913, geneg12268, geneg14561, geneg15241, geneg18181, geneg18426, geneg2901, geneg2928, geneg3512, geneg3688, geneg4490, geneg5341, geneg7423, geneg7612, geneg9122, geneg9407	7363-7618, 7850-8493, 17793-18248, 19961-20409, 22741-23201, 25169-25375, 34582-34819, 37415-38245, 41011-41928, 42921-43485, 52312-52732, 53329-53413, 54687-55402, 56570-57075, 57676-58219, 58220-58895
9	JTT+G+F	geneg16809, geneg17272	11735-12166, 15545-16116
10	JTT+G+F	geneg10785, geneg11144, geneg11236, geneg12238, geneg14697, geneg16720, geneg6144, geneg8468	16117-16434, 19247-19820, 23202-23971, 25503-25866, 28136-28365, 28572-29380, 39474-40392, 48378-49264
11	JTT+G+F	geneg10145, geneg11211, geneg6078	25867-26600, 30241-32181, 49699-50679
12	Blosum62+G+F	geneg3015, geneg6085, geneg6736, geneg9037, geneg9302	36487-37414, 38246-39072, 44978-45137, 49265-49698, 57305-57550
13	HIVw+G+F	geneg6148	47863-48377

Appendix C

List of anatomical terms and links to URI locations in the Hymenoptera Anatomy Ontology portal.

Term	Definition	URI
antenna	The anatomical cluster that is composed of the scape, pedicel and flagellum.	http://purl.obolibrary.org/obo/HAO_0000101
apical denticle	The spur that is located distally on the gonossiculus.	http://purl.obolibrary.org/obo/HAO_000157
base	The tergum that is located on abdominal segment 2 AND The tergum that is located on the abdominal segment 3.	http://purl.obolibrary.org/obo/HAO_0000053 and http://purl.obolibrary.org/obo/HAO_0000056
body	The anatomical cluster that is composed of the whole organism but which excludes the antennae, legs and wings.	http://purl.obolibrary.org/obo/HAO_0000182
club	The anatomical cluster composed of the apical flagellomeres that are differentiated by size from the basal flagellomeres.	http://purl.obolibrary.org/obo/HAO_0001185
compound eye	The compound organ that is composed of ommatidia.	http://purl.obolibrary.org/obo/HAO_0000217
costal cell	The membranous region of the forewing anterior to the submarginal vein, measured from the basal constriction that delimits the apex of the humeral plate of the wing to the point at which the submarginal vein touches the leading edge of the wing. http://purl.obolibrary.org/obo/HAO_0000226	http://purl.obolibrary.org/obo/HAO_0000226
coxa	The leg segment that is connected to the body and to the trochanter via conjunctivae and muscles.	http://purl.obolibrary.org/obo/HAO_0000228
digitus	The sclerite that is located distally on the parossiculus.	http://purl.obolibrary.org/obo/HAO_0000385
edge	The margin that extends along the border of two areas that are oriented differently.	http://purl.obolibrary.org/obo/HAO_0000285
eye margin	The margin of the compound eye.	http://purl.obolibrary.org/obo/HAO_0000672
F1	The flagellomere that is proximally attached to the pedicel.	http://purl.obolibrary.org/obo/HAO_0001148
F2	The flagellomere that is located distal to the first flagellomere.	http://purl.obolibrary.org/obo/HAO_0001883
F3	The flagellomere that is located immediately distal to the second flagellomere.	http://purl.obolibrary.org/obo/HAO_0001895
femur	The leg segment that is distal to the trochanter and proximal to the tibia.	http://purl.obolibrary.org/obo/HAO_0000327
forewing	The wing that is located on the mesothorax.	http://purl.obolibrary.org/obo/HAO_0000351
frontovertex	The anatomical cluster that is composed of the vertex and the dorsal area of the upper face dorsal to the frontofacial ridge.	http://purl.obolibrary.org/obo/HAO_0001823
genitalia	The anatomical cluster that is composed of the cupula, gonostyle, volsella and the aedeagus	http://purl.obolibrary.org/obo/HAO_0000312
head	The tagma that is located anterior to the thorax.	http://purl.obolibrary.org/obo/HAO_0000397
hind wing	The wing that is located on the metathorax.	http://purl.obolibrary.org/obo/HAO_0000400
leg	The anatomical cluster that is composed of the coxa and all distal leg segments and is connected to the pectus.	http://purl.obolibrary.org/obo/HAO_0000494
longitudinal sensillum	The multiporous plate sensillum that is elongate.	http://purl.obolibrary.org/obo/HAO_0001936

Term	Definition	URI
mandible	The sclerite that is connected to the cranium along the anterior margin of the oral foramen via the anterior and posterior cranio-mandibular articulations.	http://purl.obolibrary.org/obo/HAO_0000506
margin	The line that delimits the periphery of an area.	http://purl.obolibrary.org/obo/HAO_0001133
marginal vein	The abscissa that is located along the anterior margin of the forewing and is thought to correspond to the anterior abscissa of the radius (R1).	http://purl.obolibrary.org/obo/HAO_0000635
mesobasitarsus	The basitarsus that is located in the mid leg.	http://purl.obolibrary.org/obo/HAO_0001131
mesocoxa	The coxa that is located on the mid leg.	http://purl.obolibrary.org/obo/HAO_0001490
mesofemur	The femur that is located on the mid leg.	http://purl.obolibrary.org/obo/HAO_0000576
mesoscutum	The area that is located anterior to the transscutal articulation.	http://purl.obolibrary.org/obo/HAO_0001351
mesosoma	The anatomical cluster that is composed of the prothorax, mesothorax and the metapec- tal-propodeal complex.	http://purl.obolibrary.org/obo/HAO_0001120
mesotibia	The tibia that is located on the mid leg.	http://purl.obolibrary.org/obo/HAO_0001142
mesotibial spur	The tibial spur that is located on the mesotibia.	http://purl.obolibrary.org/obo/HAO_0001142
metabasitarsus	The basitarsus that is located on the hind leg.	http://purl.obolibrary.org/obo/HAO_0000587
metabasitarsus	The basitarsus that is located on the hind leg.	http://purl.obolibrary.org/obo/HAO_0000626
metacoxa	The coxa that is located on the hind leg.	http://purl.obolibrary.org/obo/HAO_0000631
metasoma	The tagma that is connected anteriorly to the metapectal-propodeal complex at the pro- podeal foramen and consists of abdominal segments.	http://purl.obolibrary.org/obo/HAO_0001121
metatibia	The tibia that is located on the hind leg.	http://purl.obolibrary.org/obo/HAO_0000679
metatibial spur	The tibial spur that is located on the metatibia.	http://purl.obolibrary.org/obo/HAO_0000706
mid lobe of mesoscutum	The area that is located between the notauli.	http://purl.obolibrary.org/obo/HAO_0000520
occipital margin	The edge that separates the occiput from the vertex.	http://purl.obolibrary.org/obo/HAO_0001963
ocellus	The multi-tissue structure that is located on the top of the head, composed of the corneal lens, pigment cell, rhabdoms and synaptic plexus.	http://purl.obolibrary.org/obo/HAO_0000661
ovipositor	The anatomical cluster that is composed of the first valvulae, second valvulae, third valvu- lae, first valvifers and second valvifers .	http://purl.obolibrary.org/obo/HAO_0000510
pedicel	The antennal segment that is the second segment of the antenna and is connected proxi- mally with the scape and distally with the flagellum.	http://purl.obolibrary.org/obo/HAO_0000512
phallobase	The anatomical cluster that is composed of the cupulae, gonostipites and volsellae.	http://purl.obolibrary.org/obo/HAO_0000713
posterior ocellus	The ocellus that is paired.	http://purl.obolibrary.org/obo/HAO_0000481

Term	Definition	URI
procoxa	The coxa that is located on the fore leg.	http://purl.obolibrary.org/obo/HAO_0001122
profemur	The femur that is located on the fore leg.	http://purl.obolibrary.org/obo/HAO_0001124
protibia	The tibia that is located on the fore leg.	http://purl.obolibrary.org/obo/HAO_0000350
row	The anatomical cluster that is composed of repeated units of anatomical structures.	http://purl.obolibrary.org/obo/HAO_0000901
scape	The antennal segment that is proximal to the pedicel and is connected with the head via the radicle.	http://purl.obolibrary.org/obo/HAO_0000908
sculpture	The area that is located on the sclerite and that is composed of repetitive anatomical structures.	http://purl.obolibrary.org/obo/HAO_0000913
scutellar sensillum	The campaniform sensillum that is paired and is located submedially on the mesoscutel- lum.	http://purl.obolibrary.org/obo/HAO_0001965
scutellum	The area that is located posteriorly of the transscutal line and is composed of the axillae and the mesoscutellum.	http://purl.obolibrary.org/obo/HAO_0000572
secretory pore	The anatomical space that corresponds to the distal end of an exocrine gland.	http://purl.obolibrary.org/obo/HAO_0001966
seta	The sensillum that is multicellular and consists of trichogen, tormogen, and sense cells. The area that is located between the notaulus and the parascutal carina.	http://purl.obolibrary.org/obo/HAO_0000935
side lobe	The area that is located between the notaulus and the parascutal carina.	http://purl.obolibrary.org/obo/HAO_0000466
submarginal vein	Basal-most portion of the forewing vein complex that occurs behind the costal cell; meas- ured from the constriction that delimits the humeral plate to the point at which the vein touches the leading edge of the wing apically.	http://purl.obolibrary.org/obo/HAO_0000972
T1	The tergum that is located on abdominal segment 2.	http://purl.obolibrary.org/obo/HAO_0000053
T2	The tergum that is located on the abdominal segment 3.	http://purl.obolibrary.org/obo/HAO_0000056
tarsus	The leg segment that is apical to the tibia.	http://purl.obolibrary.org/obo/HAO_0000992
third valvula	The sclerite that is located posterior to the second valvifer and is connected to the second valvifer via conjuntiva.	http://purl.obolibrary.org/obo/HAO_0001012
tooth	The projection that is located distally on the mandible.	http://purl.obolibrary.org/obo/HAO_0001019
wing	The wing that is located on the mesothorax.	http://purl.obolibrary.org/obo/HAO_0000351

Appendix D

Key to species in the *asychis* group of *Aphelinus,* male or female specimens.

1. Fore coxae yellow .....n.sp. 1

   Fore coxae brown 2

2. Profemora entirely yellow or pale ..... *semiflavus* Howard

   Profemora brown at base 3

3. Mesotibia entirely yellow .....n.sp. 2

   Mesotibia brown at base or dark with apex pale .....*asychis* Walker